Functional magnetic materials

Chih-Huang Lai

Department of Materials Science and Engineering
National Tsing Hua University, Taiwan

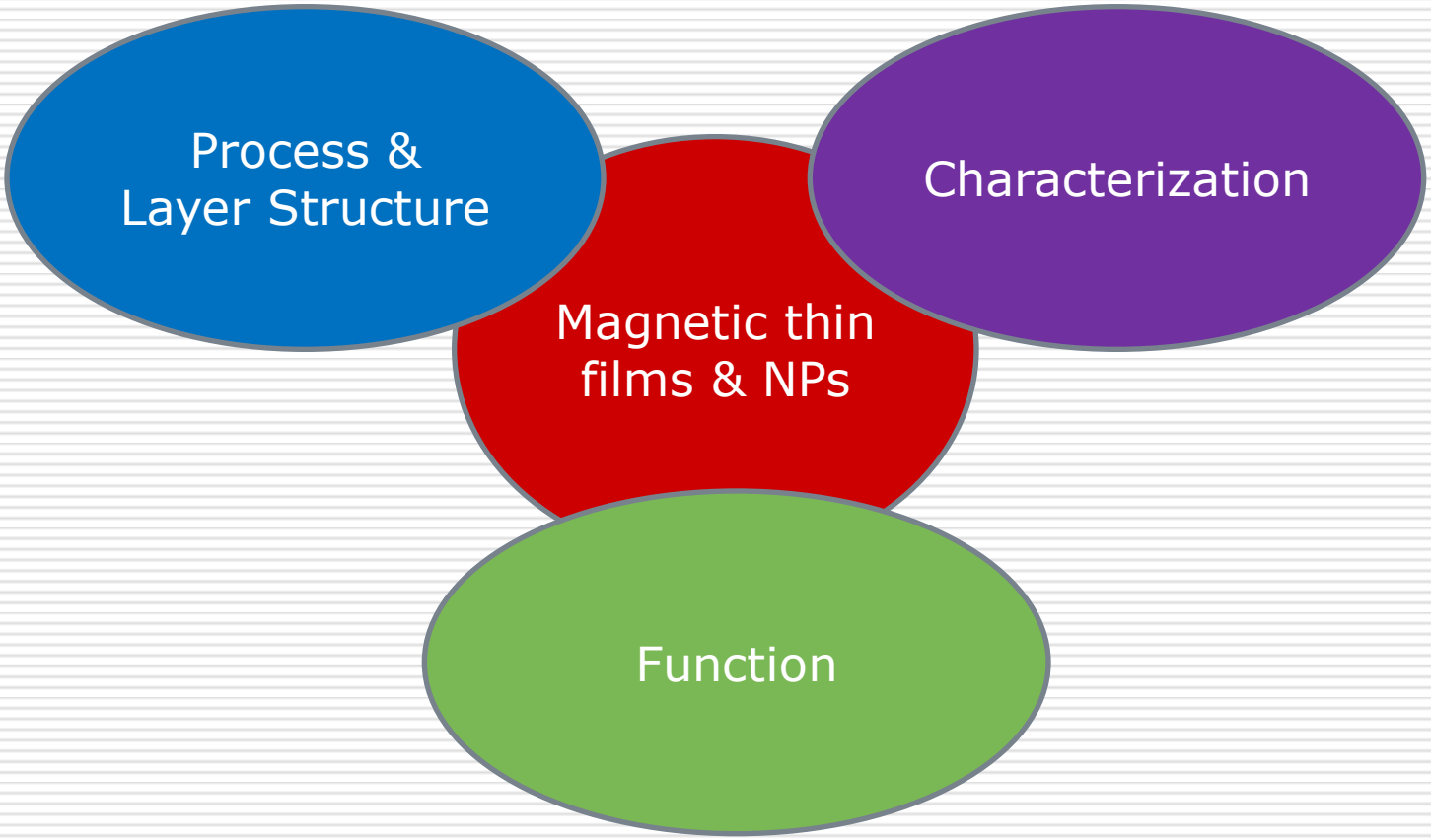
Process &
Layer Structure
Characterization
Magnetic thin
films & NPs
Function

Outline

(I) Magnetic Media:

(a) Co-based Exchange-Coupled-Composite (ECC) films
(b) FePt films

(II) Nanoparticles and Spintronics Devices:

(a)Fe_3O_4 NPs for MRI contrast agents
(b)SOT in multilayers
(c)Phase transformation

(I) Magnetic Media

(A) CO-BASED EXCHANGE-COUPLED-COMPOSITE (ECC) FILMS

Challenges of High-density Magnetic Recording

Trilemma

SNR:
→Reduced Grain Size

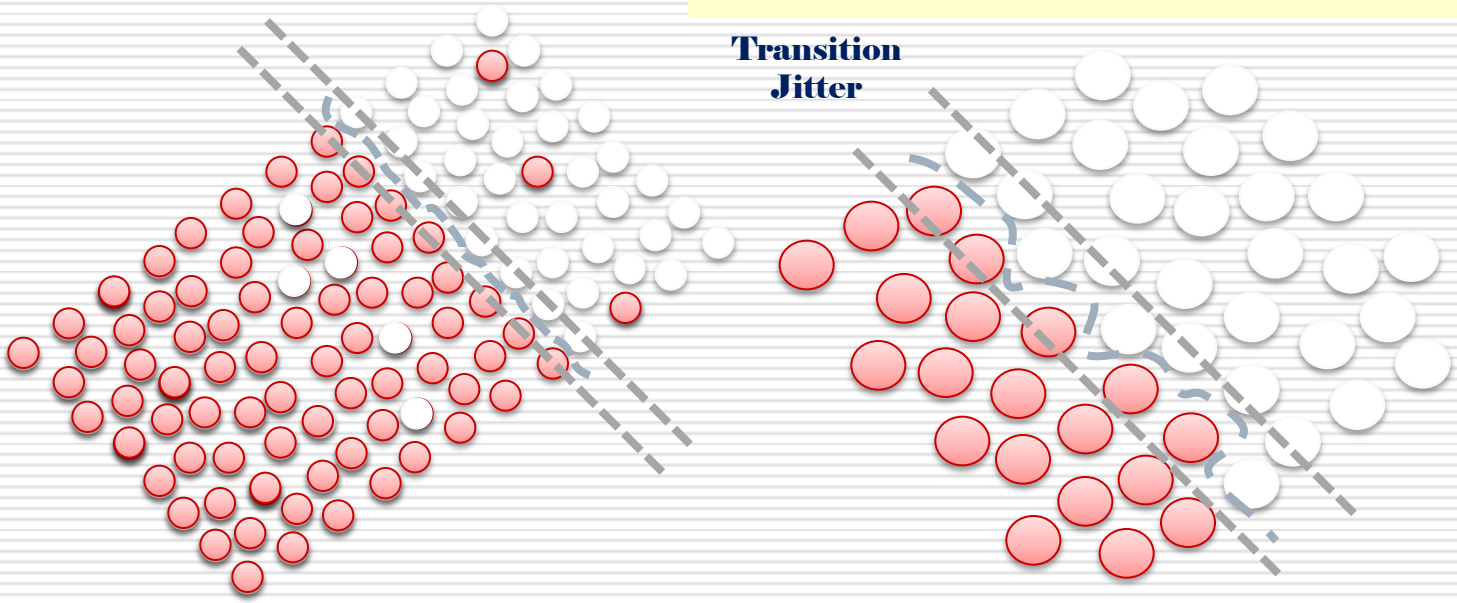

Thermal stability:
→$K_U V$=40-60*($k_B T$)
→ High K_U Material

Writability:
→Head field > H_o

Exchange Coupled Composite/Exchange Spring Media

Assisting Layer (soft layer)
Low K_u materials

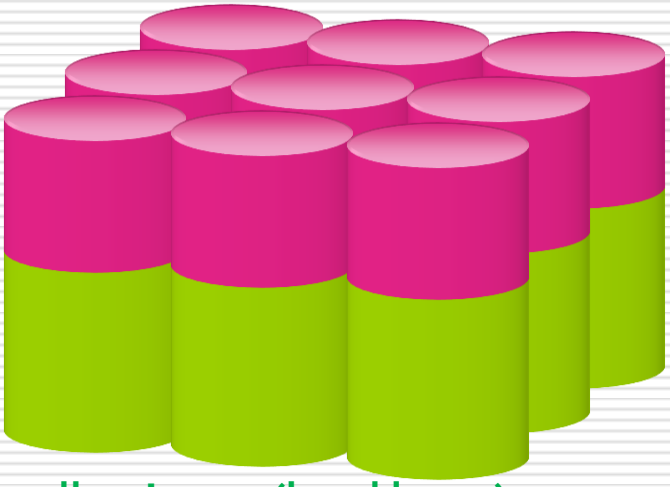

Recording Layer (hard layer)
High K_u materials → writabiltiy issue

Exchange spring reversal (spin chain model)

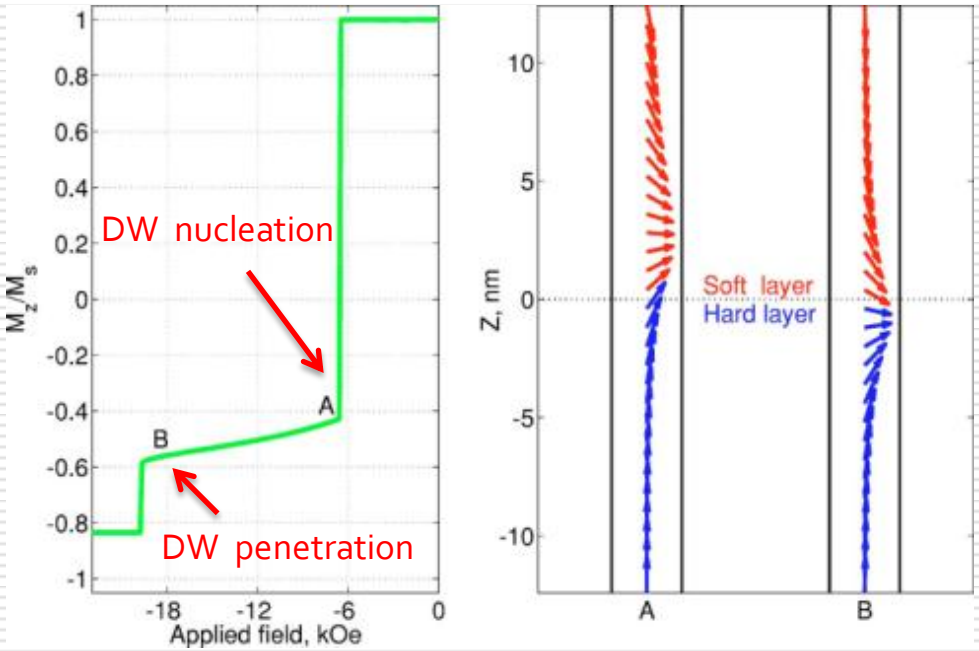

Overcome the tri-lemma effect:

➢Increase writability to thermal stability ratio

A. Yu. Dobin and H. J. Richter, Appl. Phys. Lett. 89, 062512, 2006

X-ray Magnetic Circular Dichroism

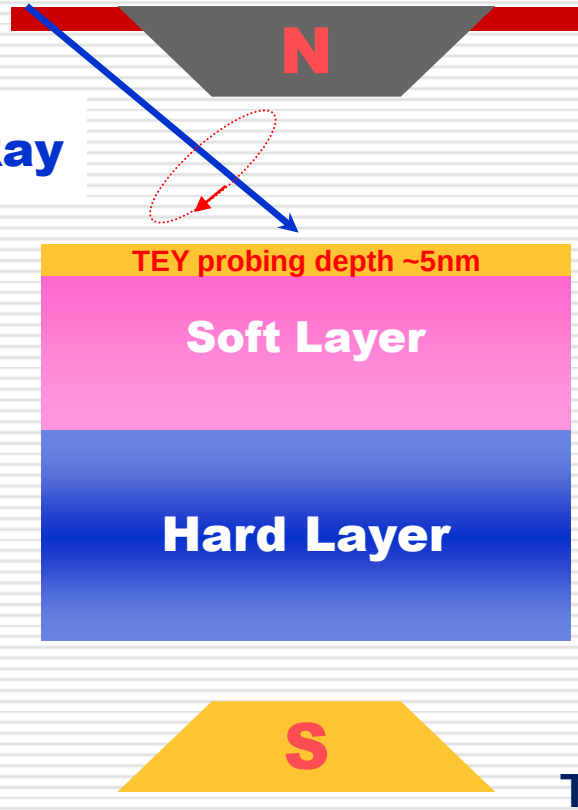

Sensitive to the M projection along X-ray incident direction

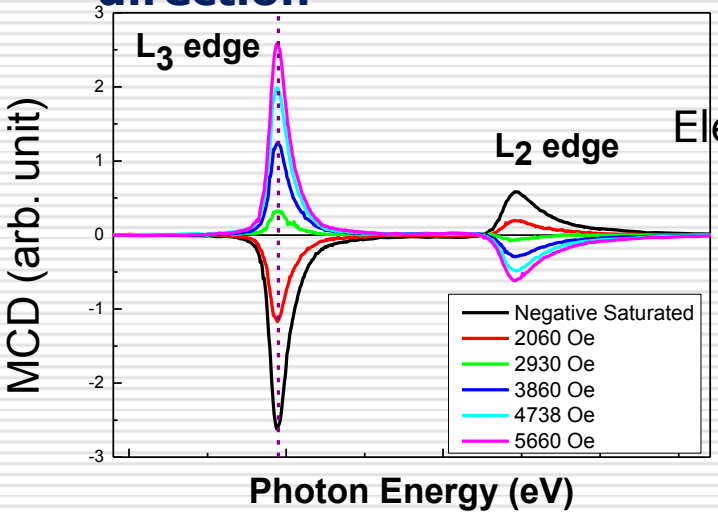

Element specific MH loop

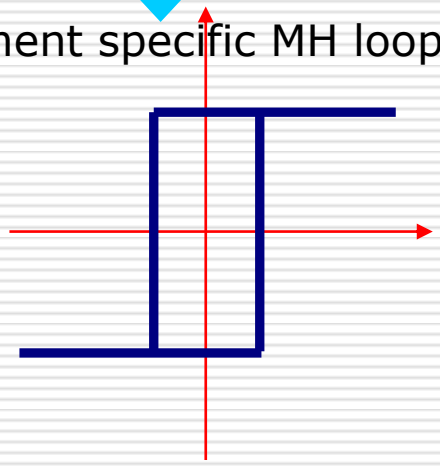

Total electron yield (TEY) :

- surface sensitivity of **5nm**

Fluorescence yield (FY) :

- Probing depth of **100nm**

Hou & Lai., J. Appl. Phys. 109, 07C104 (2011)

Granular ECC media

Ta 3/Pt 7/Ru 15/CoPtCr-SiO_2 12nm/ [Pt 0.7/CoPtCr-SiO_2 1.1]$_N$

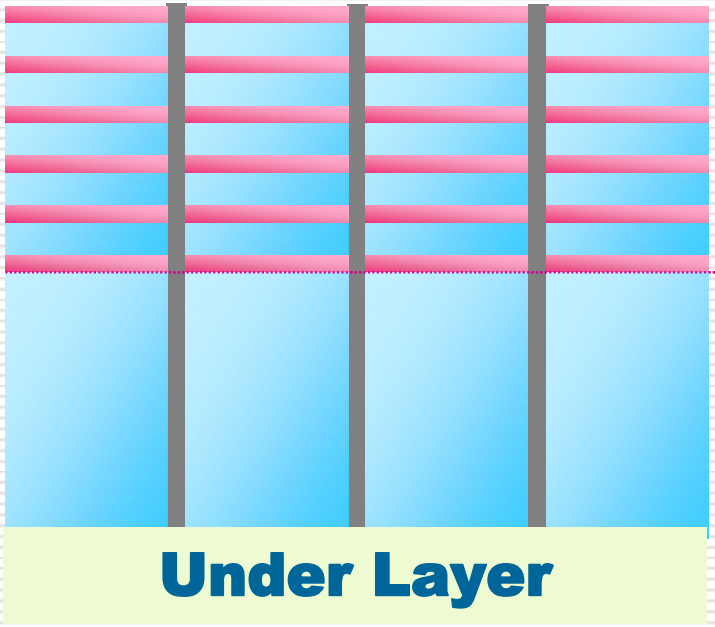

Soft Layer

[CoPtCr-SiO2/Pt]$_n$:
Granular Structure
Laminated layer design
Adjustable vertical coupling by Pt

Hard Layer

CoPtCr-SiO2:
Granular Structure
High K_u material
Commonly used in HDD

Hou & Lai. J. Appl. Phys. 105, 07B729 (2009)
Hou & Lai J. Appl. Phys. 109, 07C104 (2011)

XMCD with Fe marker

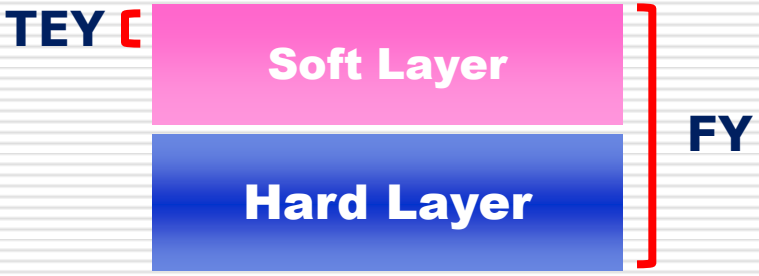

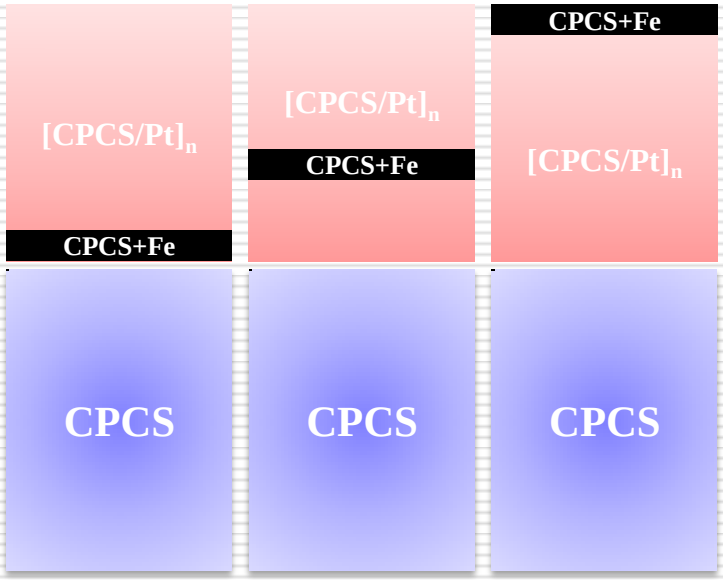

- **Florescence yield (FY) : 100nm probing depth**
- **Co-sputtered Fe-marker (4Å) at various locations → magnetization indicator**
- **XMCD loops of Fe-marker → depth-dependent reversal**

Exchange Spring Magnet

Fe-marker at the top, middle, and bottom of the soft layer (N=7)

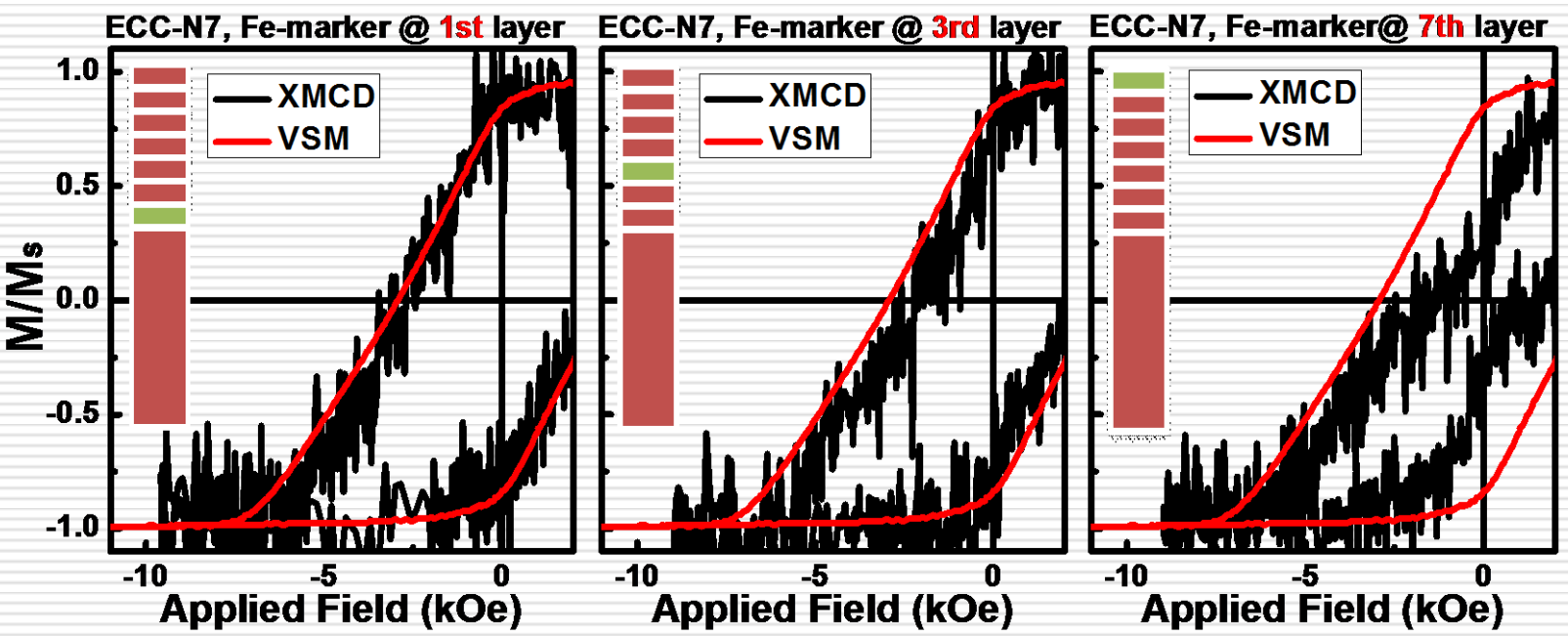

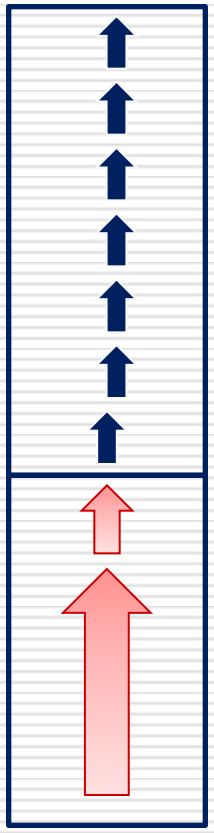

ES magnet:

- **In-depth deviation of magnetization**
- **Evidence of domain wall assisting reversal**

Hou & Lai., Appl. Phys. Lett. 98, 262507 (2011)

(I) Magnetic Media

(B) FEPT FILMS

Can Density Be Unlimitedly Increased ?

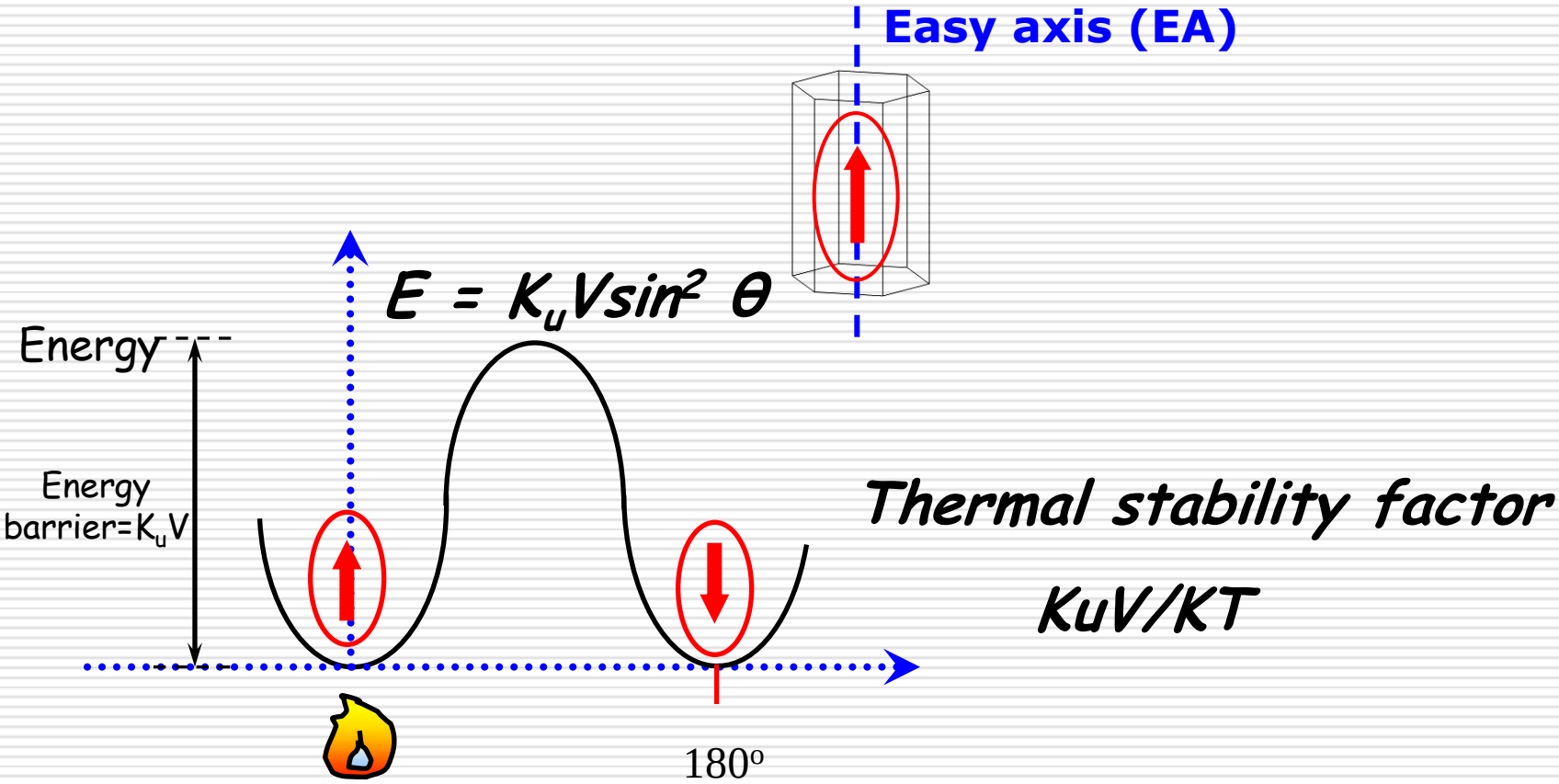

Superparamagnetic limit

Challenges of FePt for applications of media

As-deposited

Fe
Pt

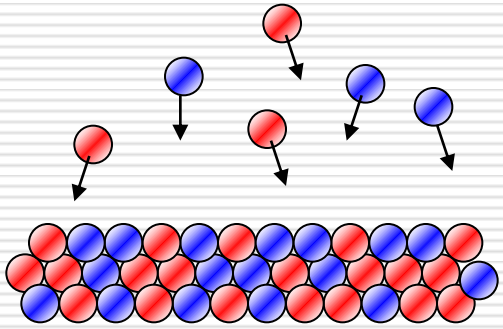

T_s: R. T.

Disordered phase

Meta-stable phase

Disordered-fcc

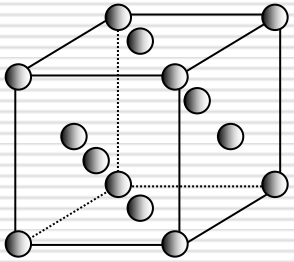

a=3.816Å

Ordered-$L1_0$

$T_a > 500℃$

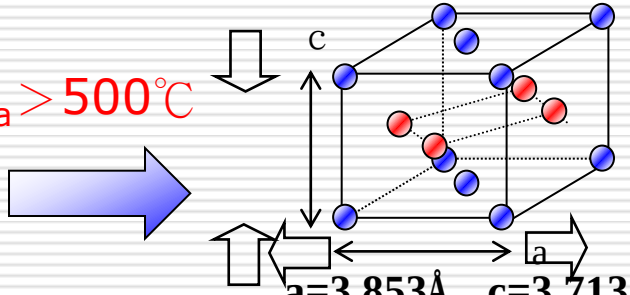

a=3.853Å c=3.713Å

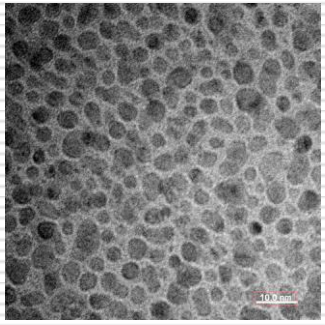

(001)-oriented

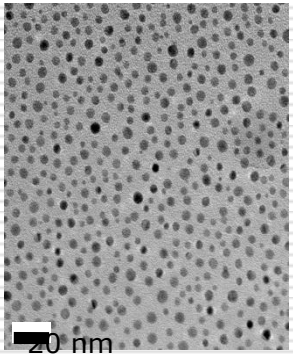

Granular

Particulate

Approaches

- Low-temperature ordering of ordered $L1_0$-FePt continuous films on amorphous substrates
- Low-temperature ordering of ordered (001) $L1_0$-FePt granular films on amorphous substrates
- (001) ordered $L1_0$-FePt nanoparticles on amorphous substrates

Enhance diffusion

–ion irradiation

- **2 MeV He-ion irradiation**
- **beam current: 1.25 μA/cm²**
- **230℃ on sample surface by beam heating**
- **ion dose: 2.4x10¹⁶ ions/cm²**
- **All He ions stop in SiO_2/Si !!**

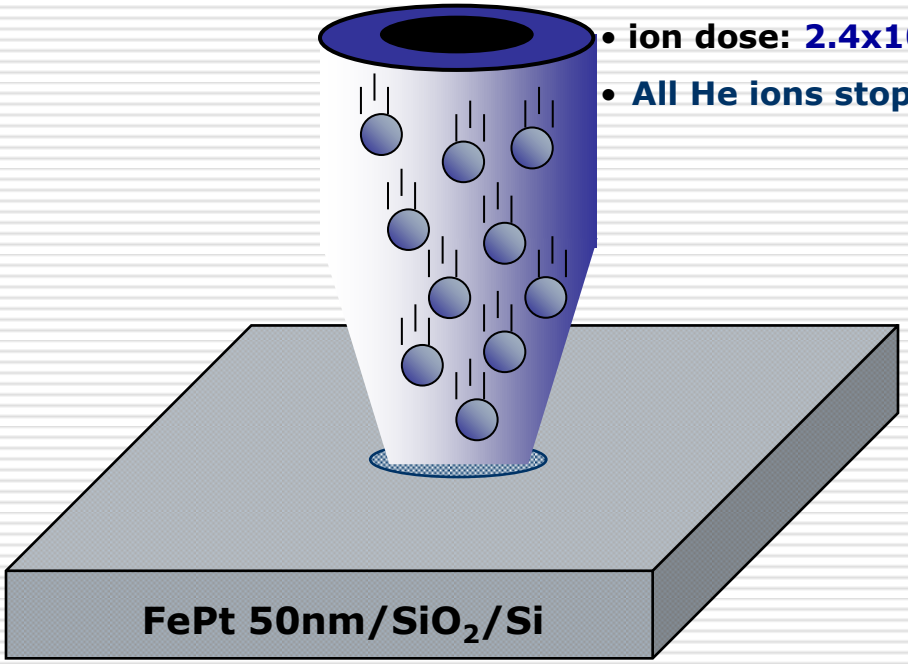

In-plane loop

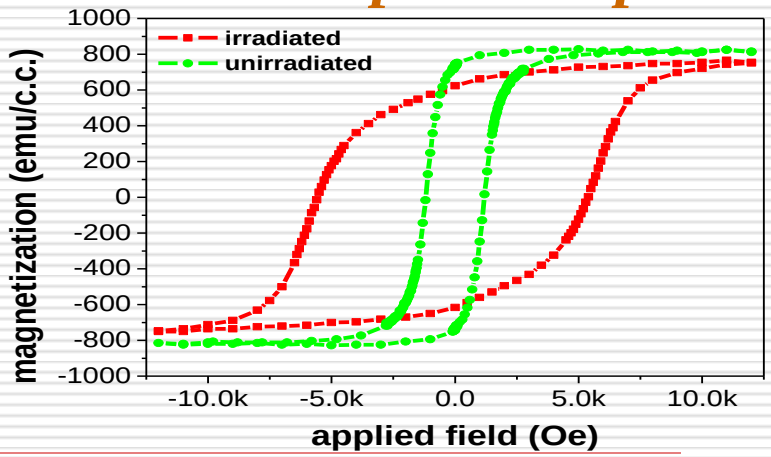

C. H. Lai et al., Appl. Phys. Lett. 83, 4550 (2003).

Dynamic-stress-induced ordering

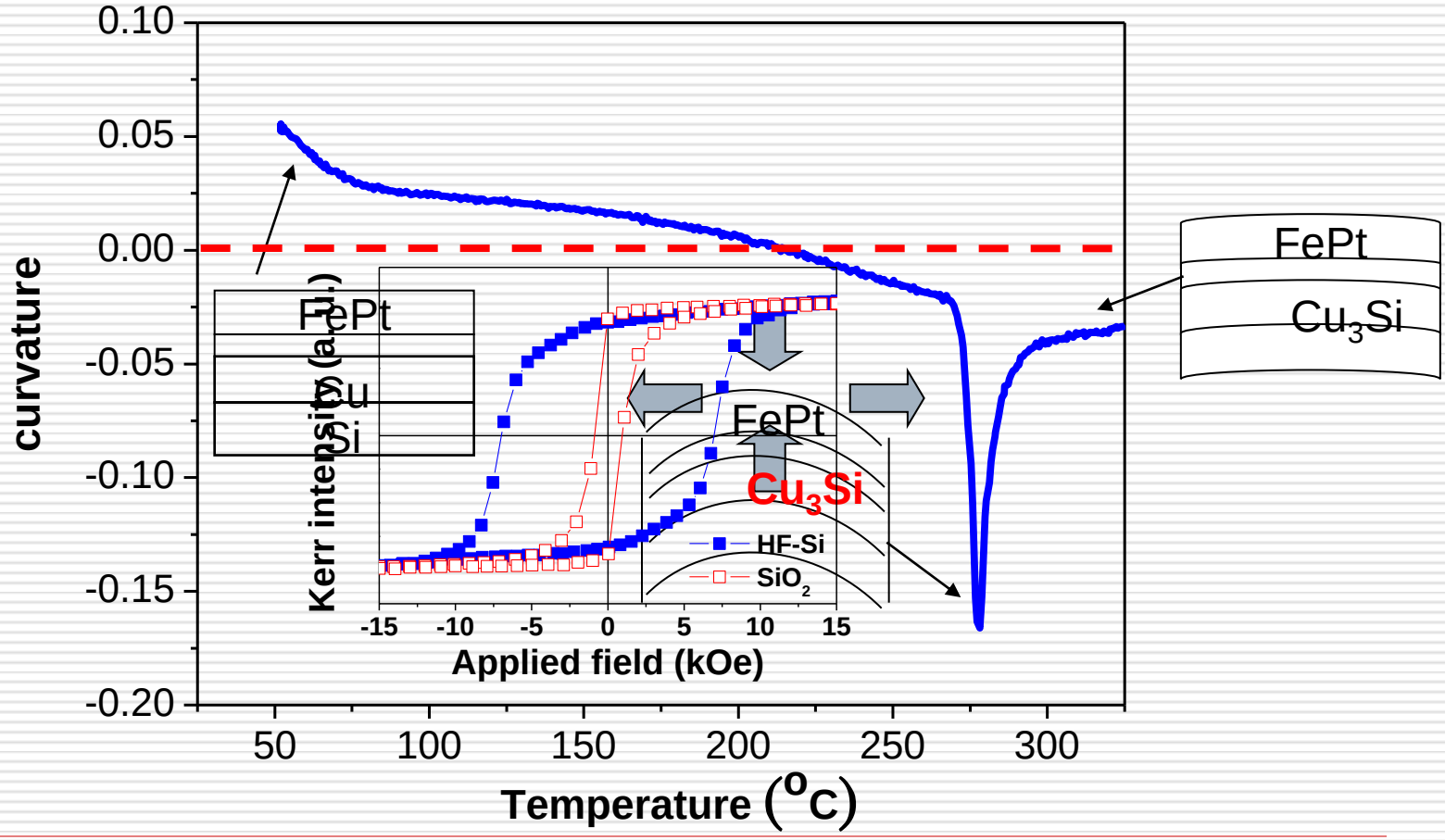

C. H. Lai et al., Appl. Phys. Lett. 85, 4430 (2004).

Reduce diffusion length

-atomic-scale multilayer (MLs)

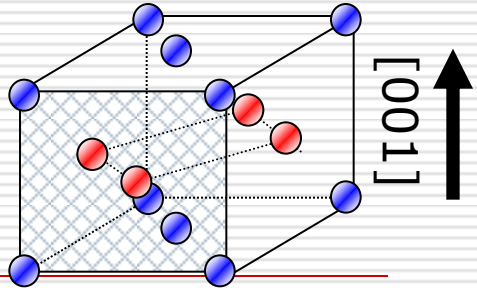

6 guns sputtering system

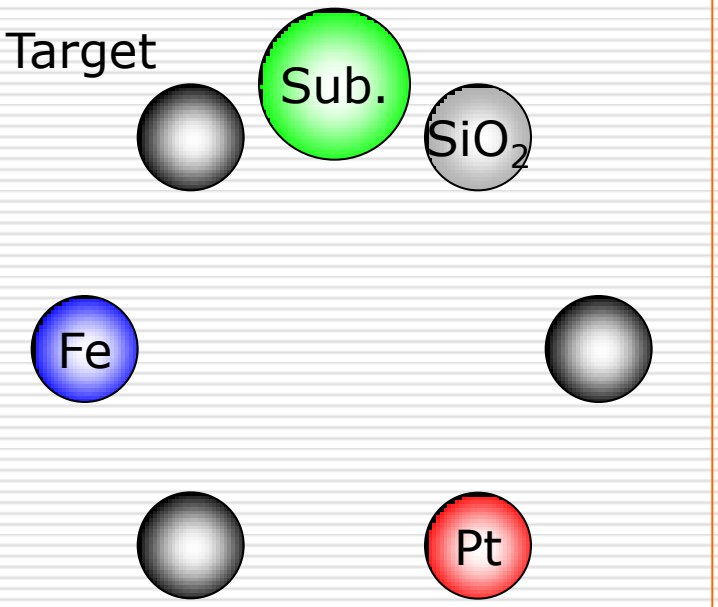

Atomic-scale $[Fe/Pt]_{18}$ MLs

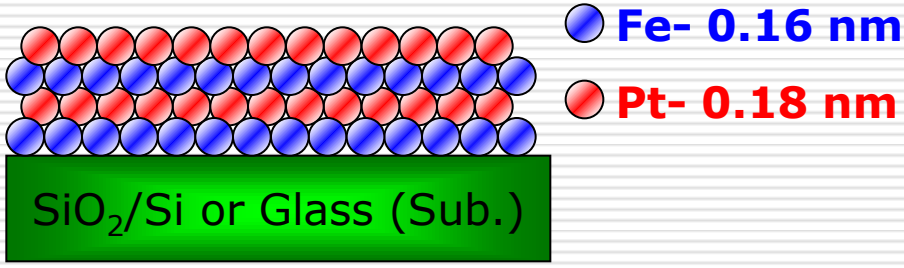

Atomic-scale $[Fe/Pt/SiO_2]_{18}$ MLs

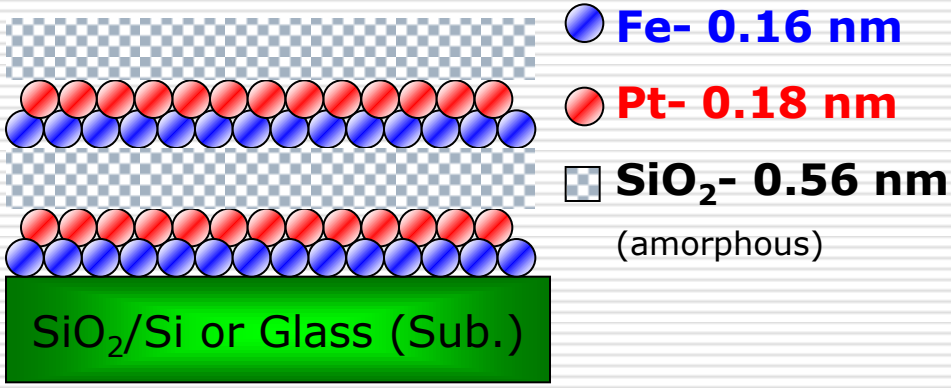

Layer-thickness dependence

6.1 nm $[Fe/Pt]_n$ MLs (n=1~18)

$(Fe/Pt)_{thickness}$ is fixed at 0.89 **($Fe_{55}Pt_{45}$)**

T_a=400℃ , t=60sec.

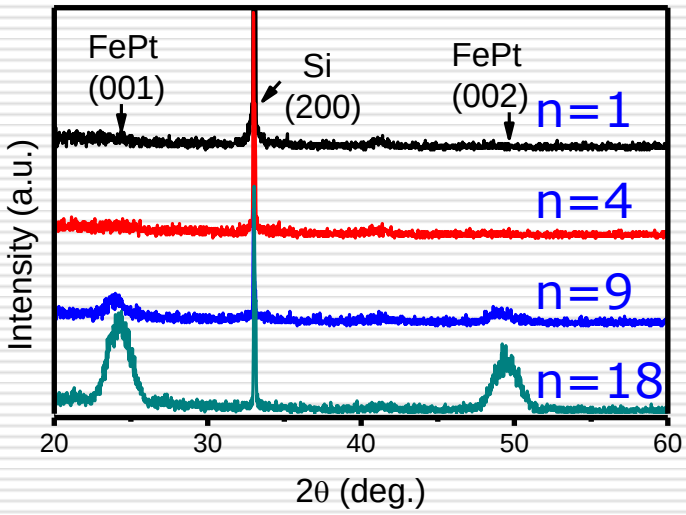

6.1 nm $[Fe(0.16)/Pt(0.18)]_{18}$ MLs

T_a=400℃ , t=60sec.

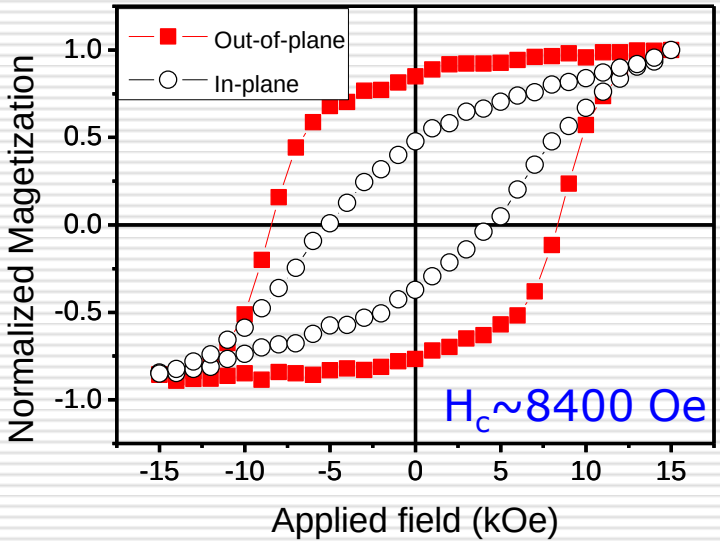

Atomic-scale Fe/Pt MLs can significantly promote the (001) preferred orientation and low-temperature ordering

Atomic-scale FePt-SiO_2 granular films

T_a= 350℃ , t=60 sec

Atomic-scale [Fe/Pt/SiO_2]$_{18}$ MLs

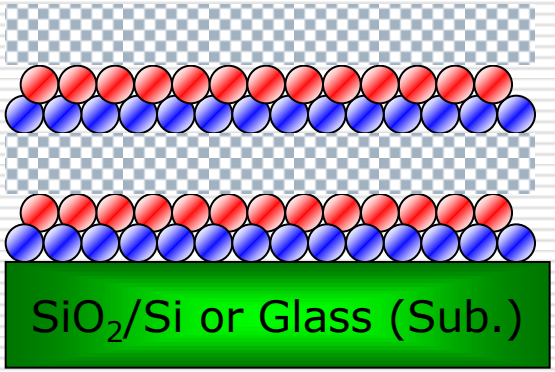

Fe- 0.16 nm

Pt- 0.18 nm

SiO_2- *x* nm (amorphous)

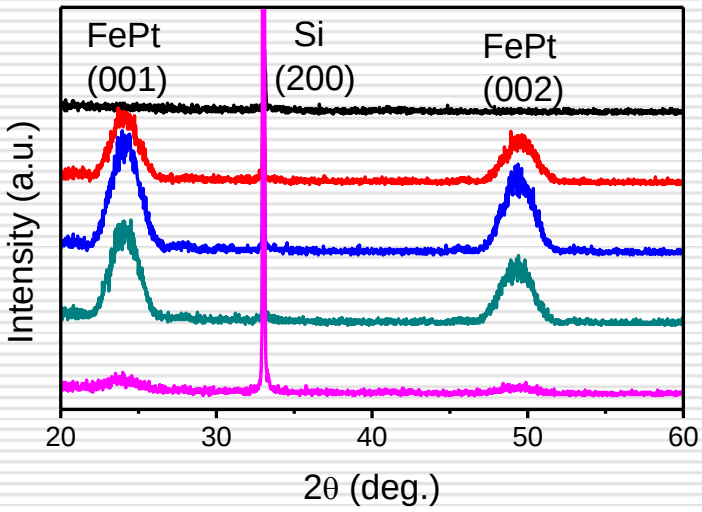

X =1.03 nm

X =0.56 nm

X =0.28 nm

X =0.19 nm

X =0 nm ([Fe/Pt]$_{18}$)

Insert ultra thin SiO_2 layer

- Ordering temperature can be further reduced to 350℃

$FePt\text{-}SiO_2$ (001) granular film

T_a = 350℃ for 60 sec.

$[Fe/Pt/SiO_2(0.28nm)]_{18}$

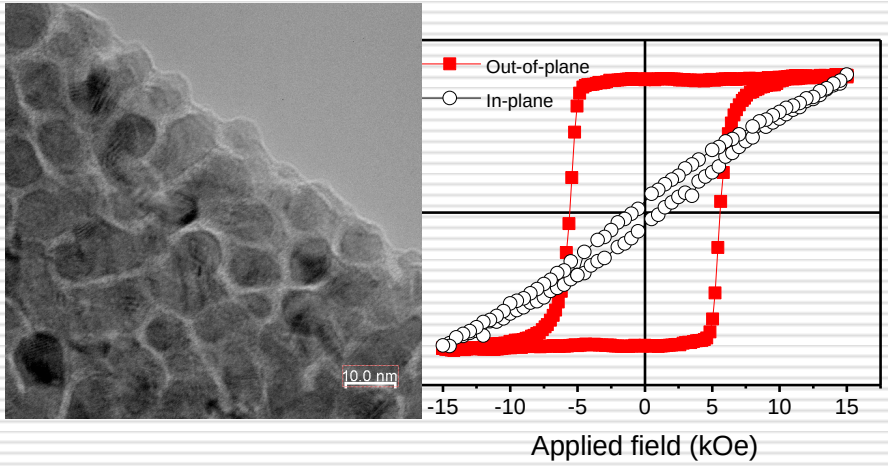

Grain size: 15.46 nm

$H_{c,\perp}$ ~5580 Oe

$[Fe/Pt/SiO_2(0.56nm)]_{18}$

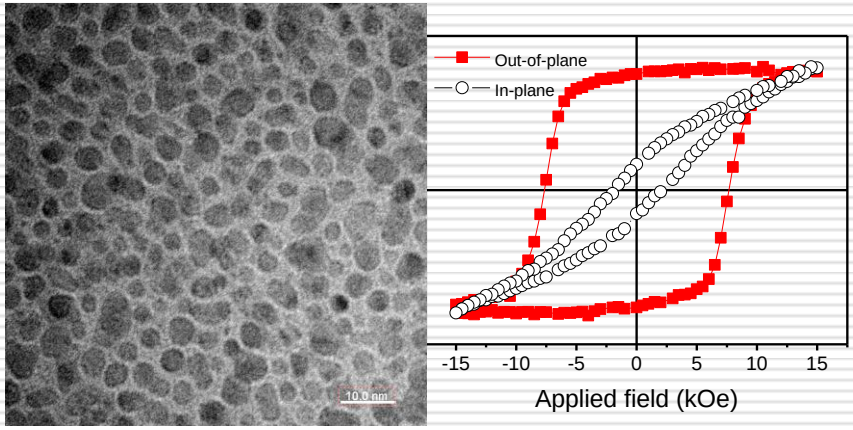

Grain size: 5.14 nm

$H_{c,\perp}$ ~7700 Oe

Mechanism

-Granular process

Diffusion-out process during annealing

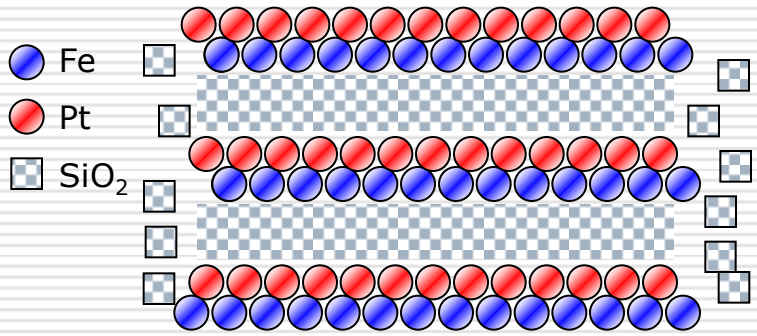

annealing

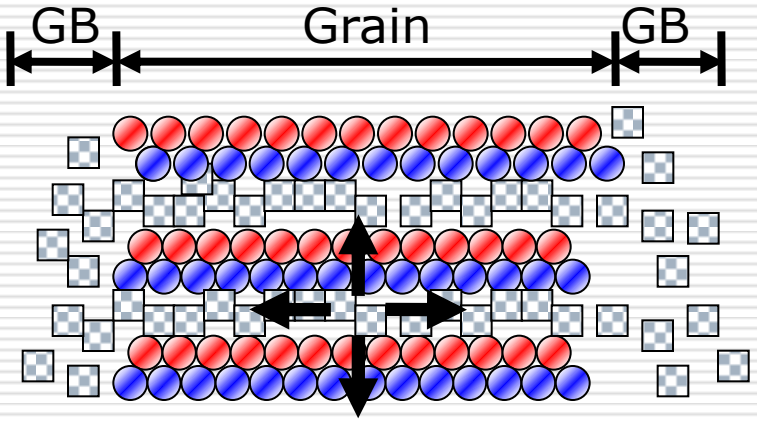

Final

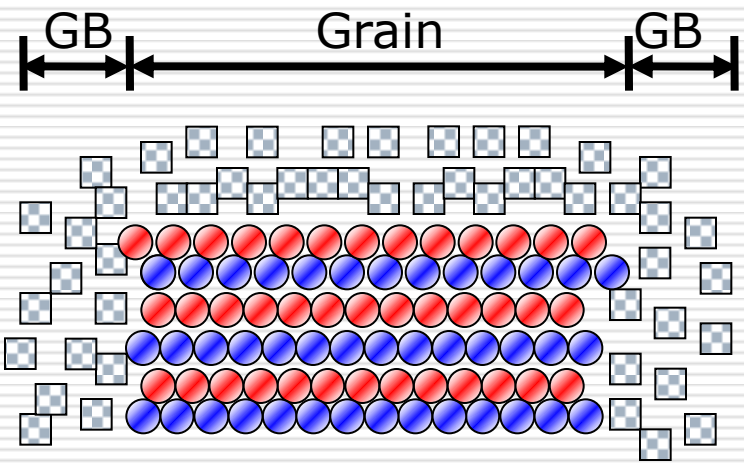

1. Insolubility and low surface energy
→ Granular microstructure

2. SiO_2 Diffusion-out

→ accelerate diffusion of Fe and Pt

Fabrication of (001) FePt NPs — Agglomeration

$[Fe/Pt/SiO_2(0.28\ nm)]_{18}$ (6.2 nm) grown on thermally oxidized SiO_2 annealed for 2 sec.

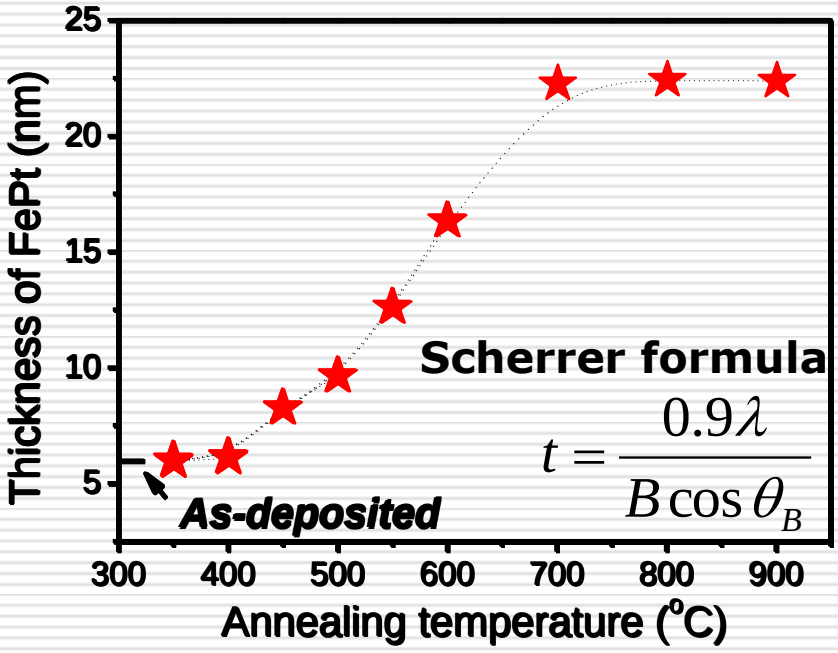

TEM Cross-sectional image

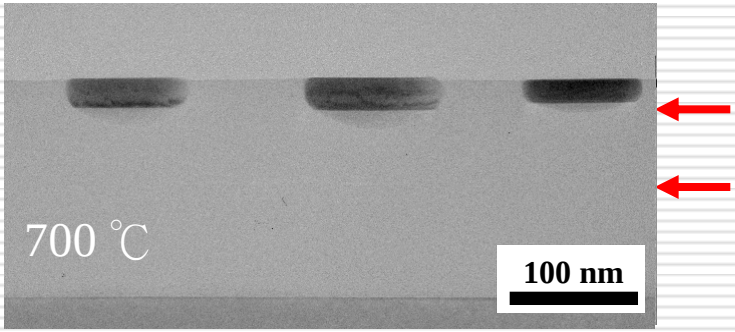

TEM Plane-view image

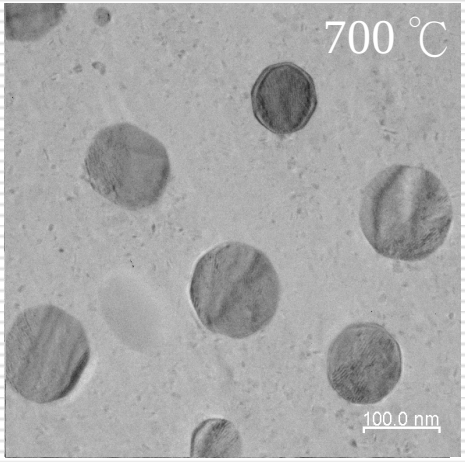

Flattened truncated octahedral NPs

Wulff's construction:

Top view

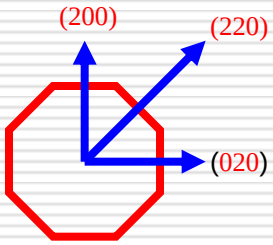

Truncated-octahedron

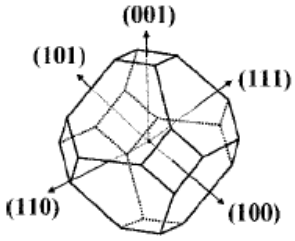

Side view

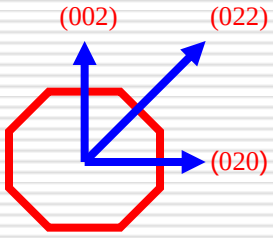

$[Fe/Pt/SiO_2(0.28\ nm)]_{18}$ annealed at 700 ℃ for 2 sec.

TEM plane-view image

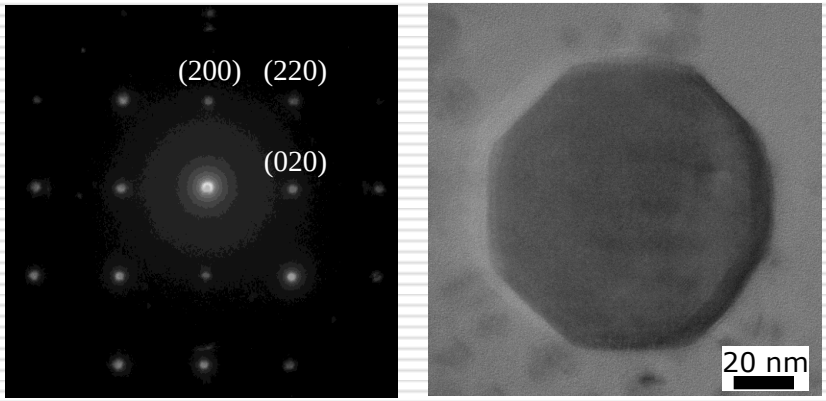

TEM cross-section image

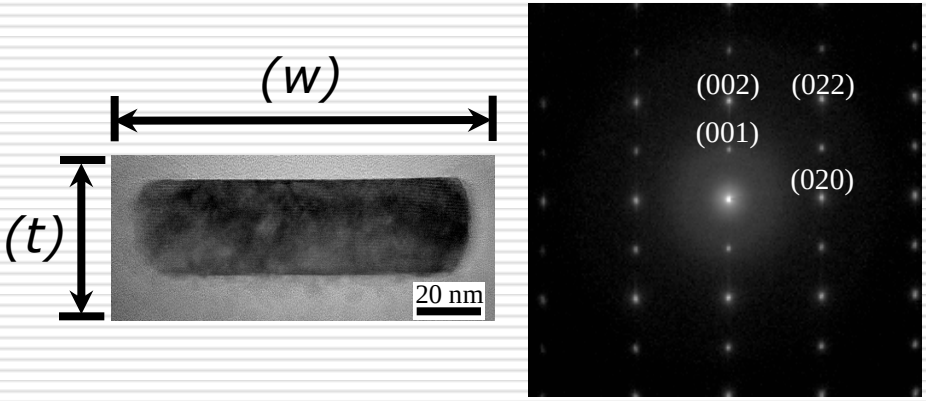

Octagonal nanopariticles

Larger width/thickness ratio

Mechanism of Agglomeration

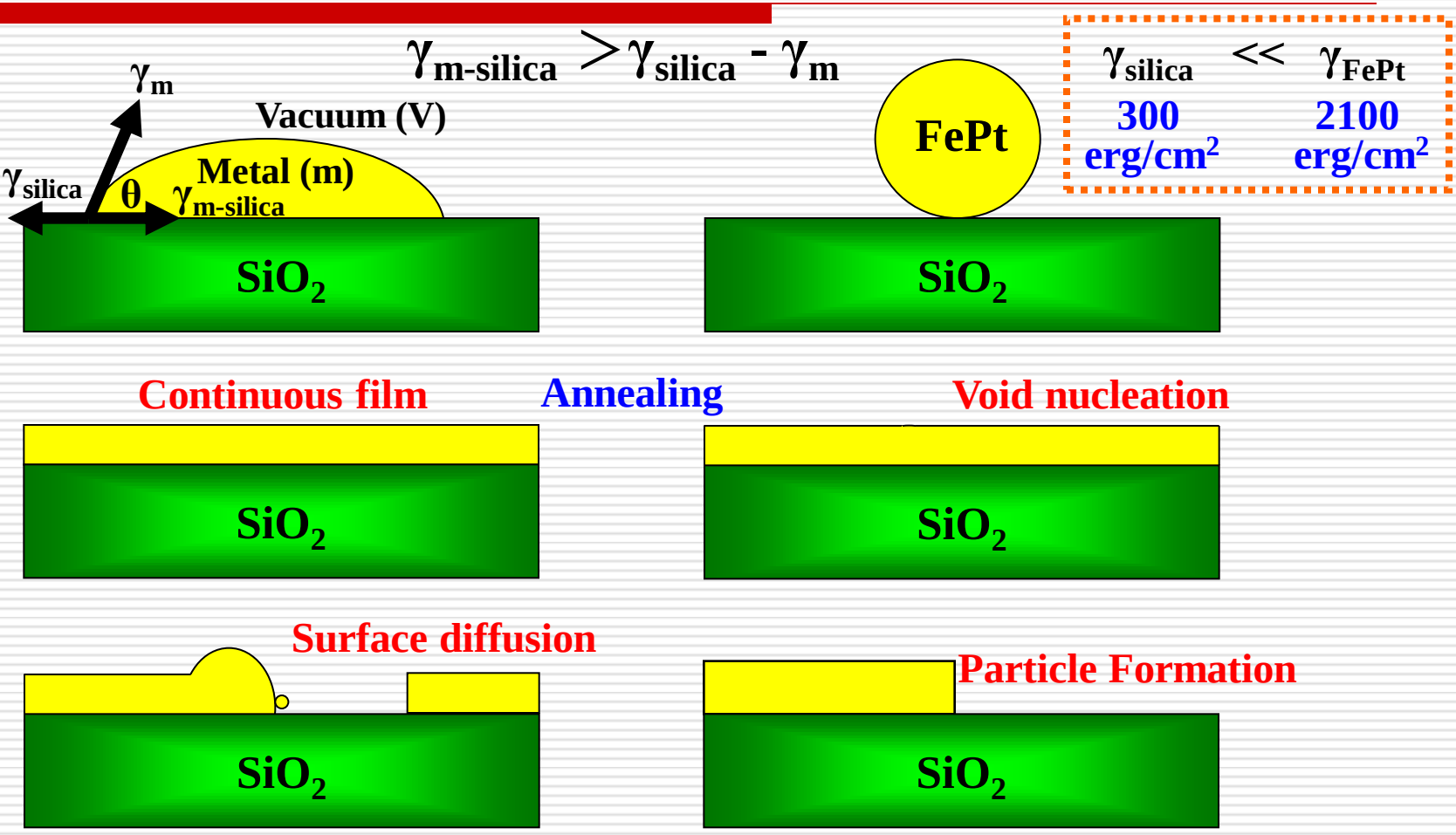

Ultra-high density (001) FePt NPs

[Fe/Pt/SiO_2]$_3$ annealed at 700 °C for 12 hr

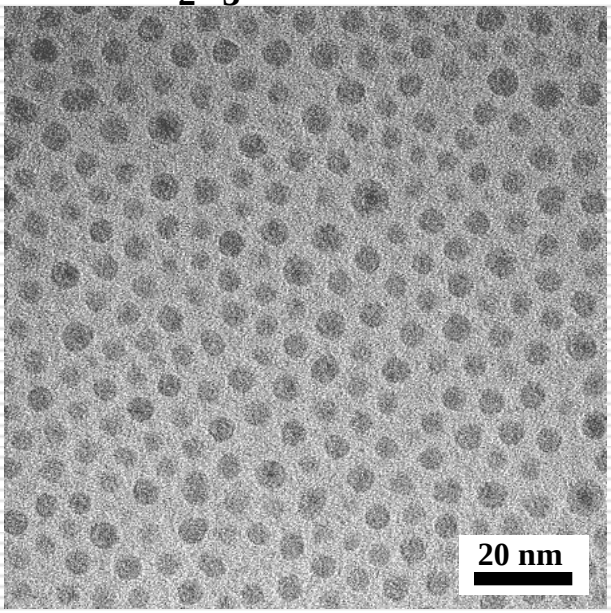

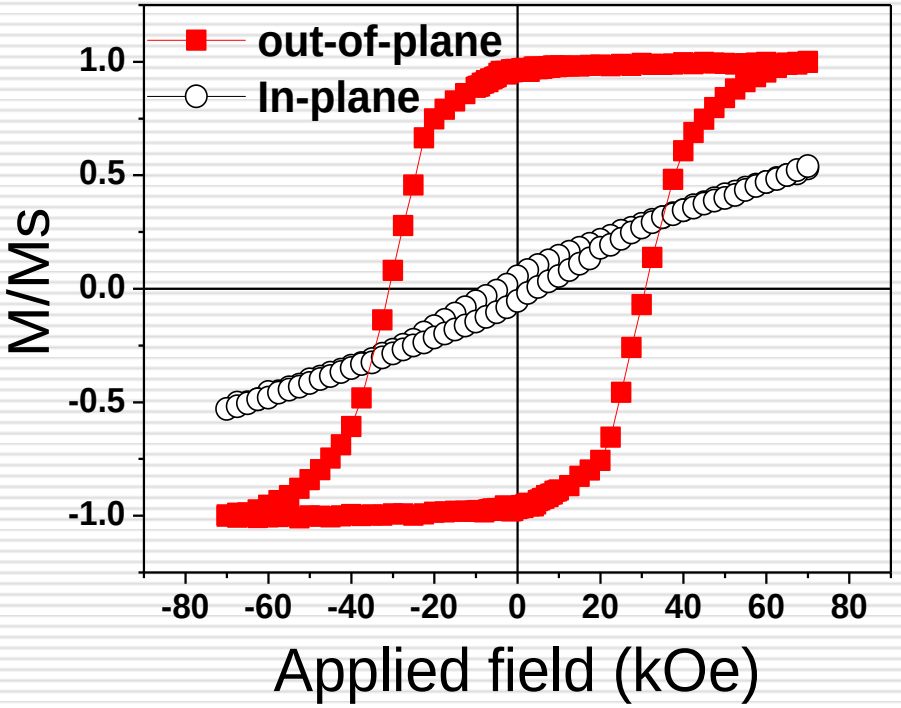

Particle size ~ 5.6 nm

Size distribution ~ 14.1%

Distance ~ 8.3 ± 1.7 nm

Areal density ~ 1.0×10^{13} dots/in.^{2}

H_c ~ 31 kOe

Perpendicular anisotropy

C. H. Lai , APL 2008

Fabrication Process for Self-assembled FePt NPs

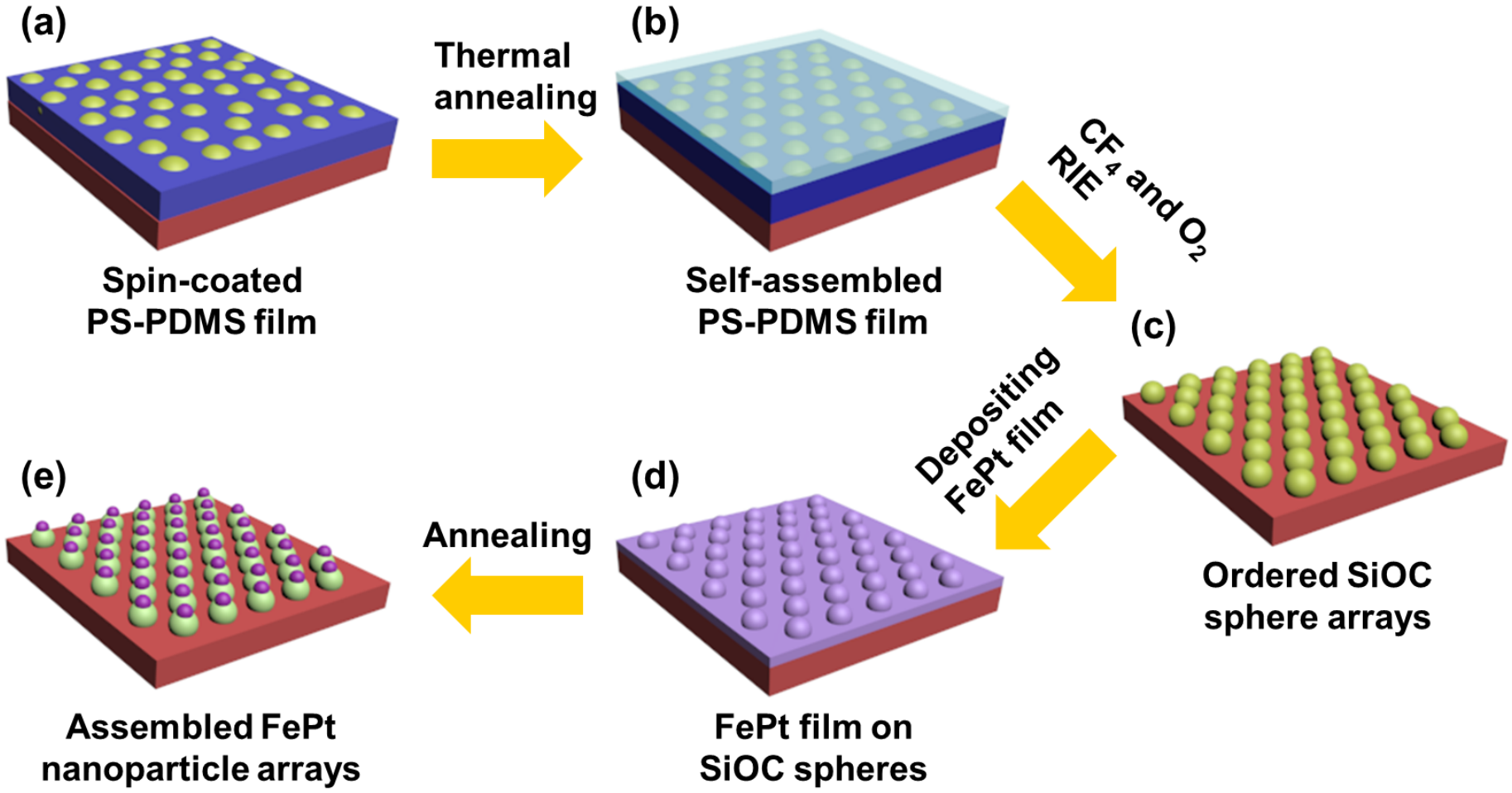

PDMS Spheres after O_2 Treatment

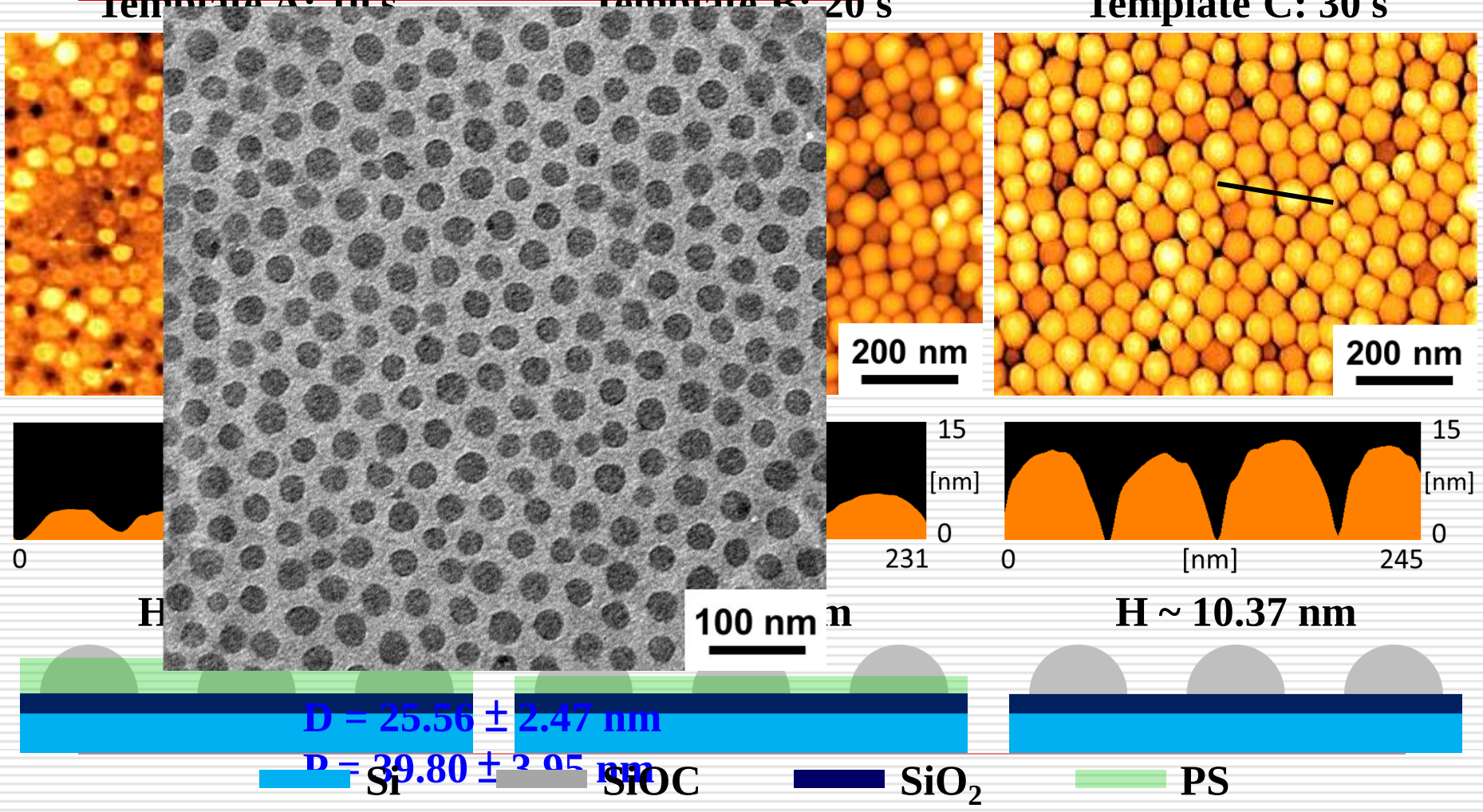

Volcano-shape FePt NPs

FePt on template C (30s)
Annealed at 700 ˚C for 1 min, heating rate of 50 ˚C/s.

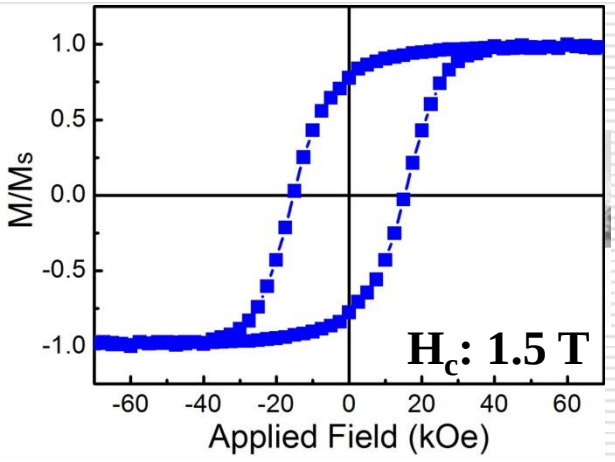

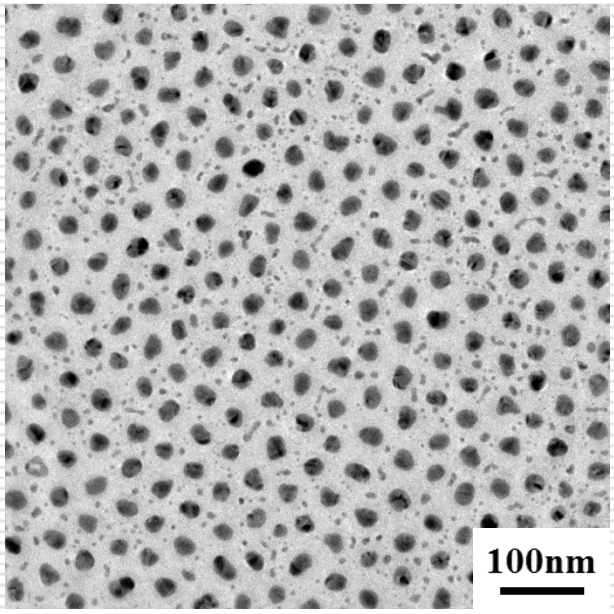

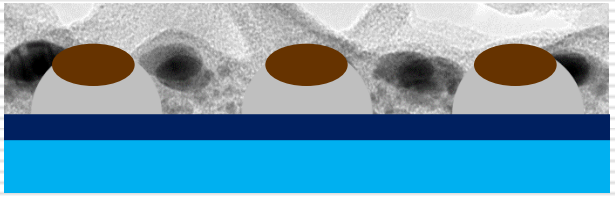

Volcano-shape composite NPs

Mechanism of Nanoparticle Assembly

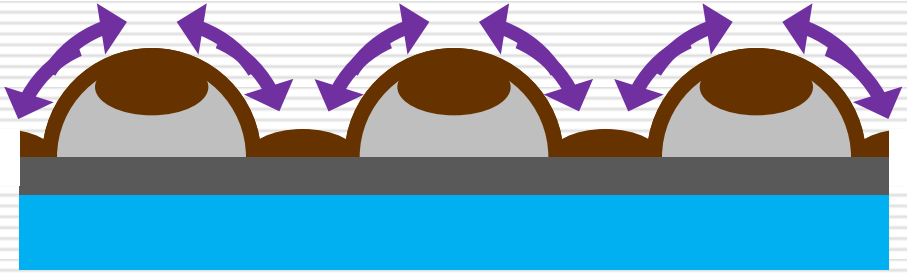

Chemical potential:

$\Delta\mu = \kappa\gamma\Omega + E_s$

κ: local curvature,
γ: surface energy
Ω: atomic volume
***E_s*: strain relaxation energy**

Yang *et al.*, *Phys. Rev. Lett.* 92, 025502 (2004)
Chen *et al.*, *Appl. Phys. Lett.* 93, 083101 (2008)

(II) Nanoparticles and Spintronics Devices:

(A) Fabrication of Fe_3O_4 Nanocubes for MRI contrast agent

Modified Hot-injecting Method

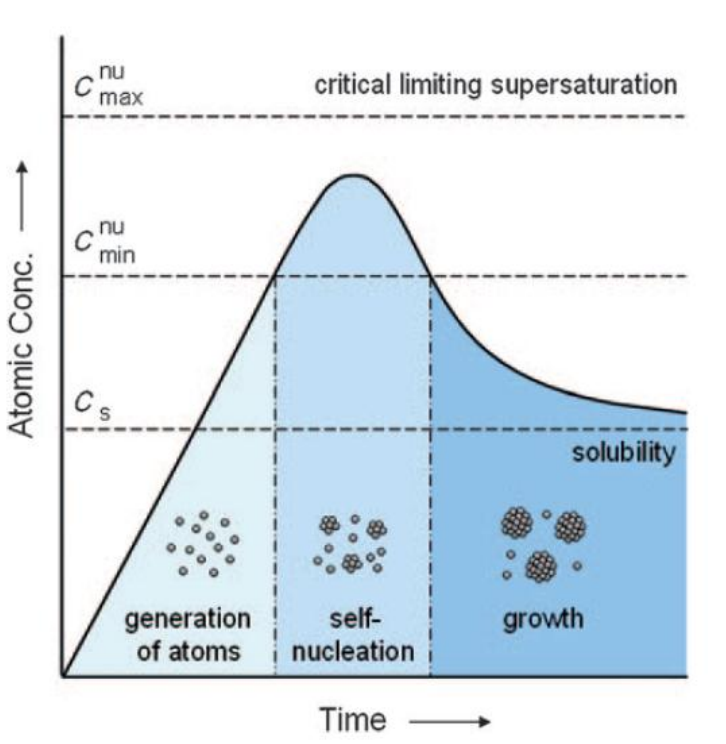

Modified hot-injecting method:

a. Slowly injecting the precursor into hot solution
b. Nucleation and growth are separated
c. The monomer concentration can be controlled

Reaction solution:

Surfactant: oleic acid, oleylamine
Reductant: tetradecanediol
Solvent: Benzyl ether

Precursor solution:

Precursor: $Fe(acac)_3$
Solvent: Benzyl ether

Xia ***Angew. Chem. Int. Ed.***, 2009, 48, 60

Synthesis of Core/Shell Nanocubes

Precursor: 1 mmol
Solvent: 5 ml

Solvent: 15 ml
Surfactant: 40 ul
Reductant: 5 mmol

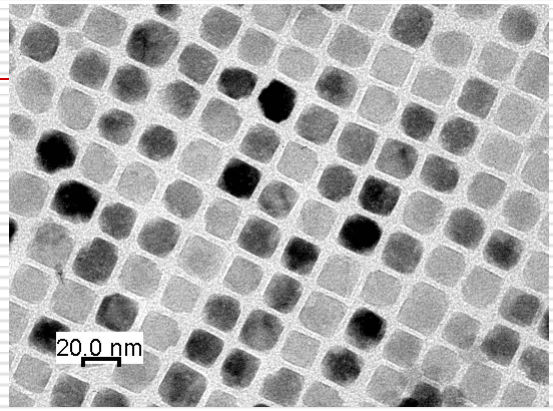

Solvent: 15 ml
Surfactant: 40 ul
Reductant: 5 mmol
Metal/alloy NPs

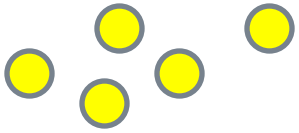

FePt NPs

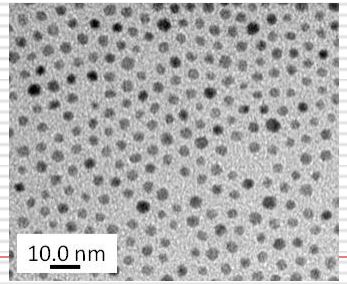

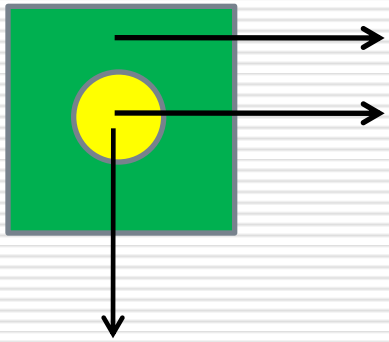

Fe_3O_4 cubic shell

FePt core

FePt core
(disordered phase)

Structure analysis

Avg. size: 16.1 ± 0.9 nm

Avg. size: 14.7 ± 1.1 nm

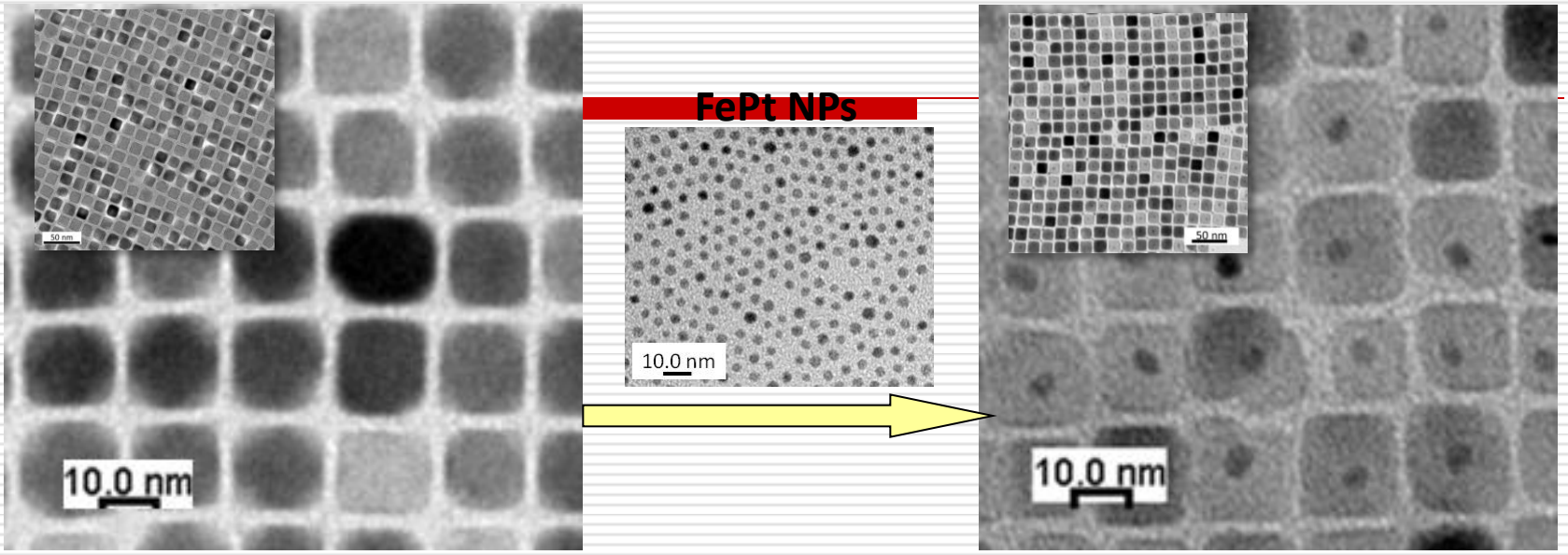

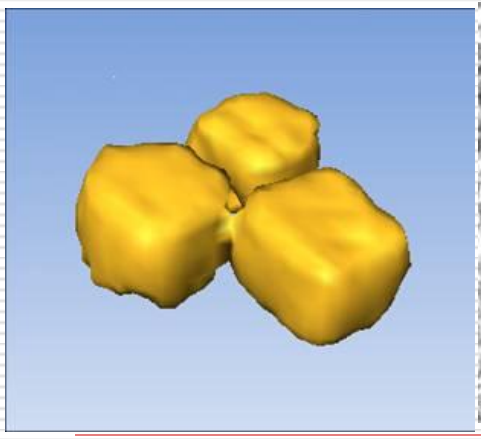

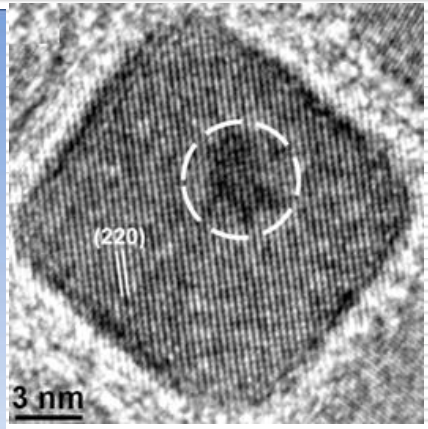

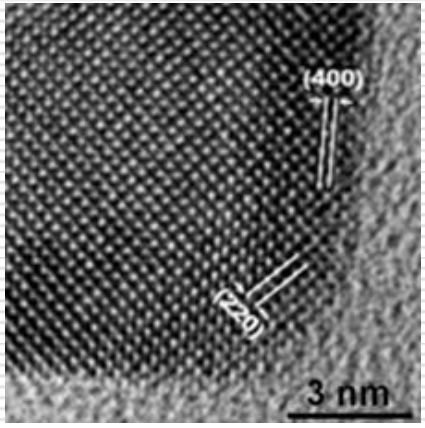

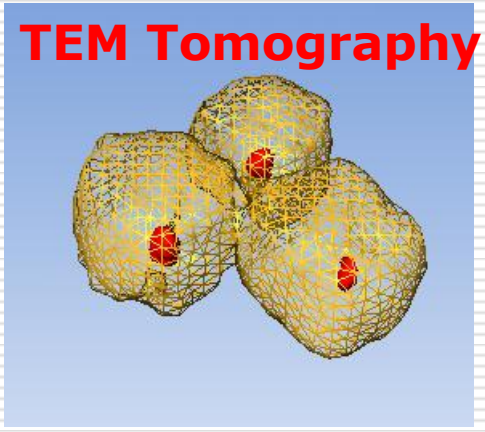

XMCD for Fe_3O_4

- Inverse spinel structure:
  $Fe^{3+}{}_A(Fe^{2+}Fe^{3+})_BO_4$
- A: tetrahedral site, Td
- B: octahedral site, Oh
- Spin arrangement:
  $(Fe^{3+}\downarrow)_A(Fe^{2+}\uparrow Fe^{3+}\uparrow)_BO_4$

  ➔ $4\mu_B$ /u.c.

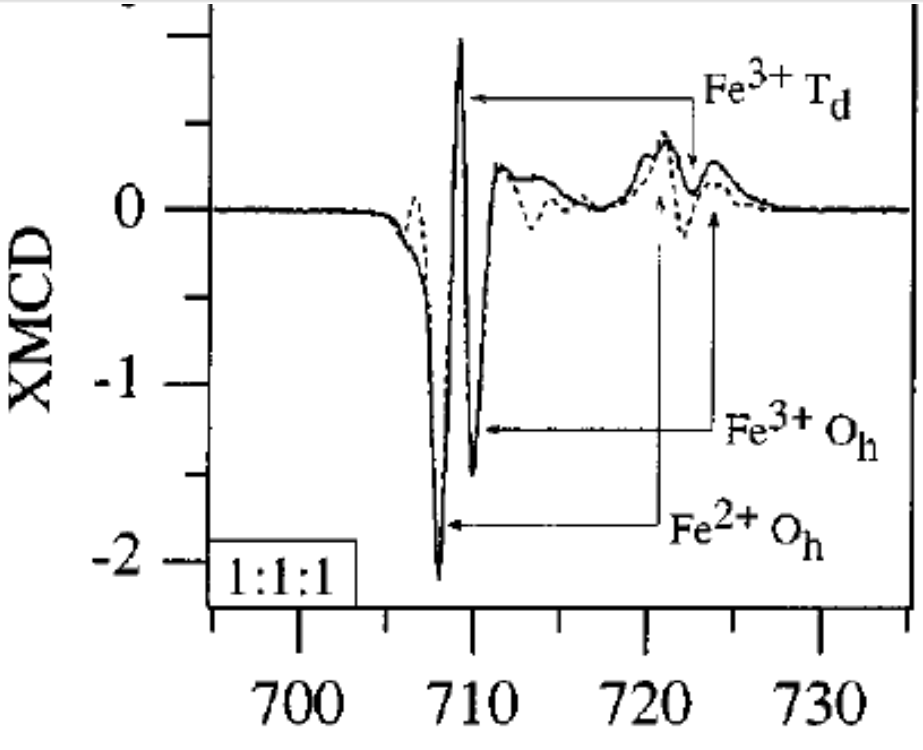

XMCD Measurements: shape effects

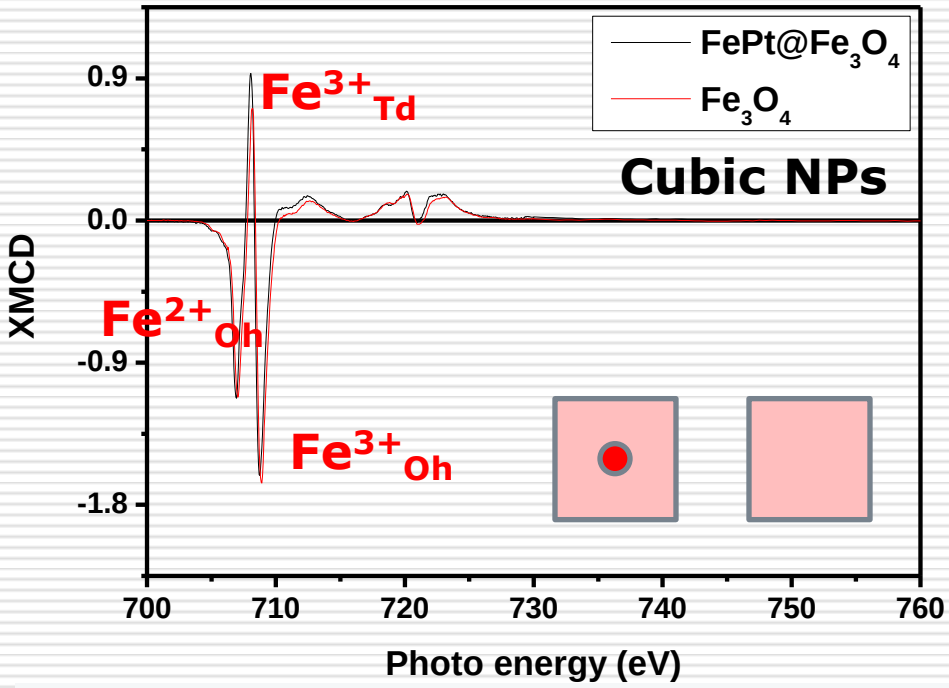

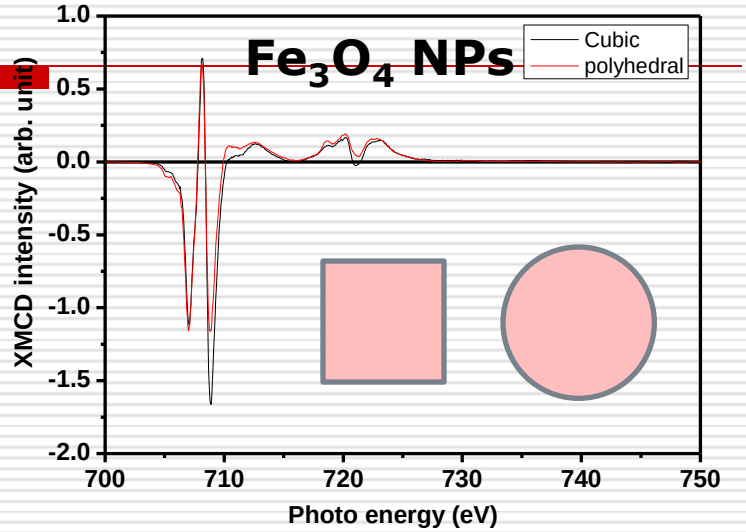

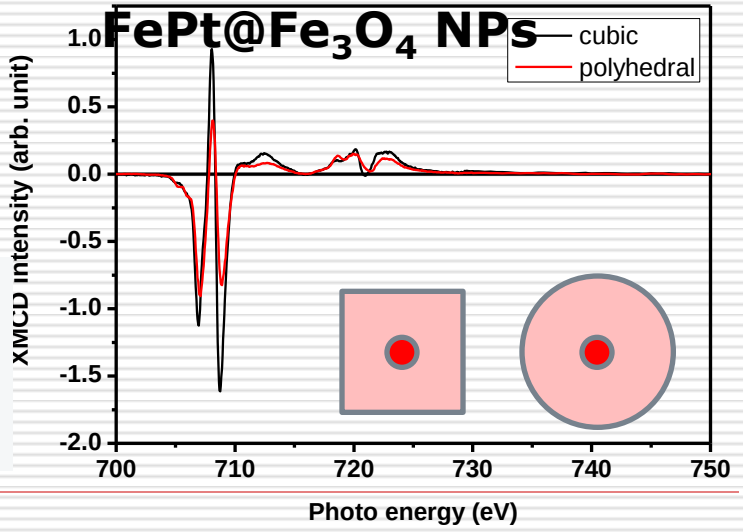

The Fe^{3+} is more stable at the octahedral sites when the shape of Fe_3O_4 NPs becomes cubic.

Ho & Lai Chem. Mater. 2011, 23, 1753–1760

MRI

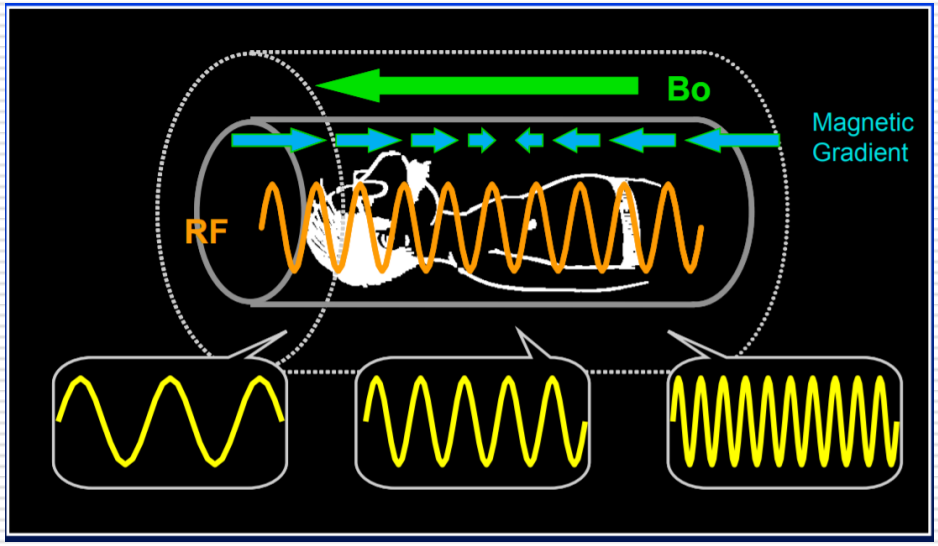

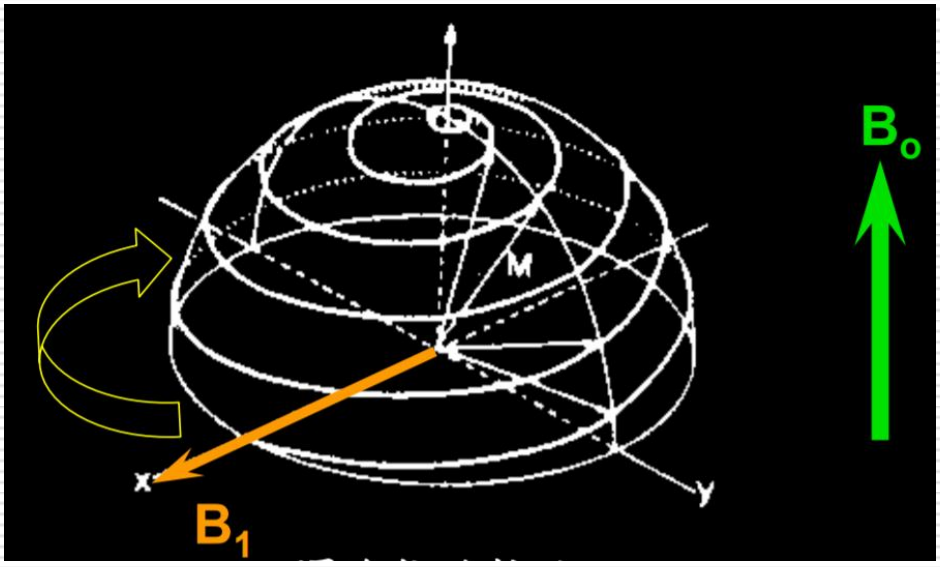

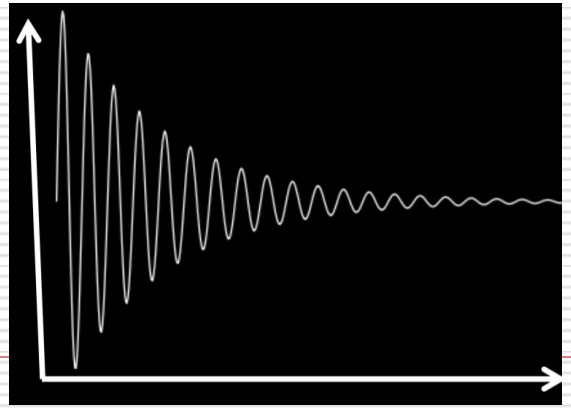

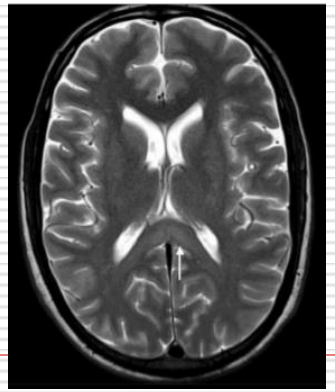

Iron oxide for MRI application

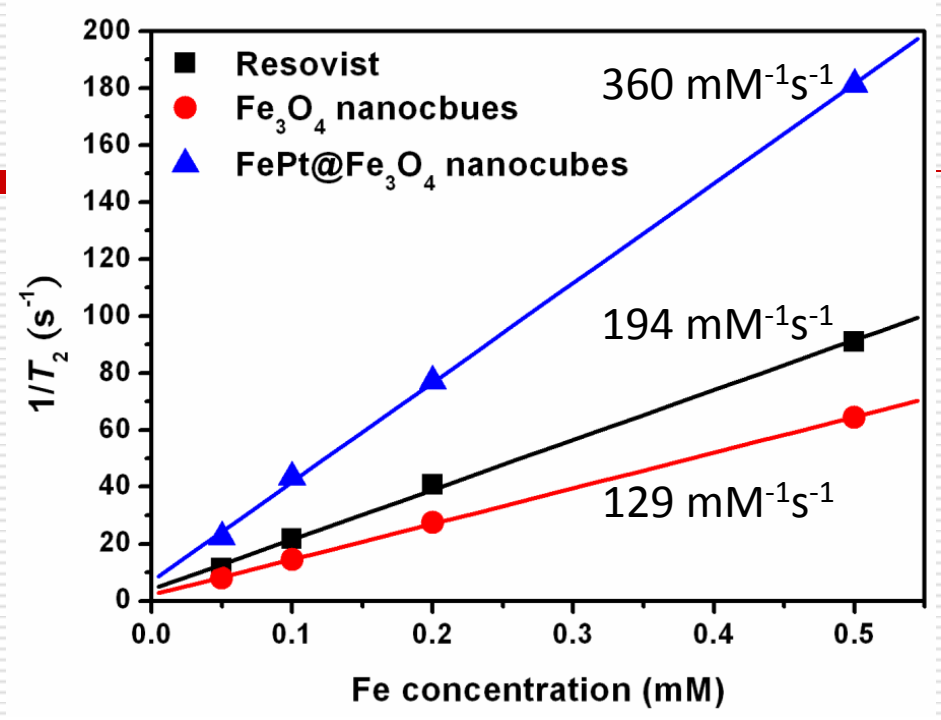

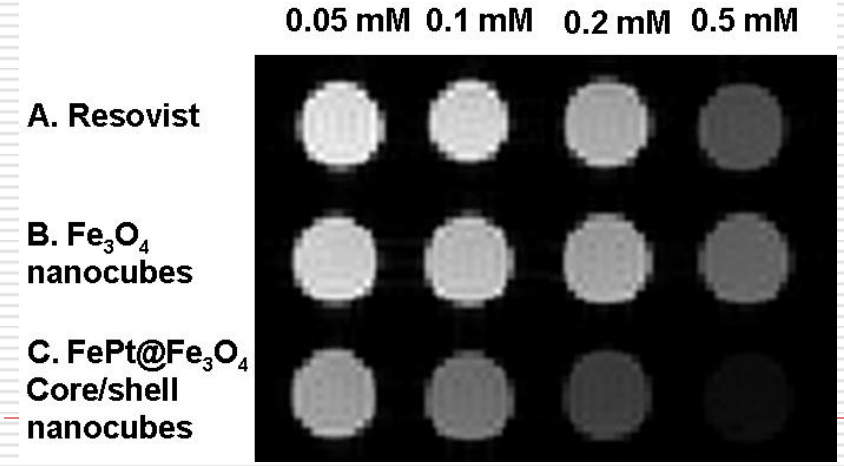

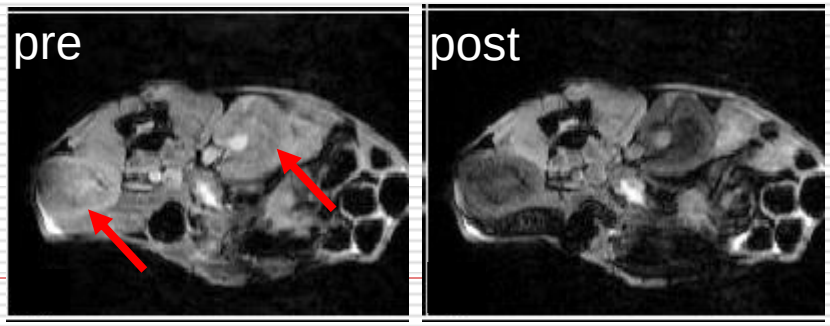

Relaxivity

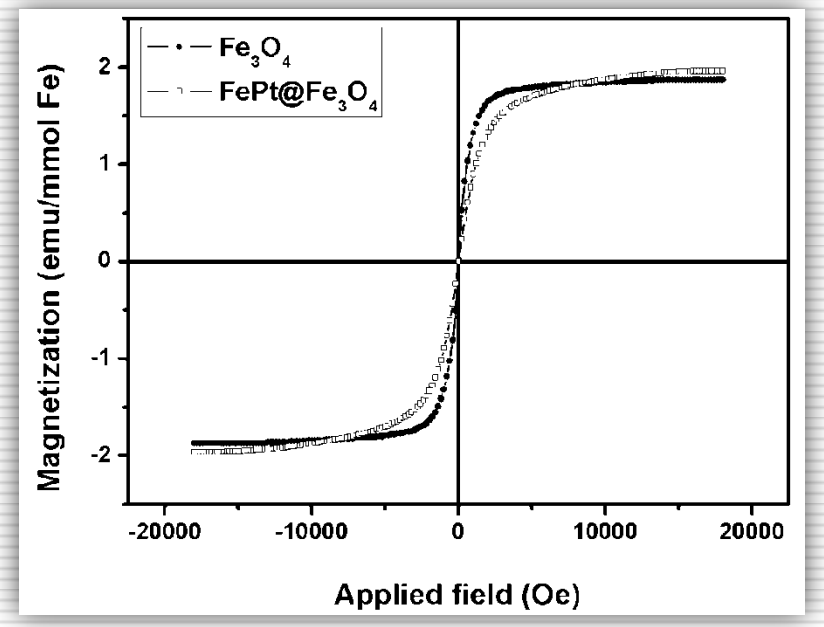

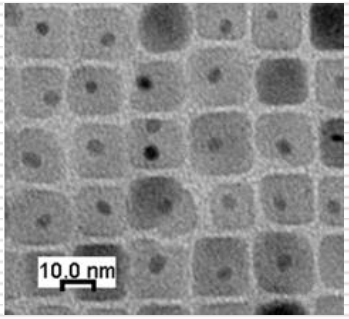

14.7 nm ± 1.1 nm

r_2 = 360 $mM^{-1}s^{-1}$

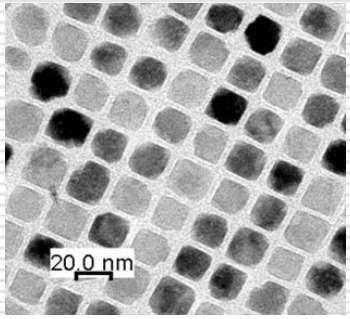

16.1 nm ± 0.9 nm

r_2 = 129 $mM^{-1}s^{-1}$

for single particle $r_2 = (256\pi^2\gamma^2/405)\kappa M_s^2 r^2 / D(1 + L/r)$

for many particles Interaction among particles ?

Interaction between NPs

Electron Holography

IONP

FePt@IONP

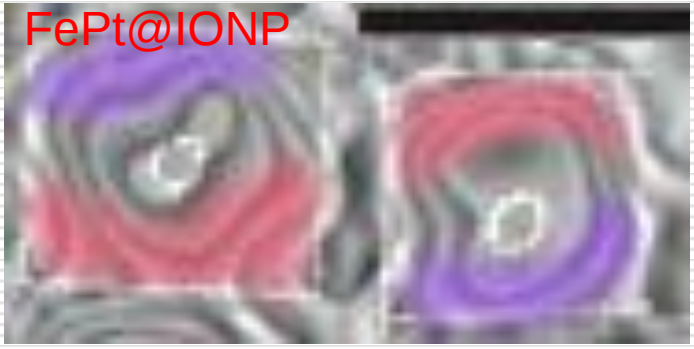

OOMMF simulation (remanent state)

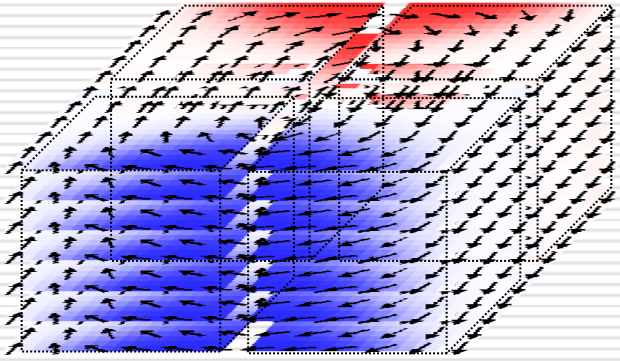

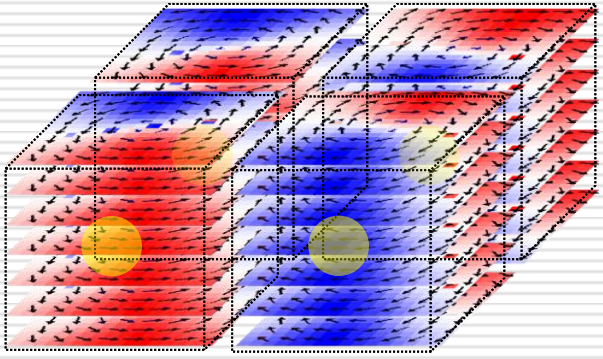

Interaction between NPs by Small-Angle Neutron Scattering (SANS)

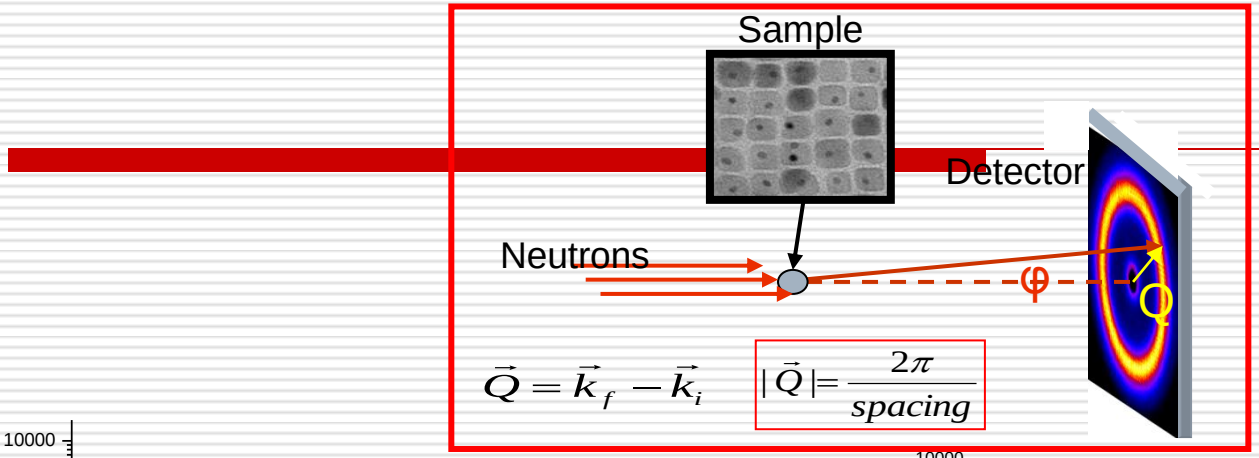

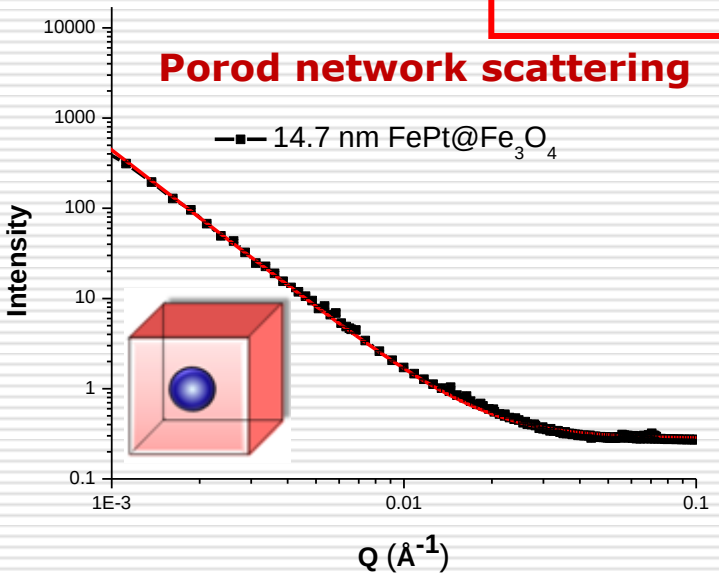

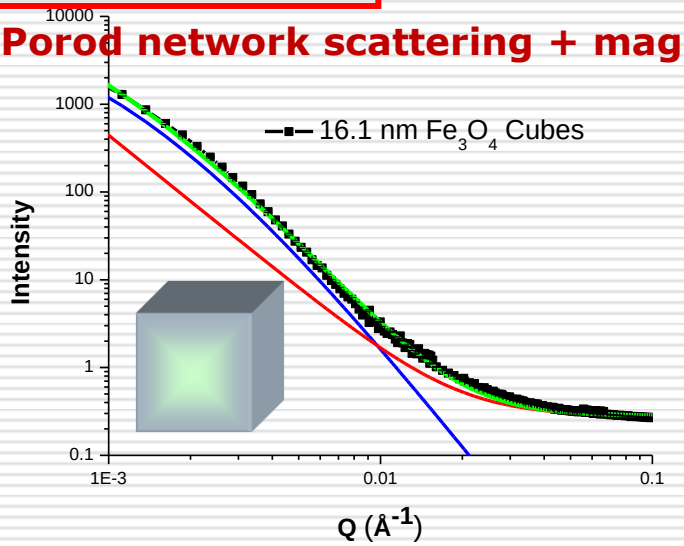

1. Both samples display same Porod "network" scattering ($Q^{-2.5}$ curve).

2. Fe_3O_4 cubes display additional "hump" that is consistent with magnetic clusters of approx. 5-8 cubes across

Arrangements of NPs by magnetic fields

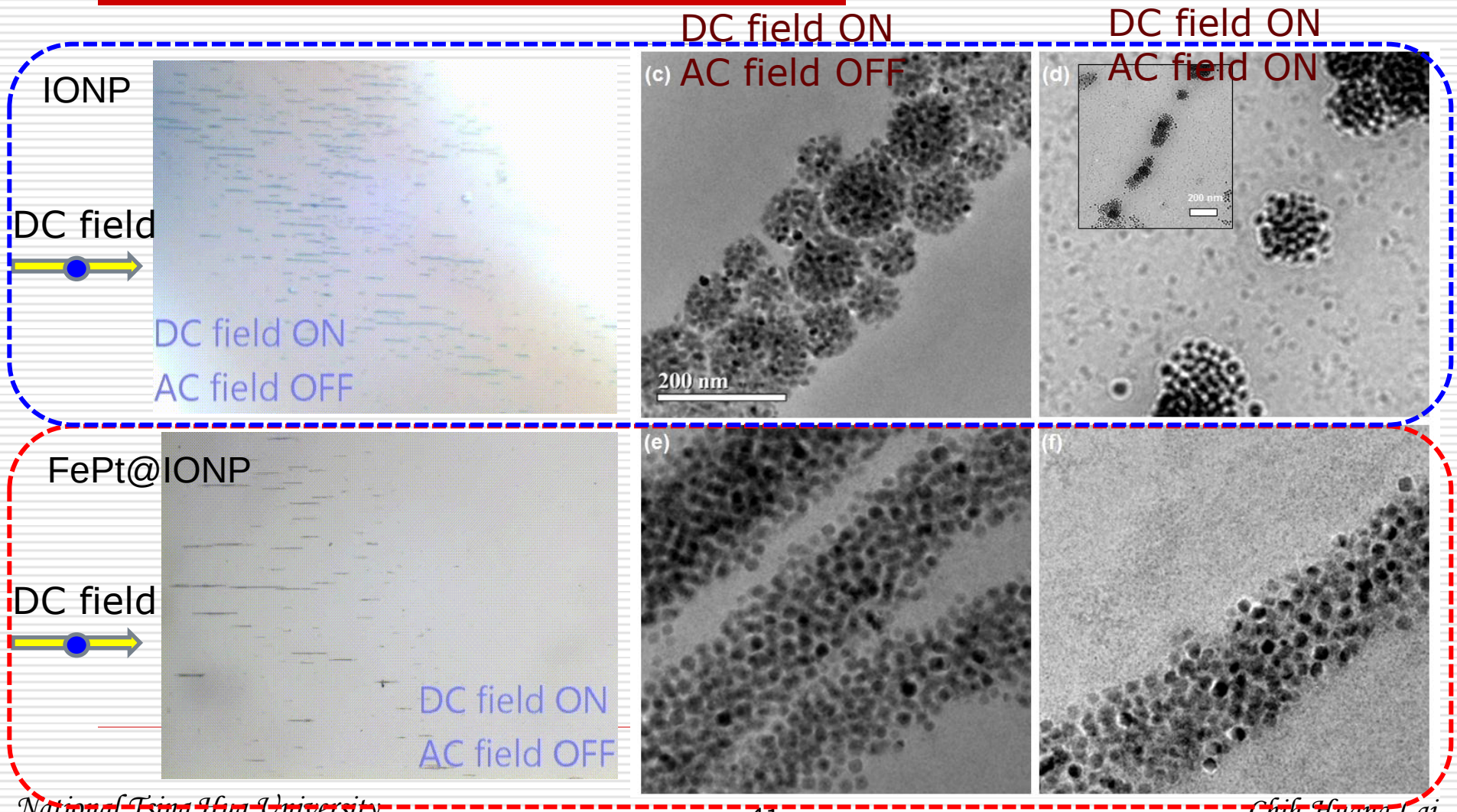

Dipole filed generated by NPs

1. Reduced dipolar interaction in zero field helps the circulation of NPs in the bloodstream.

2. Under a strong DC field, the FePt core is strongly aligned by the DC field such that the NPs chains are not disturbed by the applied AC pulse field.

3. The chain configuration reveals a stronger dipolar field around the chain, which corresponds to a faster dephasing of the proton and therefore an enhancement of the MRI performance.

Monte Carlo simulations

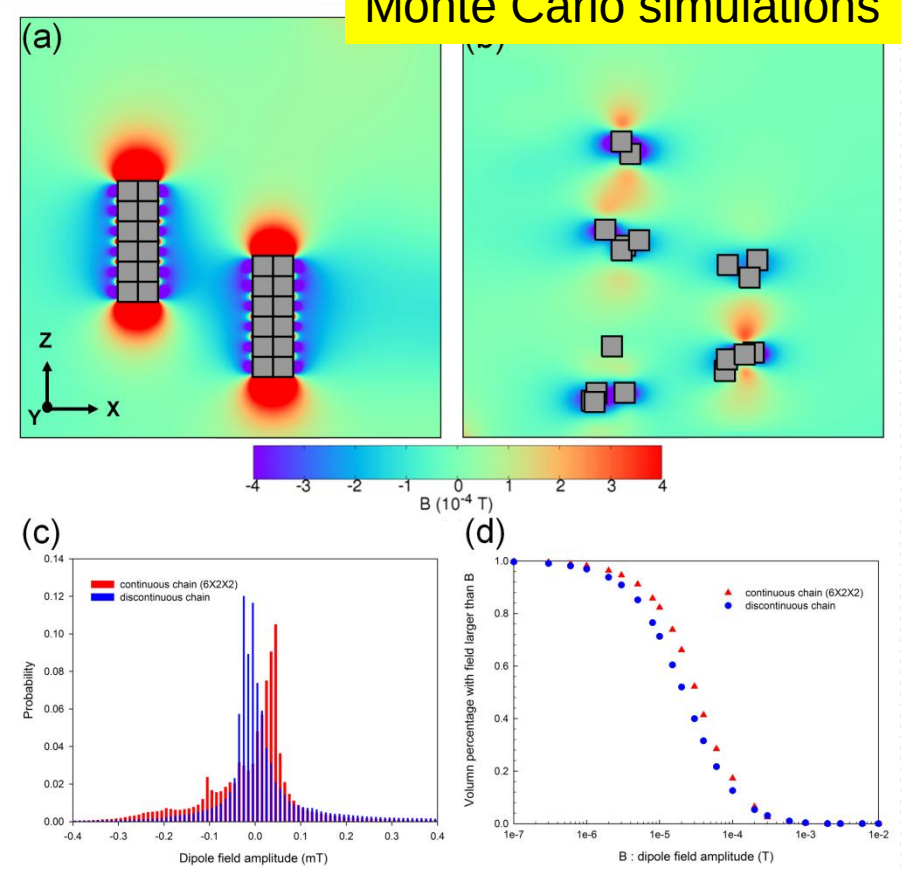

Yang and Lai, Adv. Mater. 2018, 1802444

(II) Nanoparticles and Spintronics Devices:

(B) SOT in multilayers

SOT in (Pt/Co) multilayers

[HM/FM]

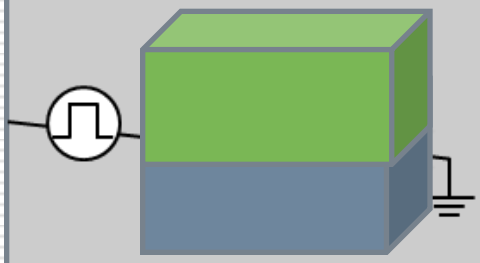

[Pt/Co]

Multilayer

$[HM/FM]_N$

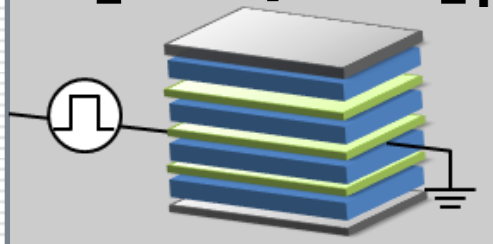

$[Pt/Co]_N$

Effective fields induced by Spin-orbit torque in Co/Pt MLs

- Spin Hall effect dominated ($\Delta H_L >> \Delta H_T$)
- Spin-orbit torque efficiency increases with increasing repeating layers.

sub./ Ta (2.5 nm)/[Pt (2 nm)/ Co (0.9 nm)]$_N$/ Pt (2 nm)

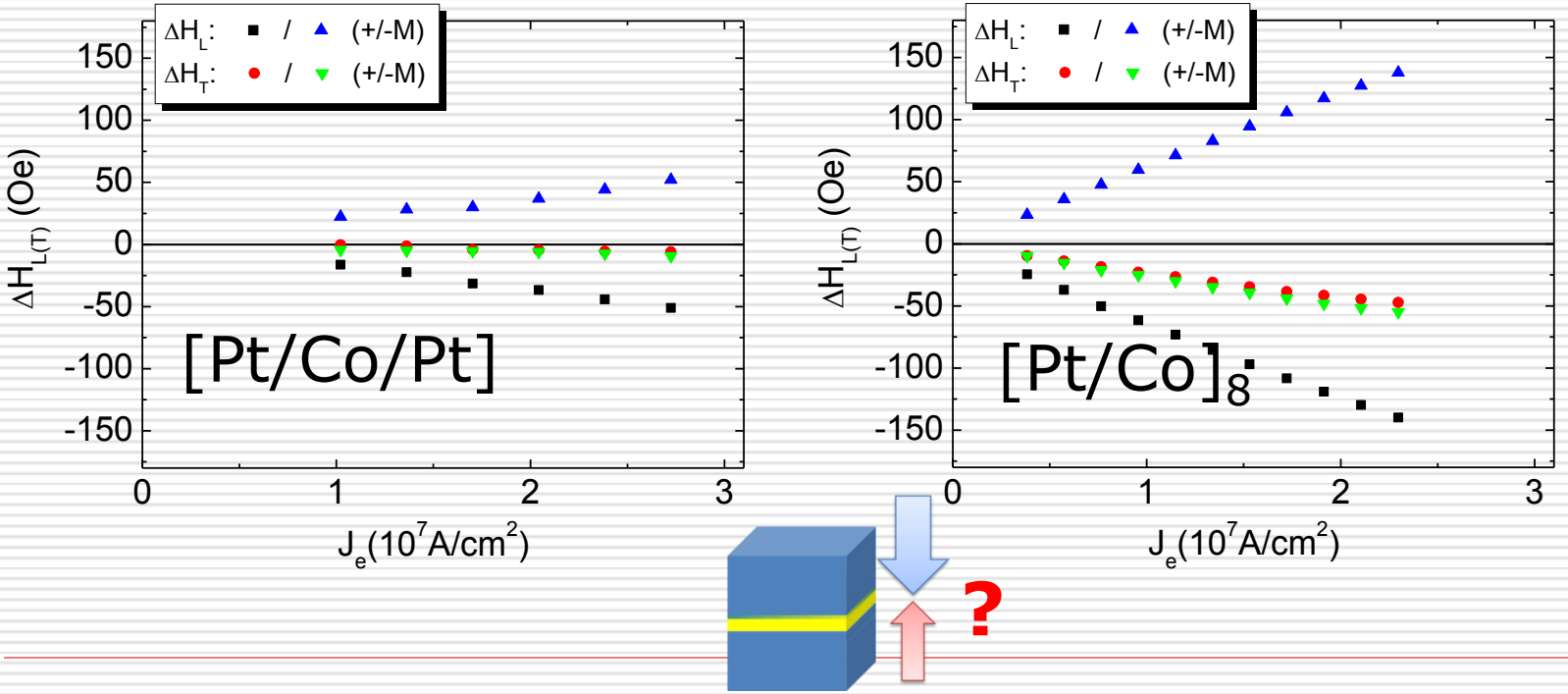

Huang and Lai, APL, 107, 232407(2015)

Net spin current in symmetric tri-layers

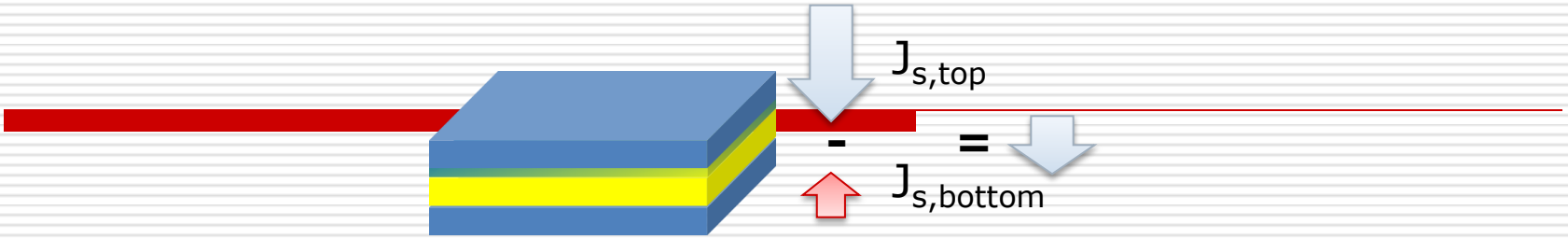

Different interface structure

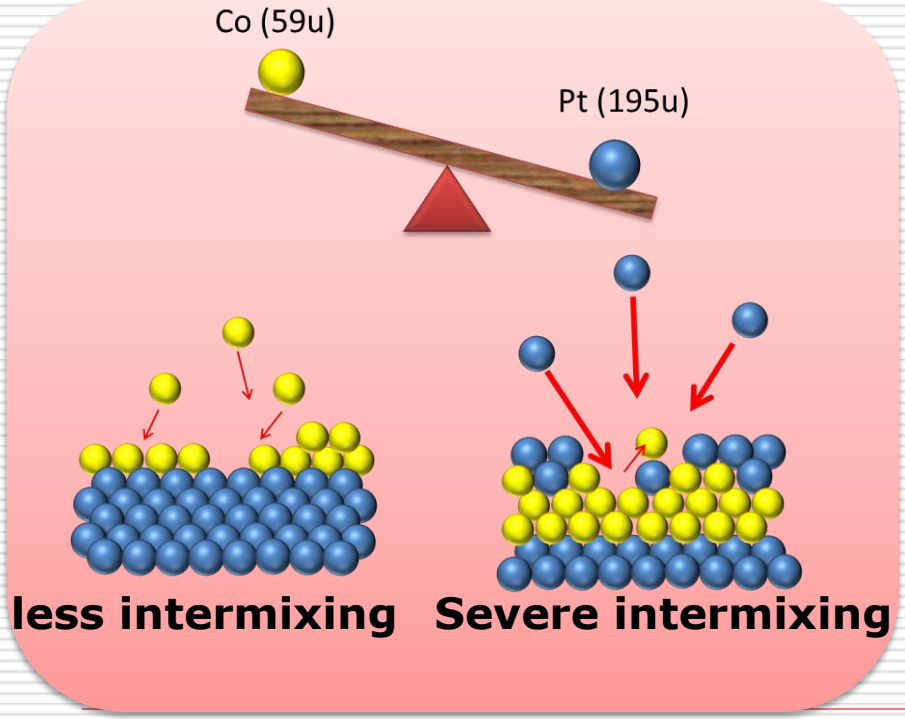

Different Spin current transparency

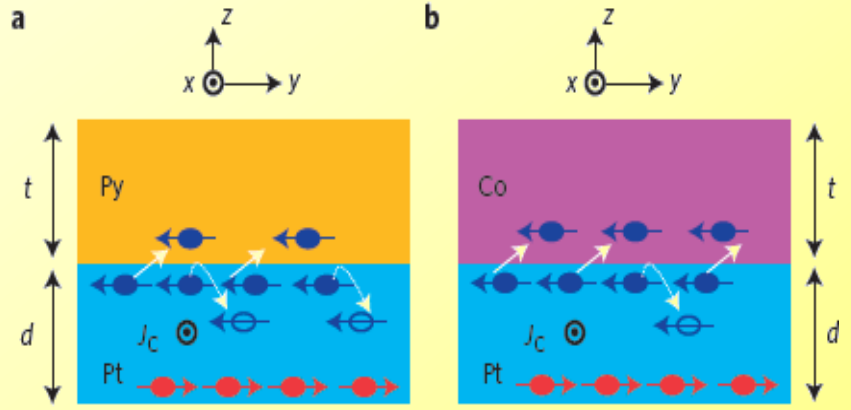

Lower transparency Higher transparency

Nature Physics **11**, 496-502 (2015)

Huang and Lai, Appl Phys Lett **100**, 142410 (2012).

SOT-driven switching in Co/Pt multilayers

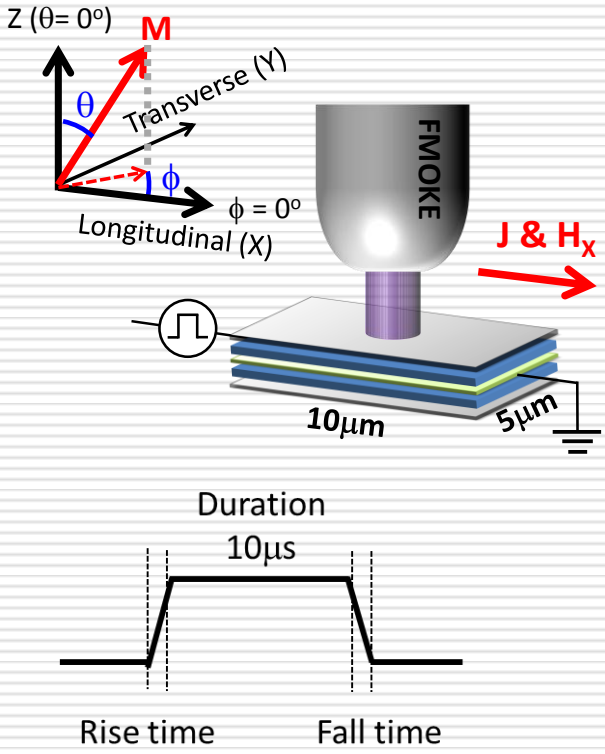

Pulses: Rise/Fall time: 20 ns

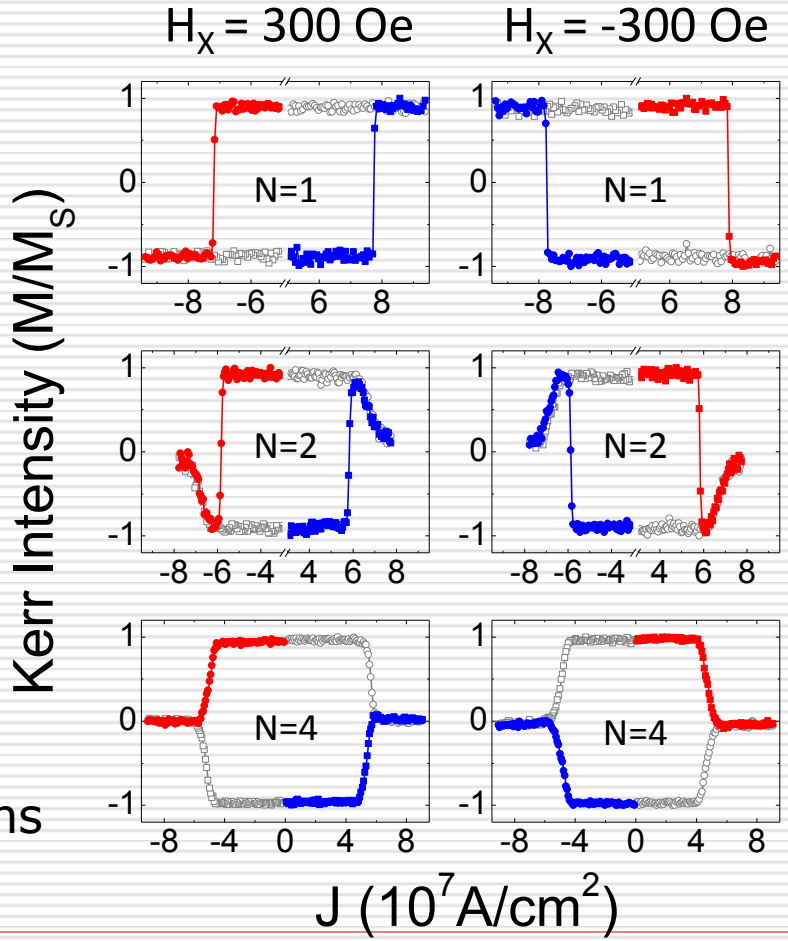

Binary switching

Continuously changed M

Demagnetization state

Initialization-free SOT switching for N=2

- Resultant magnetization converged when $J>J_c$
- Magnetization can be tuned solely by the electric pulse
- Initial state independent ➔ Initialization free for multilevel

Randomly write pulse sequence

(5.5~9x10^{7}A/cm^2 ; Duration : 100ns) Jc:6.9x10^{7}A/cm^2

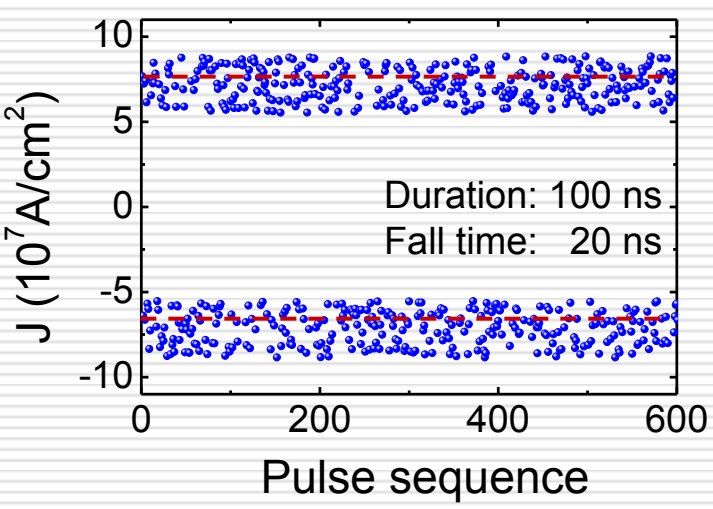

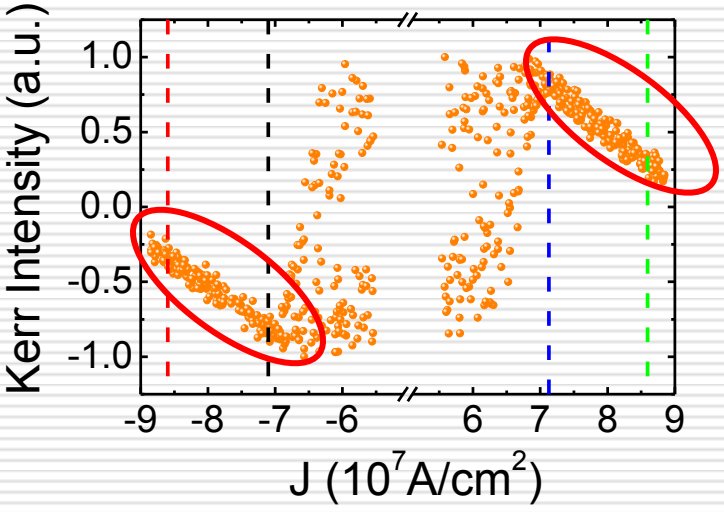

Initialization-free multilevel states

- 4 different states are written without initialization step

4-level read/write test

(Duration : 100 ns)

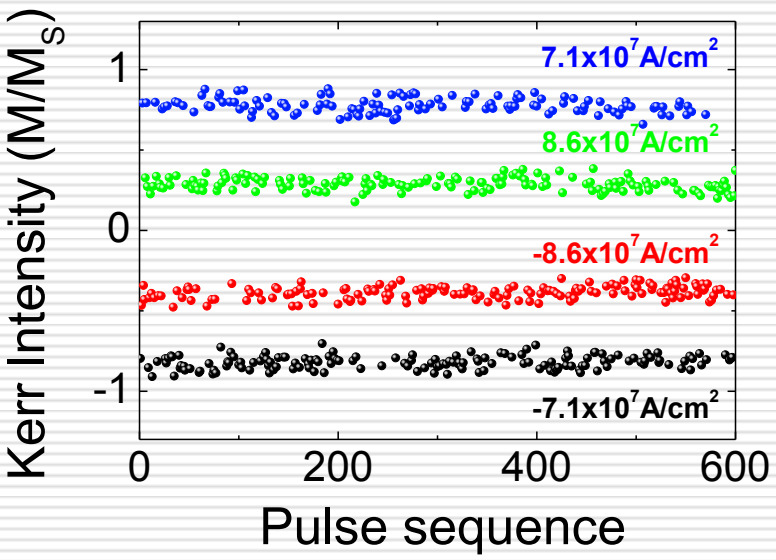

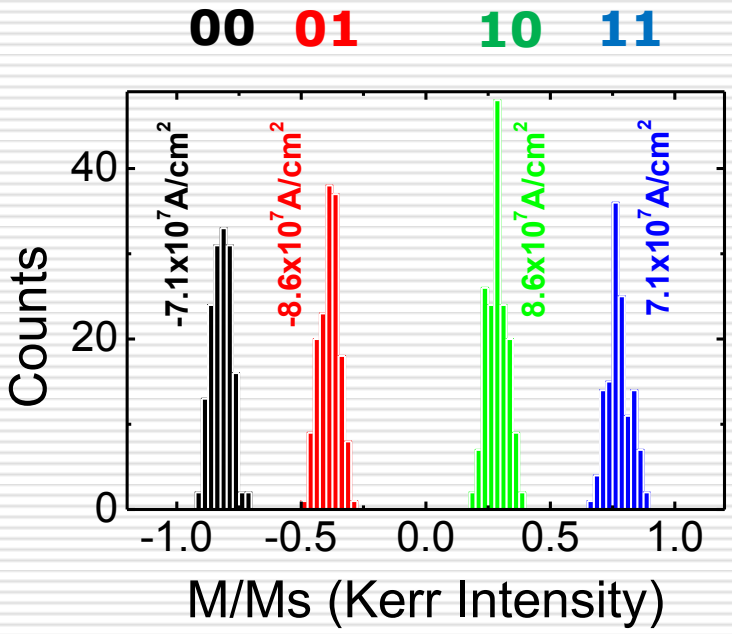

Huang and Lai, Adv. Mater. **29**, 1601575 (2017)

Self-organized domain structure during magnetic relaxation

Initial State

Dipolar interaction

Intermediate State

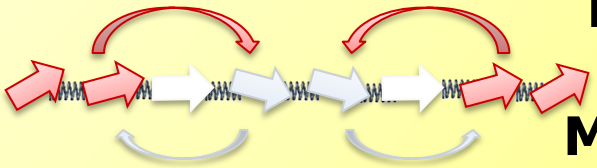

Exchange energy

Domain wall energy E_{DM} v.s. Magnetostatic energy E_{MS}

Final State

Multi-domain formation

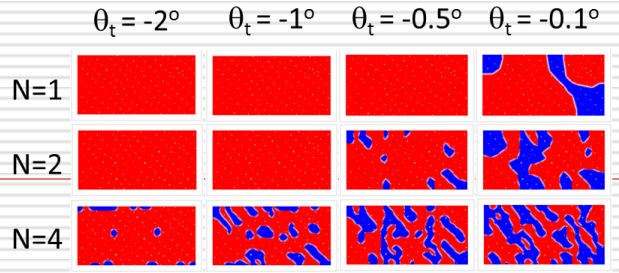

M_s*t (N) ⇧ → E_{MS} ⇧

Multi-level: a statistical consequence after magnetization relaxation

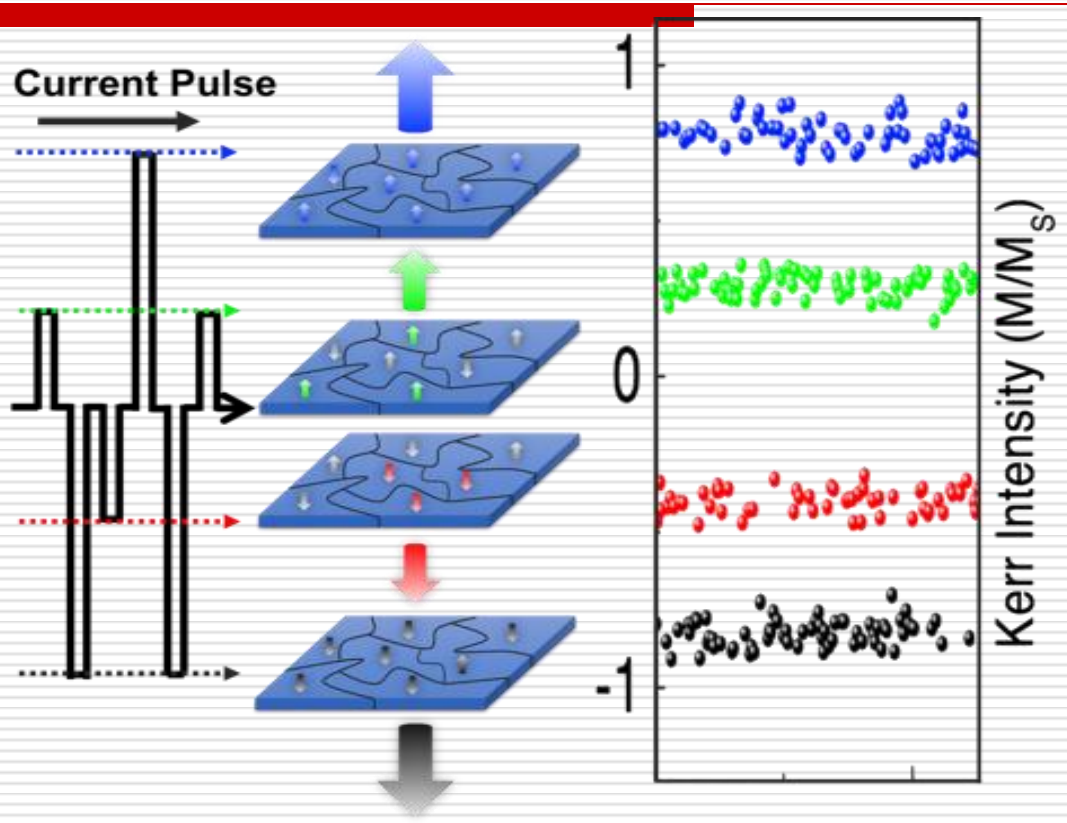

No requirement for the domain patterns to be the same at the microscopic scale for each SOT switching.

SOT switching curve for HM/FM/AFM

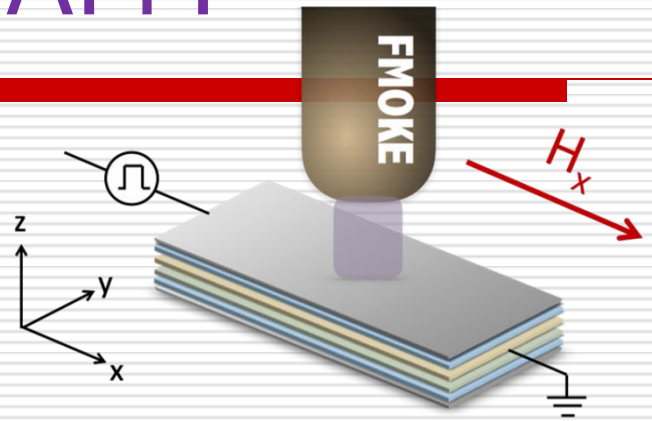

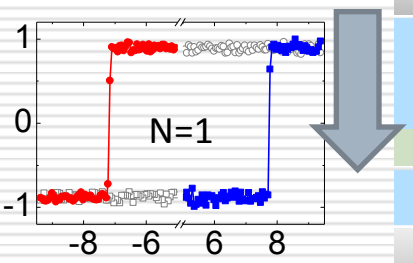

Ta 2.5
Pt 4
Co 1.2
Pt 2
Ta 2.5

Device: 5×10 μm² Hx= 300 Oe

Ta 2.5
Pt 4
IrMn 8
Co 1.2
Pt 2
Ta 2.5

Js

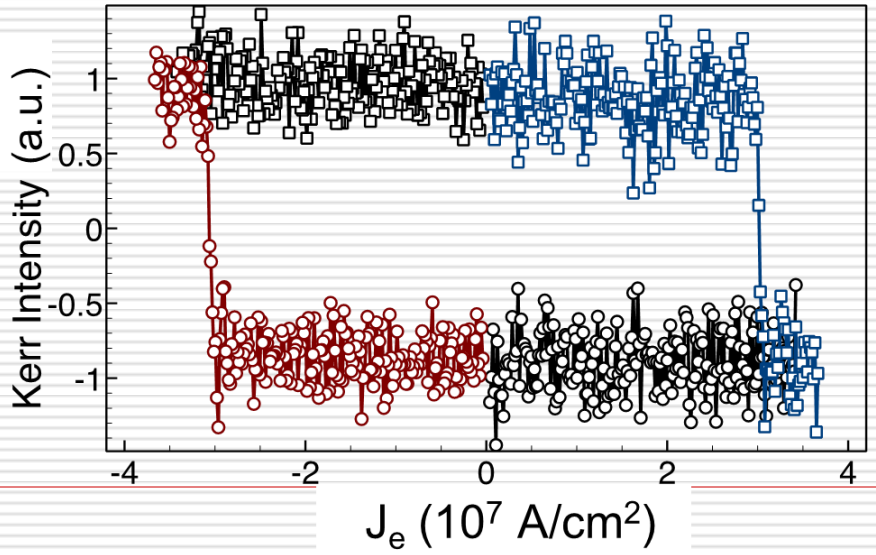

Dominant spin current source with different t_{IrMn}

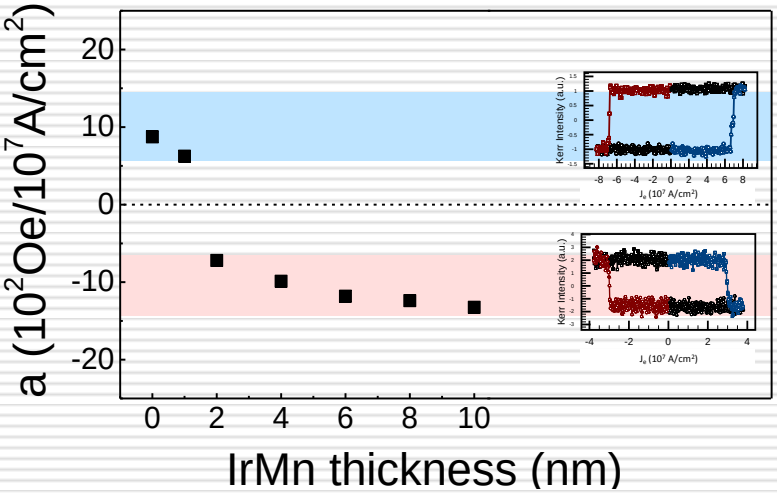

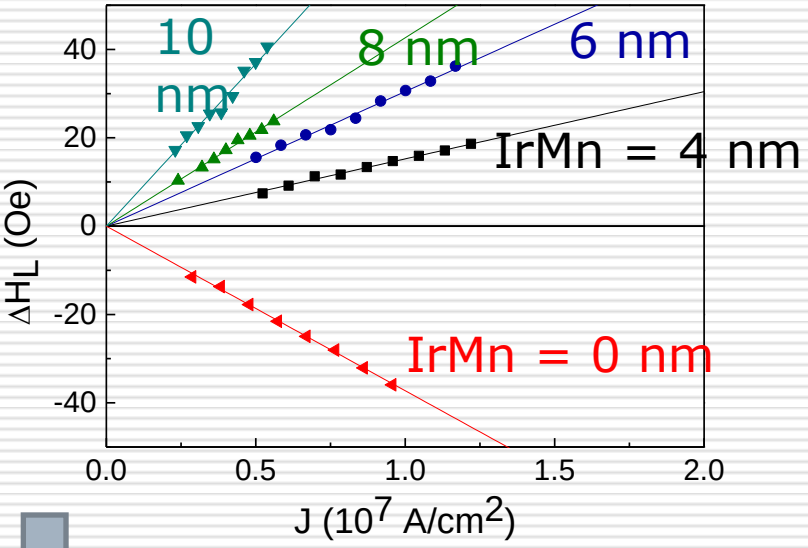

SOT efficiency

$\alpha = H_K / J_c$

H_K :anisotropy field

J_c :threshold current density

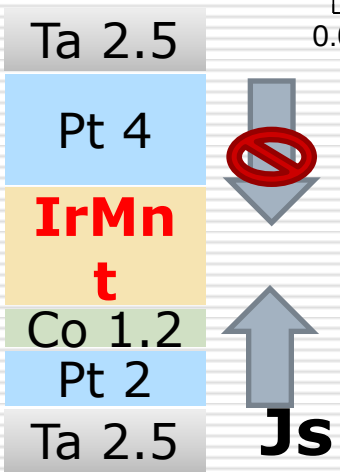

Current-pulse-induced EB switching

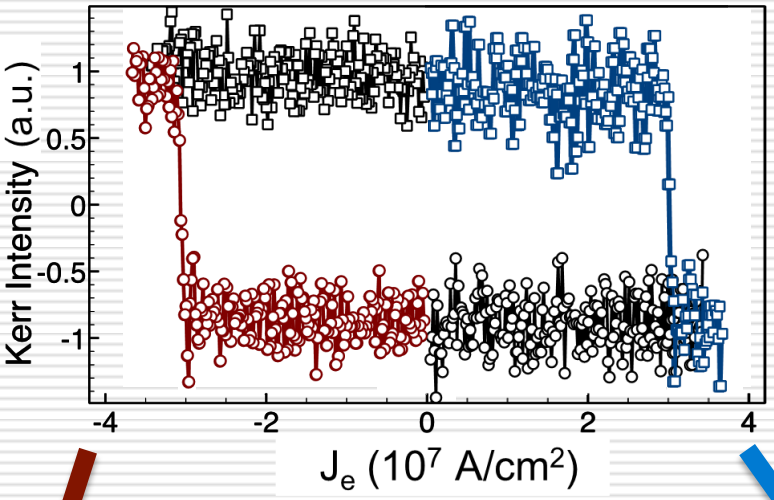

Initial EB

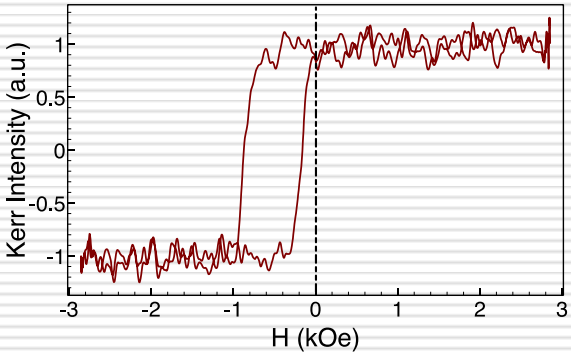

After -I SOT switching

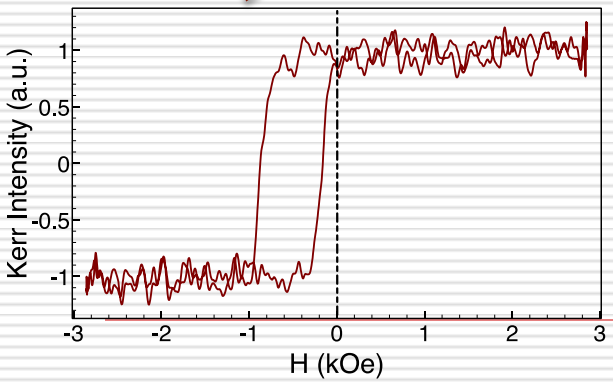

After +I SOT switching

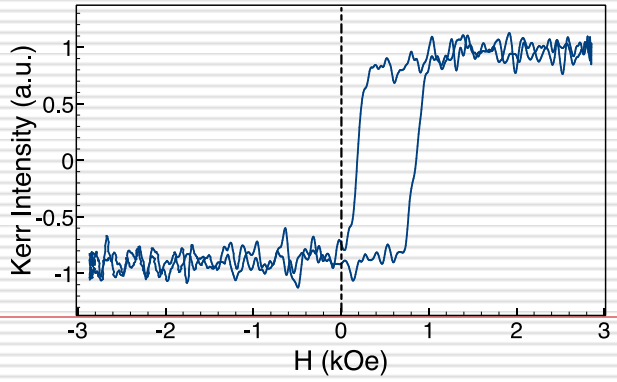

Lin and Lai, Nature Materials, **18**, 335 (2019)

(II) Nanoparticles and Spintronics Devices:

(c) Phase Transformation

NiMn structure

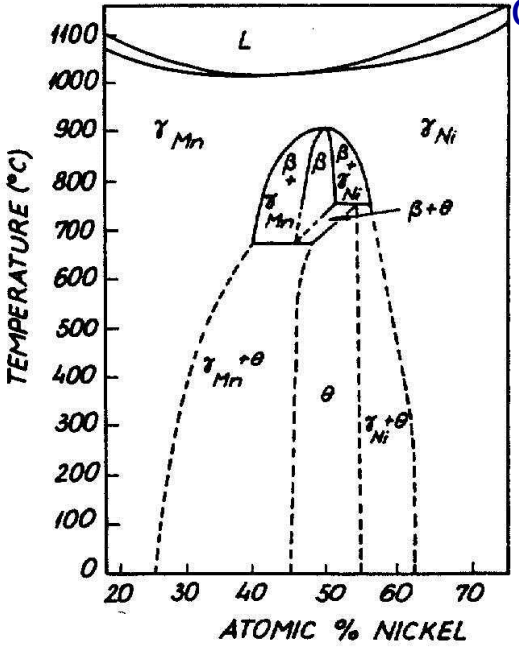

disordered, f.c.c. (γ phase)

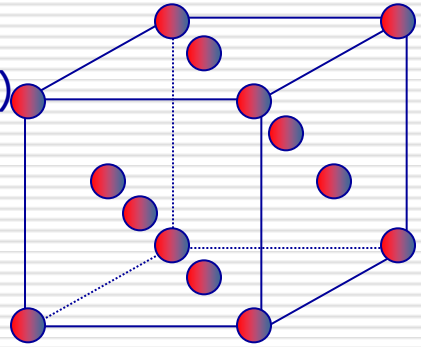

a=3.65Å

(as-deposit, **paramagnetic**)

ordered, $L1_0$ (θ phase)

- Mn
- Ni
- ⟶ spins

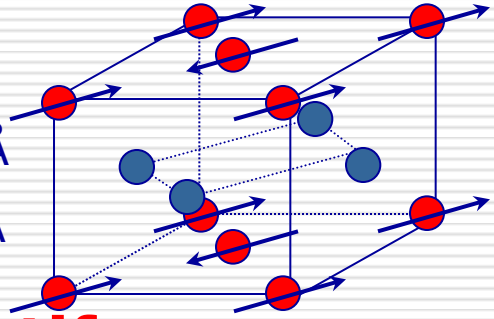

a=3.74Å

c=3.52Å

(after annealing, **antiferromagnetic**)

Identification of NiMn order phase

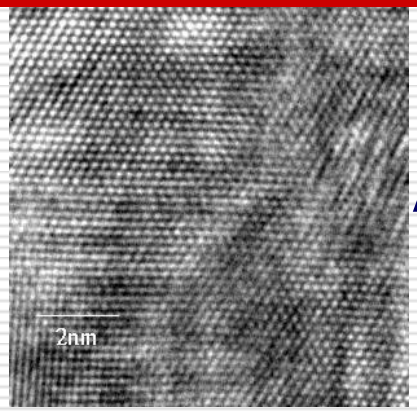

As-deposited

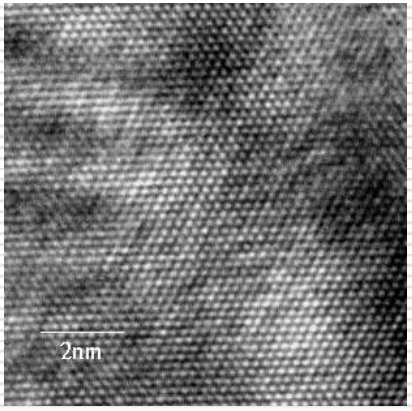

annealed

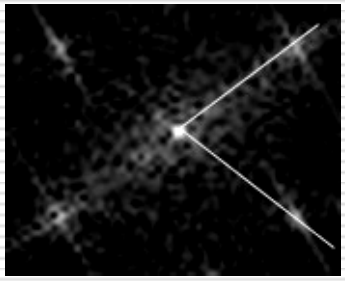

70.57°

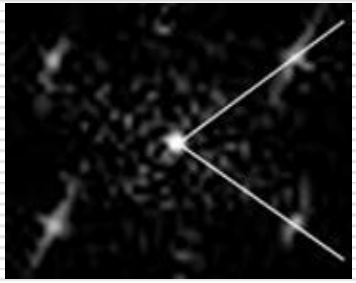

69.12°

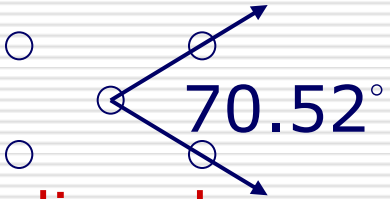

disorder

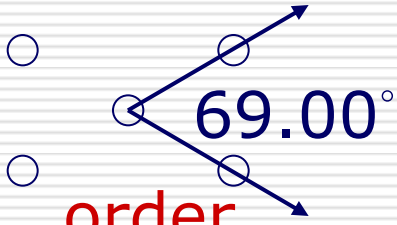

order

HRTEM processed by low-pass filter

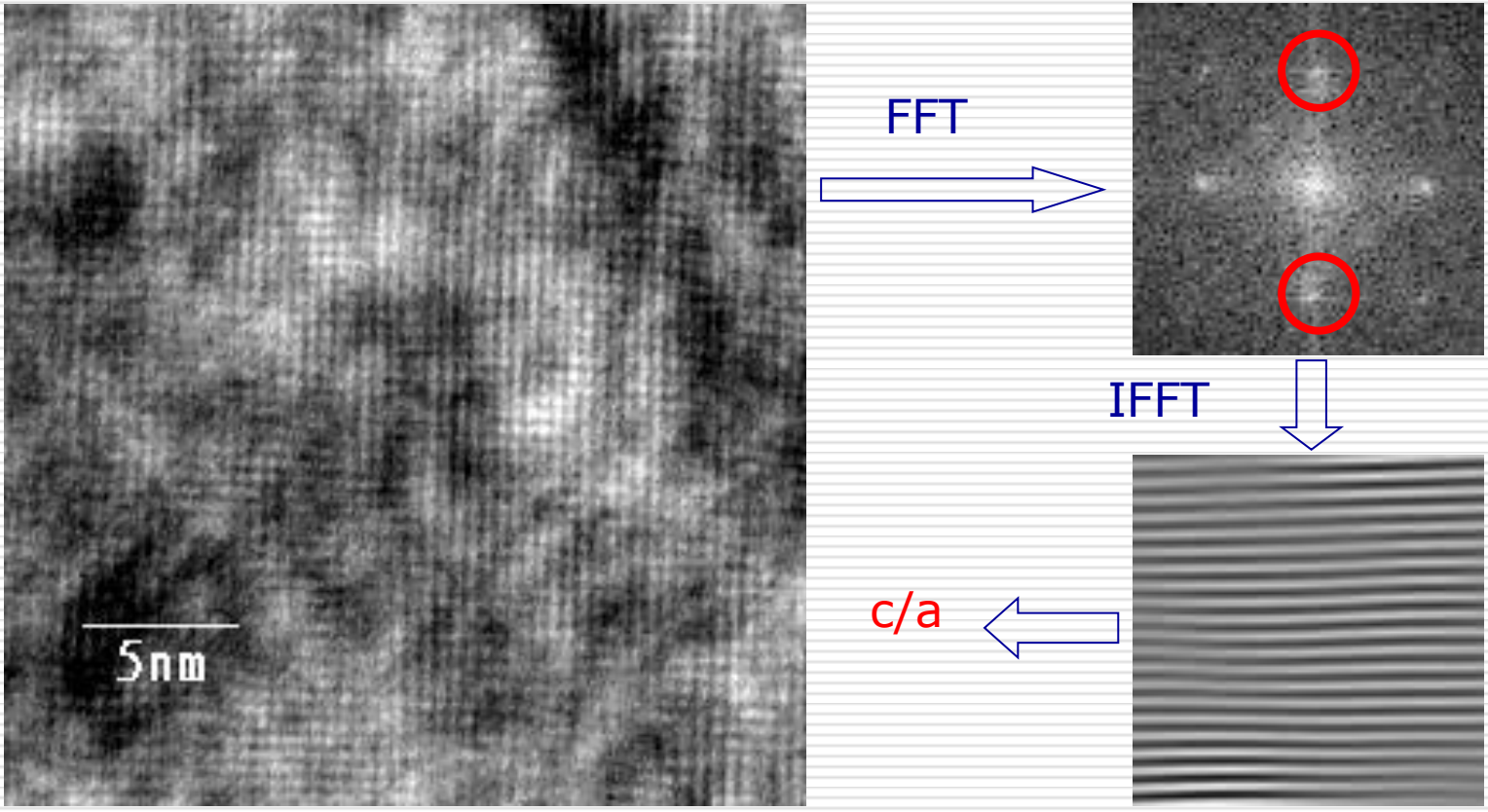

TEM analysis

280 ˚C 1hr-annealed sample

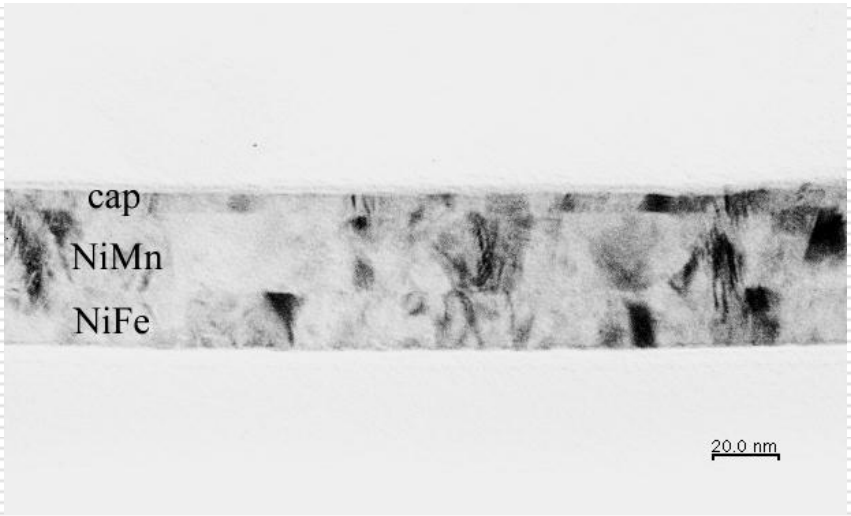

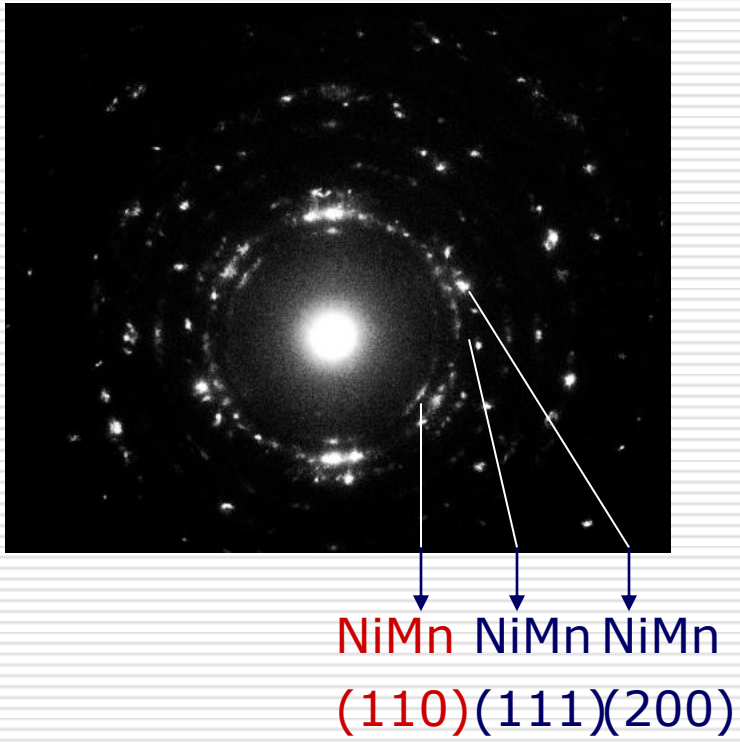

Dark field image contributed by different orientations

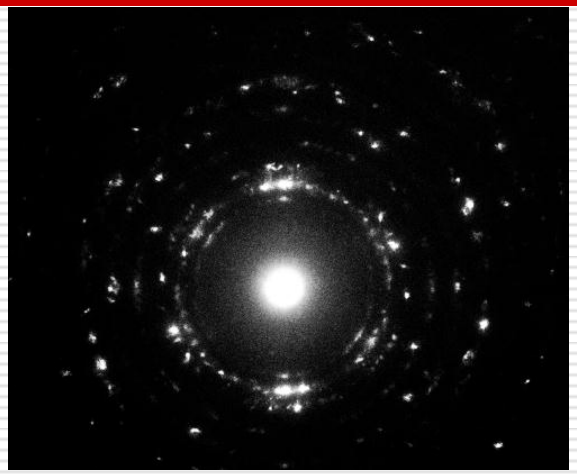

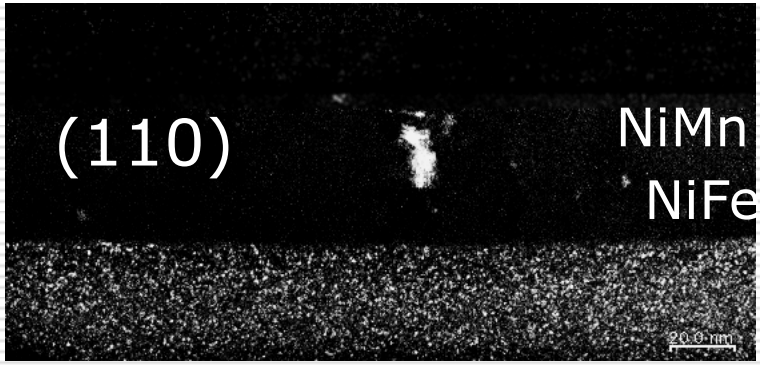

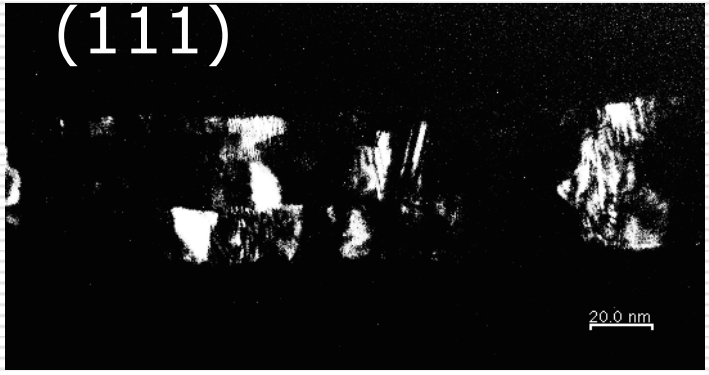

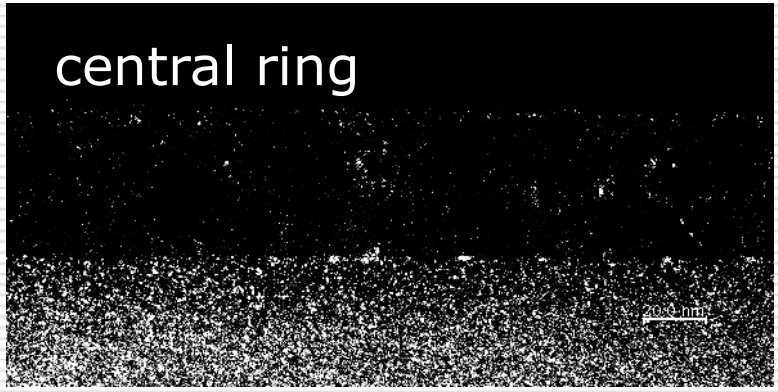

Distribution of ordered phase by dark field images

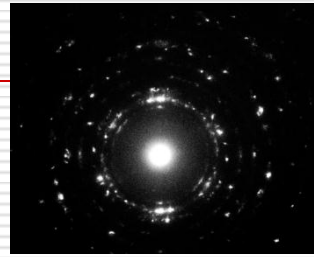

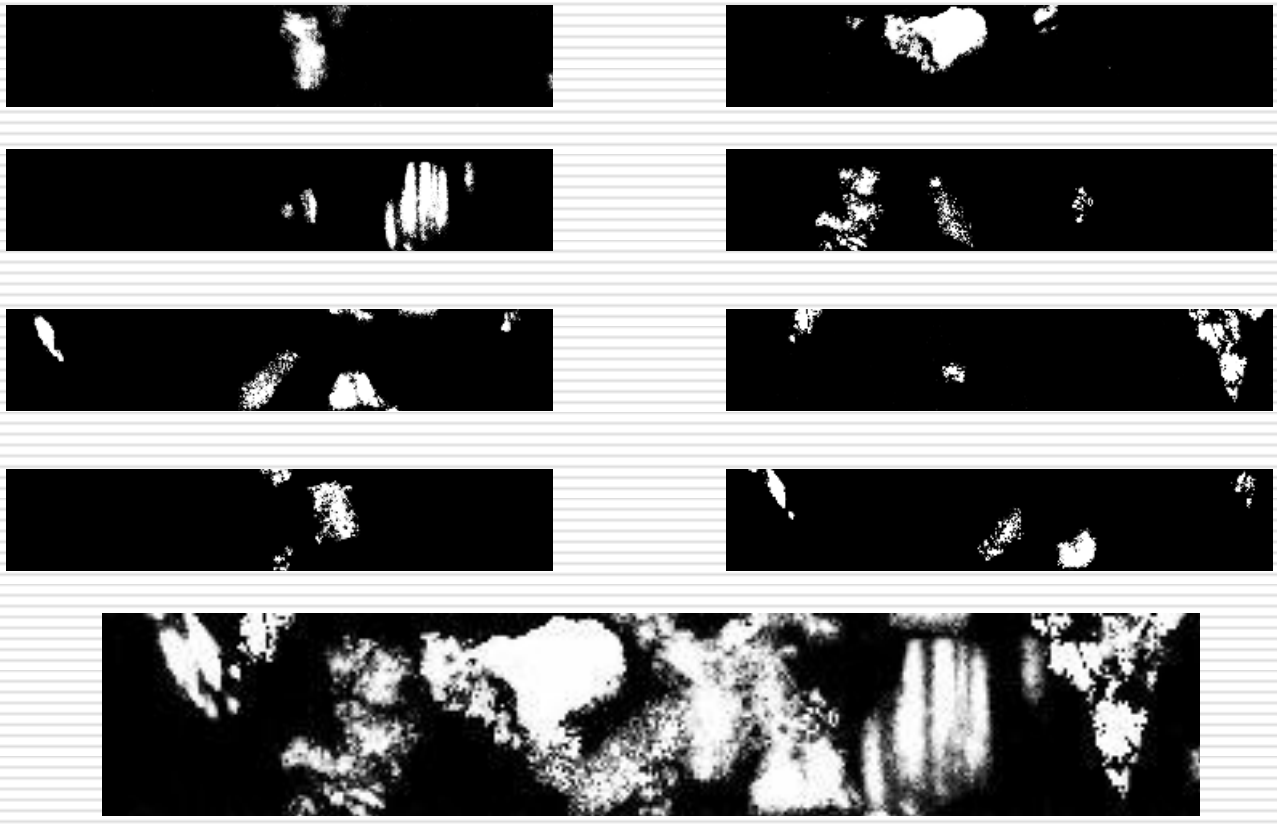

Volume fraction of order phase=72 %

Relationship between Hex and ordering factor

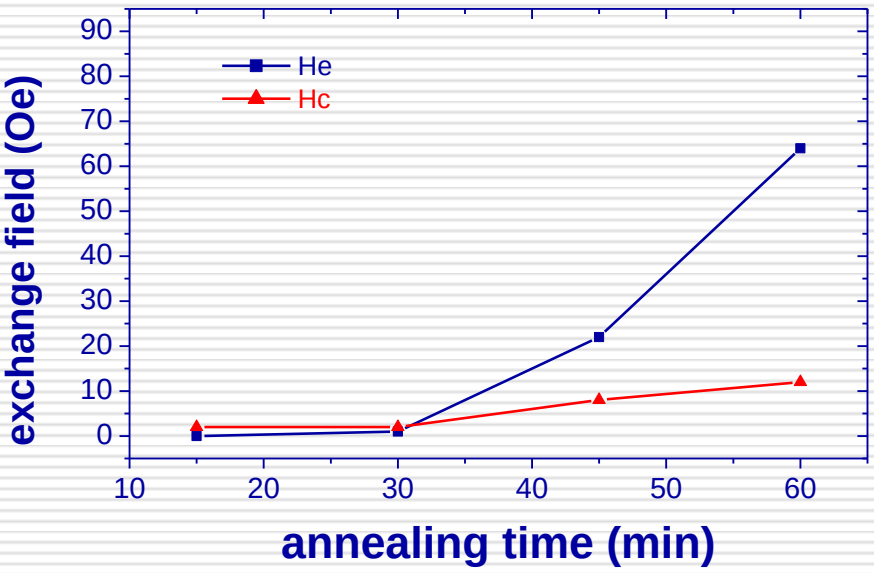

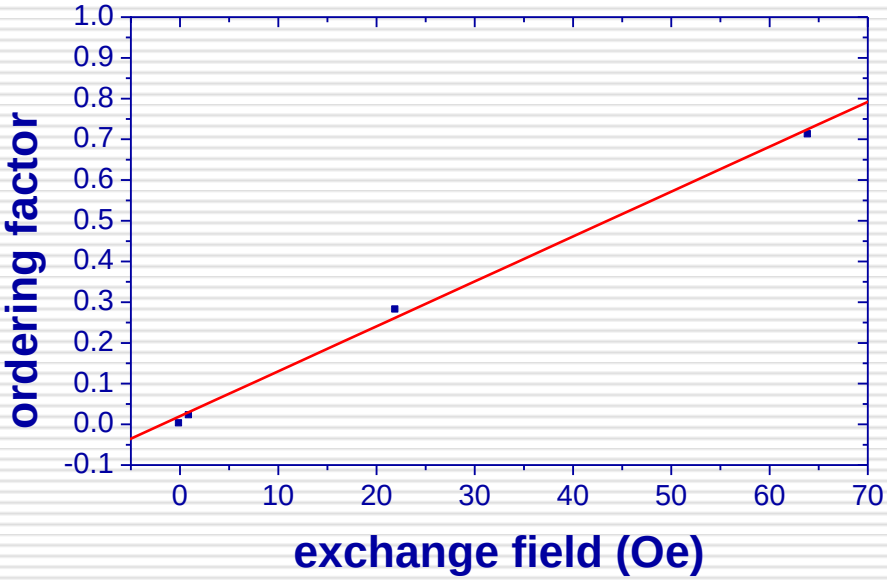

Annealing temperature=240 °C

Acknowledgments

Group members in NTHU

Y. C. Wu
C. C. Chiang
L. W. Wang
C. H. Yang
H. C. Ho
C. H. Ho
K. F. Huang
D. S. Wang
P. H. Lin
J.W. Liao
M.D. Yang

Collaborators

York Univ. Roy Chantrell

NIST Brian Kirby
kathryn Krycka

Colorado State Univ. MingZhong Wu

Georgetown Univ. Kai Liu

Univ. of Vienna Dieter Suess

NTHU Hsiu-Hau Lin

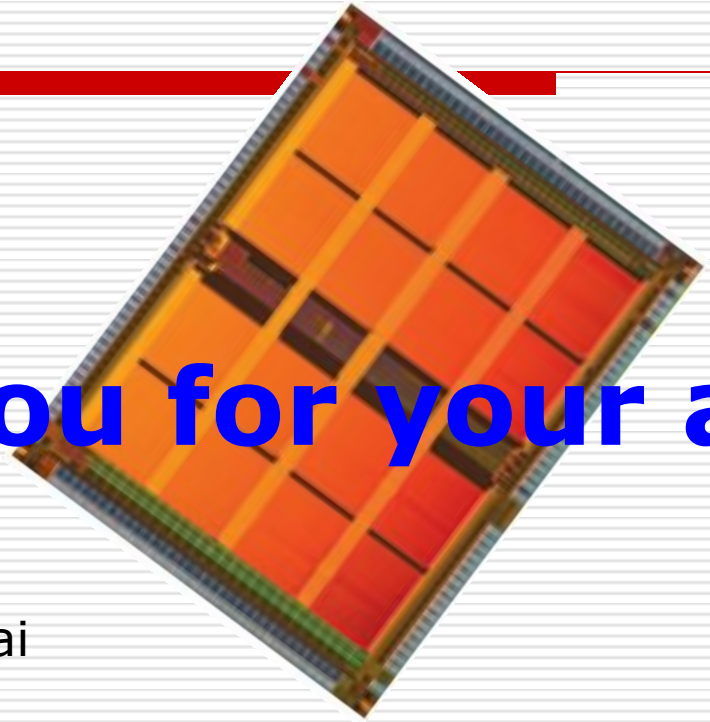

Thank you for your attention!

Web page of lab:
Prof. Chih-Huang Lai

Chih-Huang Lai
chlai@mx.nthu.edu.tw

(I) Magnetic Media

(S1) PATTERNED MEDIA

Agglomeration of Thin FePt Films

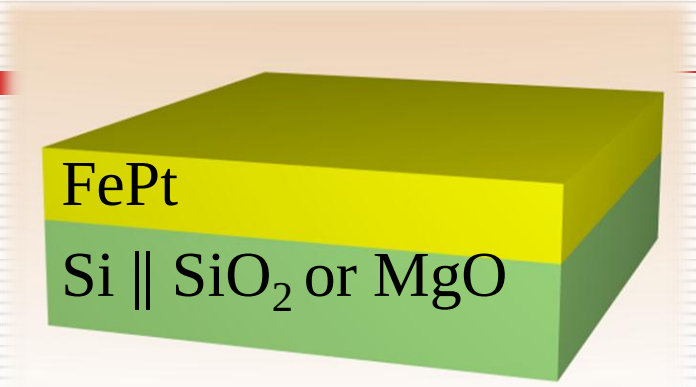

- **High Temperature Process**

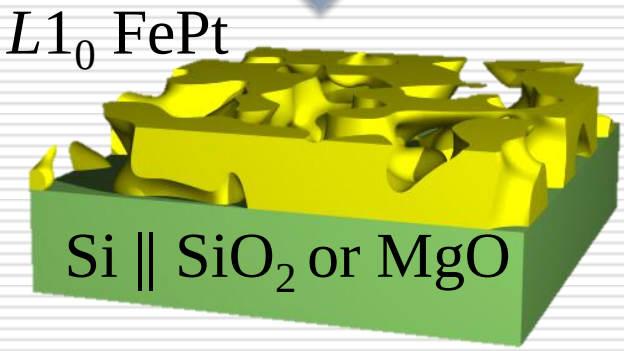

- **Discontinuous film**
  Thermal de-wetting (Agglomeration)

Capping-layer effects

$[Fe/Pt]_{18}$ MLs/5nm SiO_2

T_a = 350℃ for 60 sec.

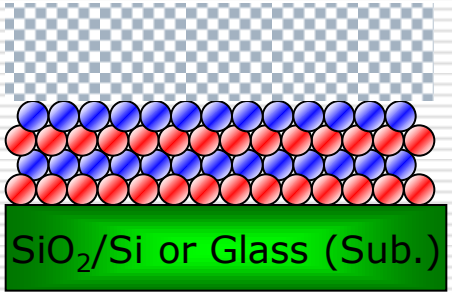

Fe- 0.16 nm

Pt- 0.18 nm

SiO_2- *x* nm (amorphous)

$[Fe/Pt/SiO_2(0.56nm)]_{18}$

T_a = 350℃ for 60 sec.

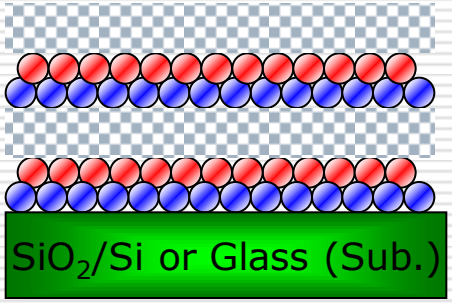

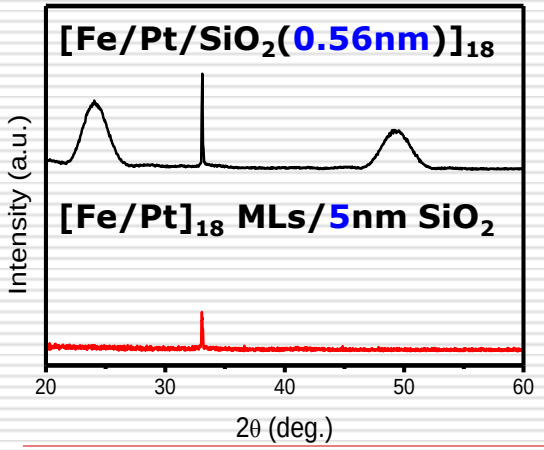

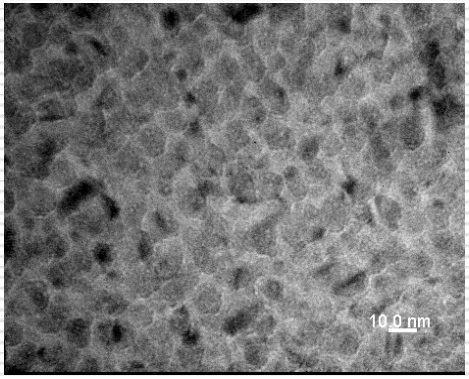

12±1.4 nm

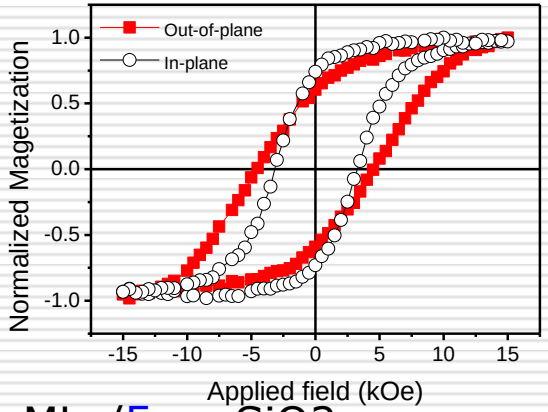

$[Fe/Pt]_{18}$ MLs/5nm SiO2

Experimental-Oxide Cap

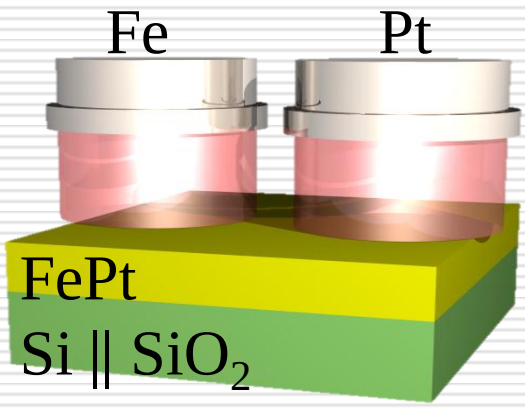

◆ **Film deposition @ RT**

$Fe_{52}Pt_{48}$

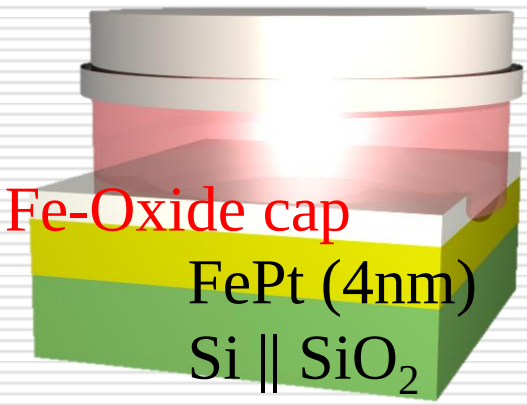

◆ **Plasma oxidation**

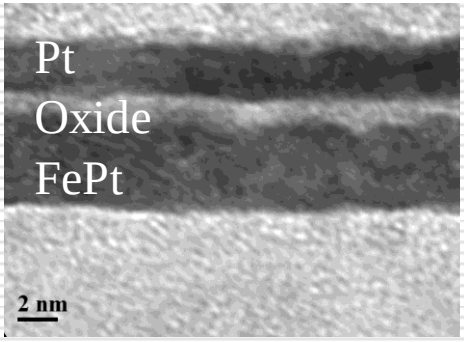

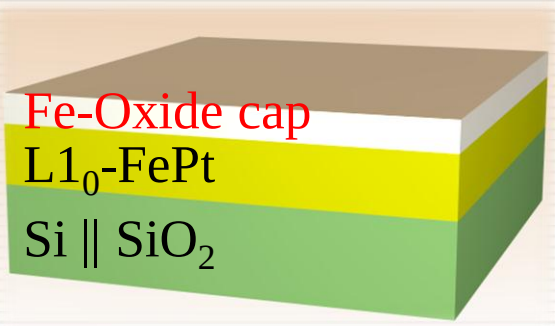

◆ **RTA @ 500 ^{0}C for 10 s**

Agglomeration and Crystalline Orientation

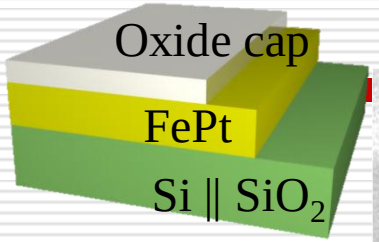

- 0 nm
- 0.9 nm

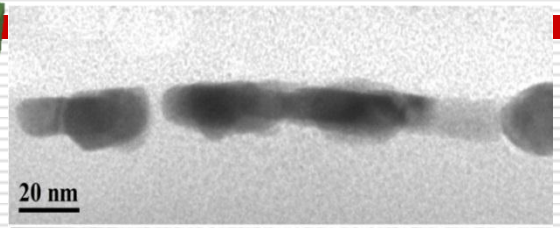

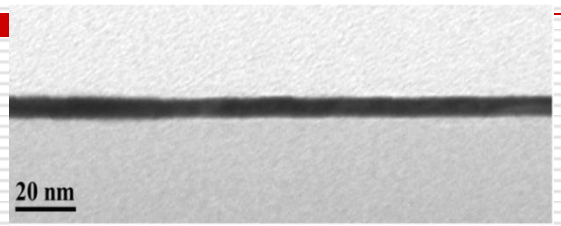

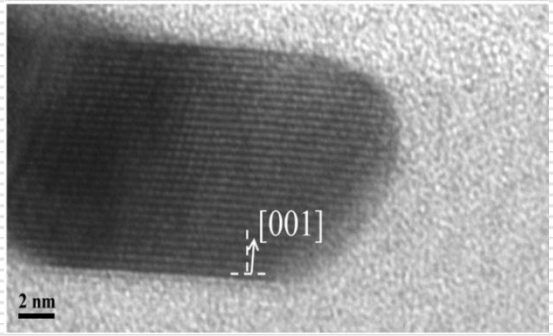

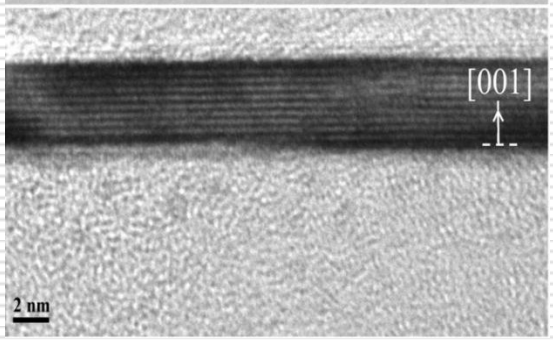

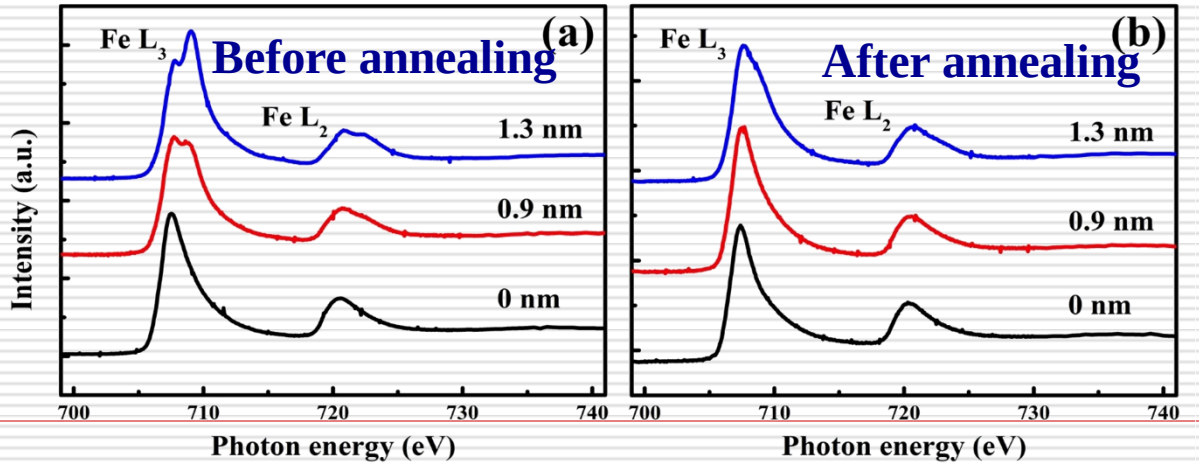

Patterning Process

Continuous FePt film (4nm)

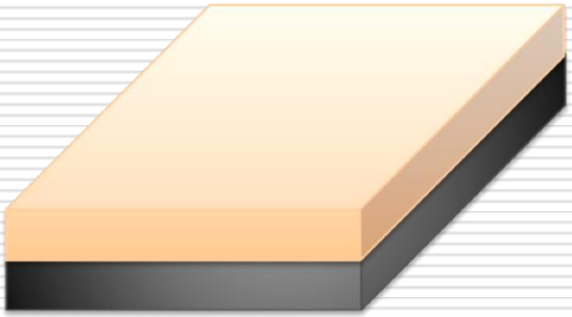

$L1_0$ FePt
Substrate

Copolymer by spin coating

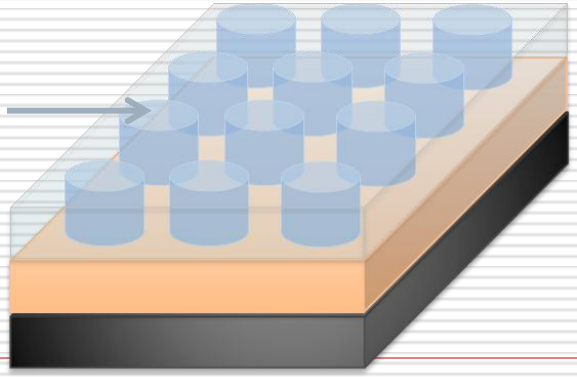

PDMS

PS

O_2 plasma etching

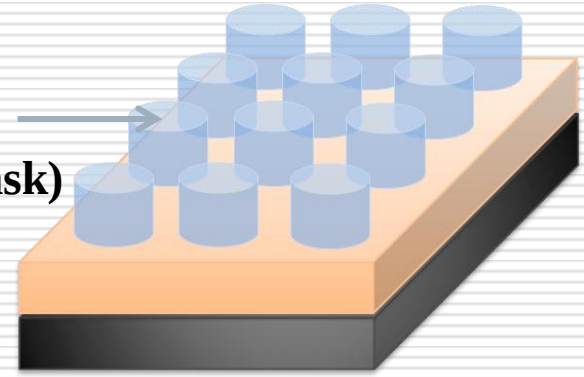

PDMS
(Hard Mask)

$CO + NH_3$ plasma etching

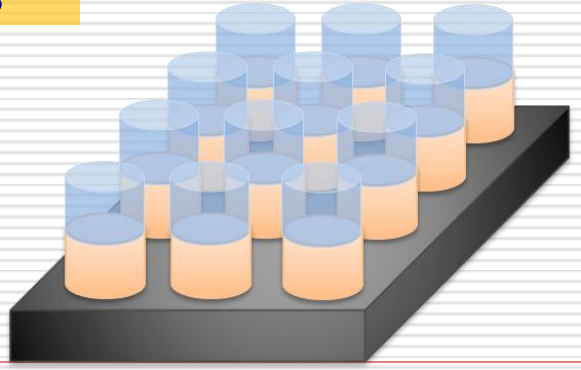

Magnetic Property for Patterned Films

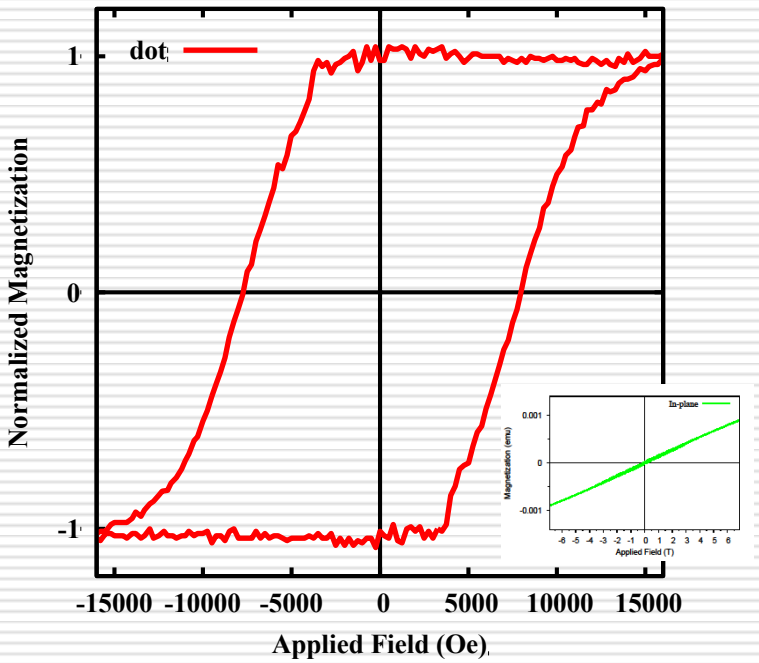

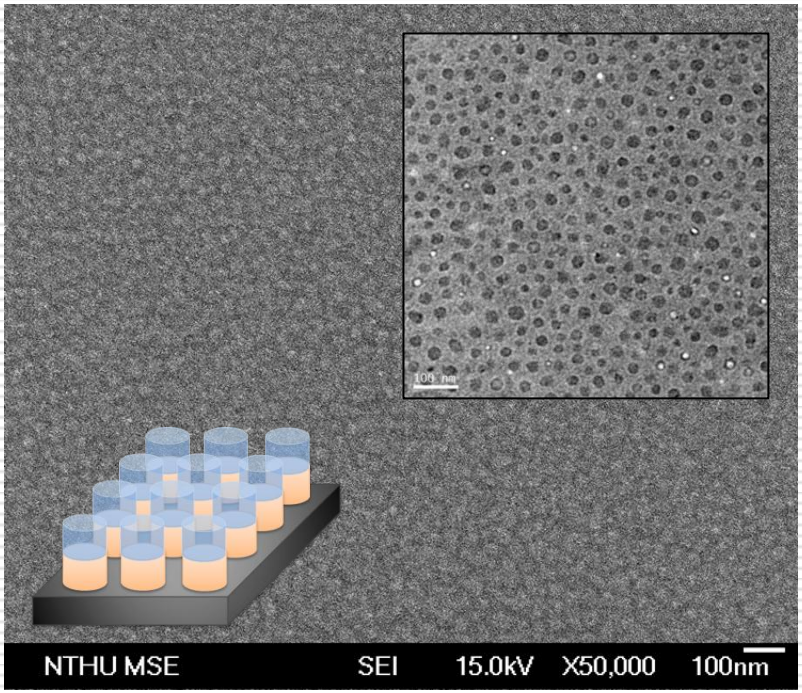

- Average dot diameter of 25 nm
- Dot-to-dot distance: 40 nm

(II) Nanoparticles and Spintronics Devices:

(S2) Perpendicular Magnetic Tunneling Junctions

Perpendicular Magnetic Tuning Junction

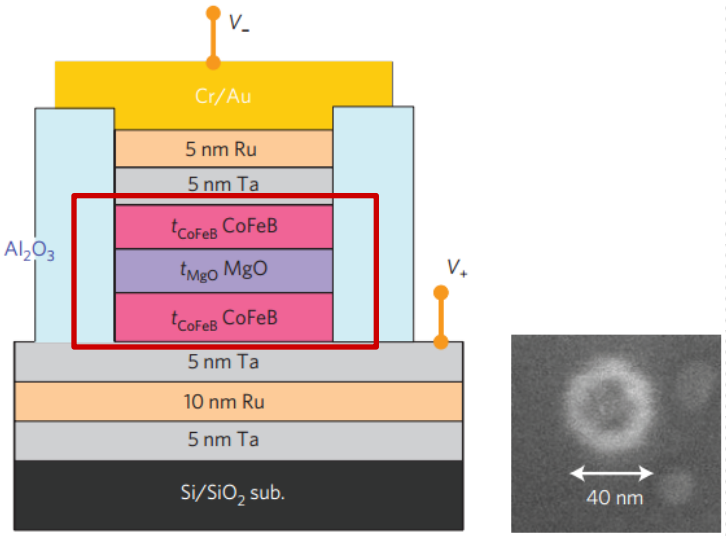

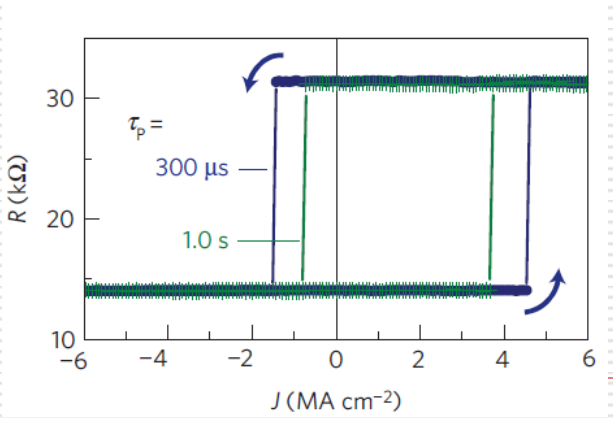

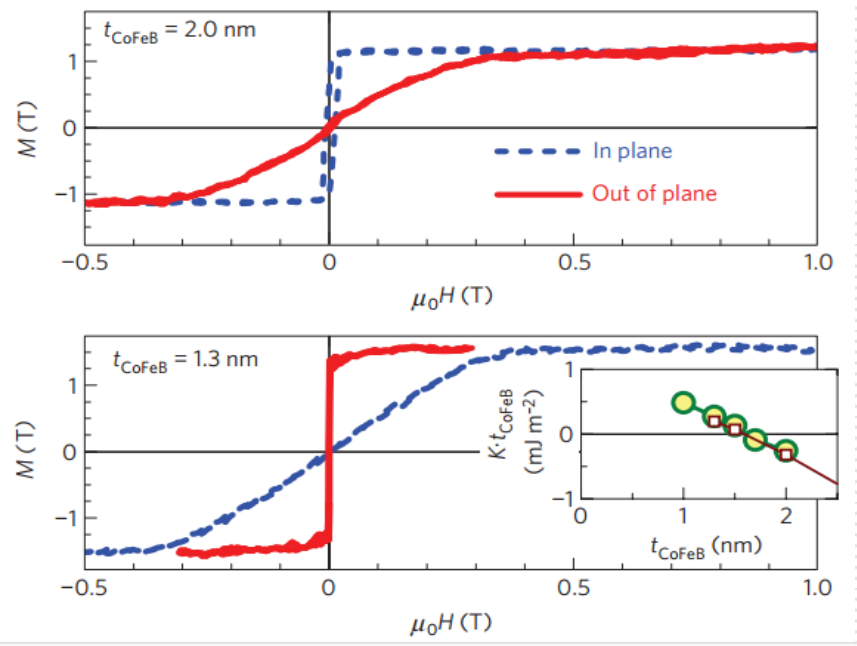

Origin of PMA
Damping constant

S. Ikeda *et al.*, Nat. Mat. (2010)

Mg oxidation vs. PMA

SiO_2// MgO_x / CoFeB(1.5 nm)/ Pt(2 nm)

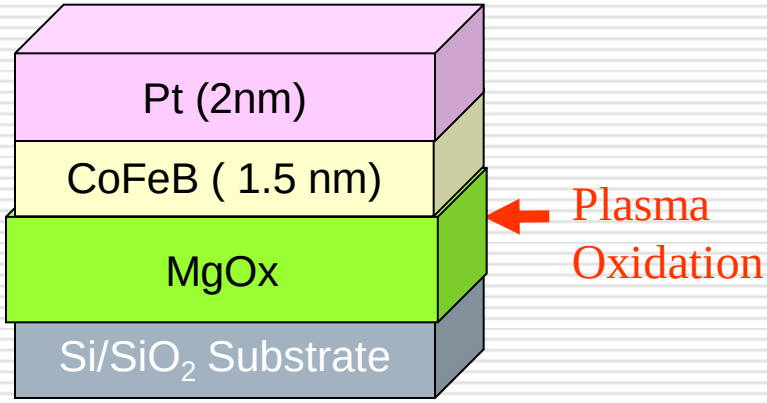

Control MgO_x / CFB interface by Mg oxidation time.

SiO_2//MgO_x /CoFeB(1.5 nm)/Pt(2 nm) annealed @ 330℃-30min

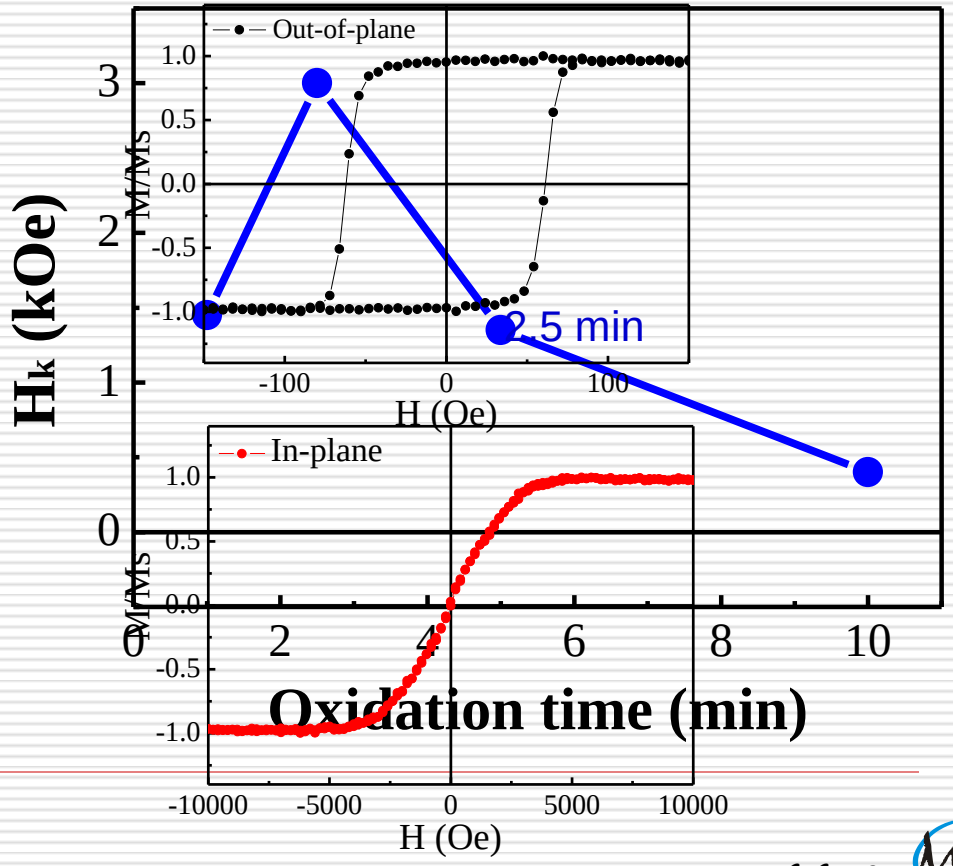

XAS (Fe & O)

- XAS: X-ray Absorption Spectroscopy
- Dragon Beamline, BL-11A1, NSRRC, Taiwan

t_{ox} = 2.5min
T_{ann} = 330℃

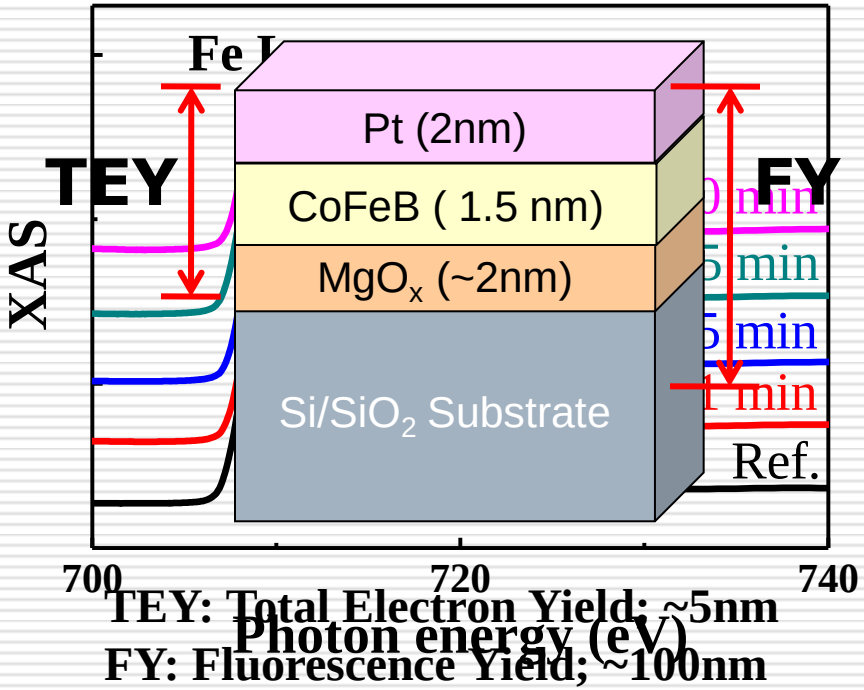

TEY: Total Electron Yield; ~5nm
FY: Fluorescence Yield; ~100nm

(Ref. = SiO_2//CoFeB/Pt, as-deposited state)

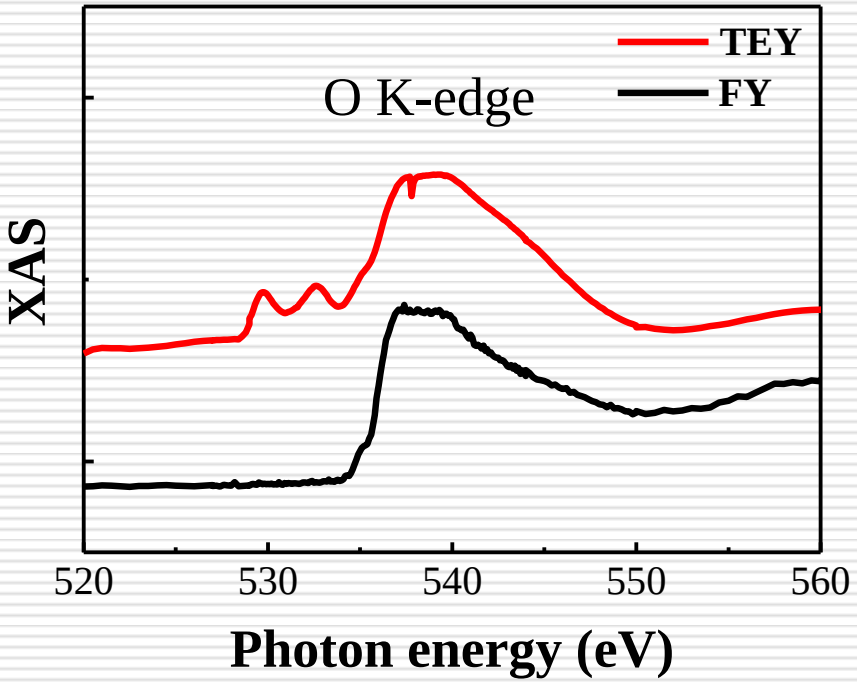

Pre-edges came from FeO_x

PRB **48**, 2109 (1993)

XMCD & Sum rules

- XMCD: X-ray Magnetic Circular Dichroism
- Dragon Beamline, BL-11A1, NSRRC, Taiwan

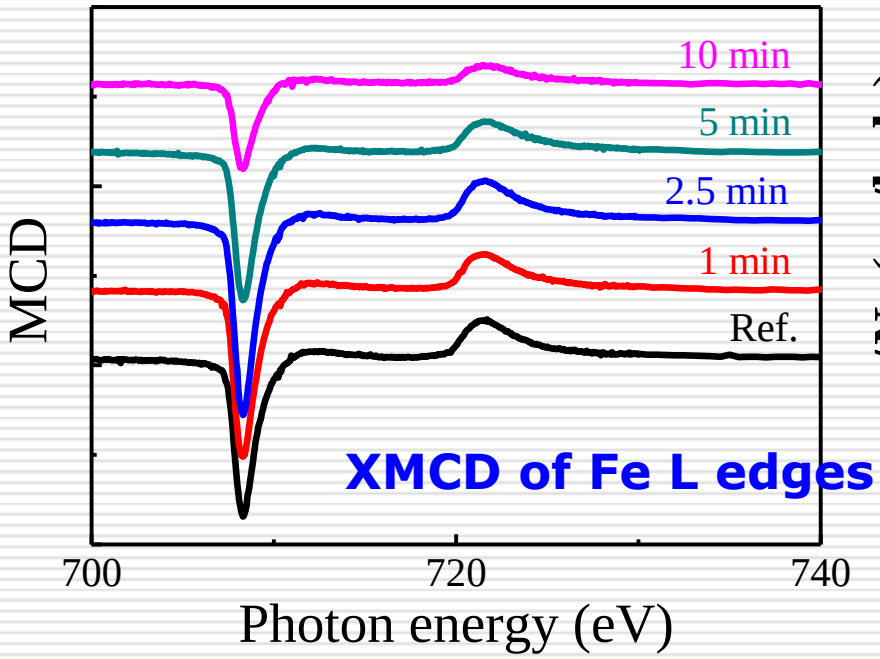

Sum rules calculation

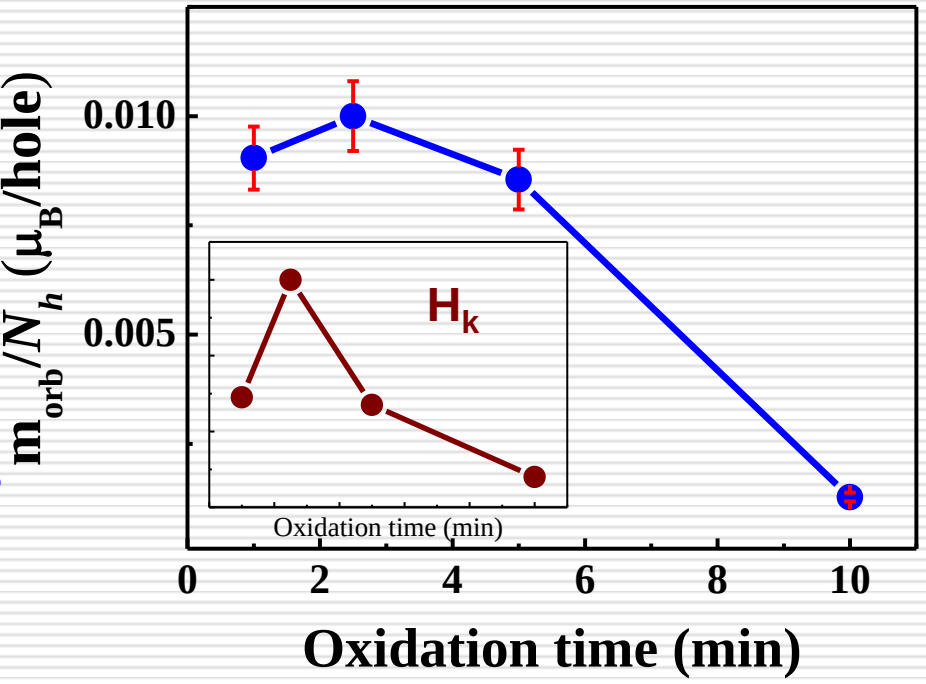

Fe-O bonding ⇨ PMA

W. C. Tsai, C. H. Lai., APL 100, 172414 (2012)

Effects of capping on PMA

Film structure:

Sub.// Pd (3)/ CoFeB (1)/ MgO (0.4)/ OX/ MgO (1.2)/ Al (X)/ Pd (3)

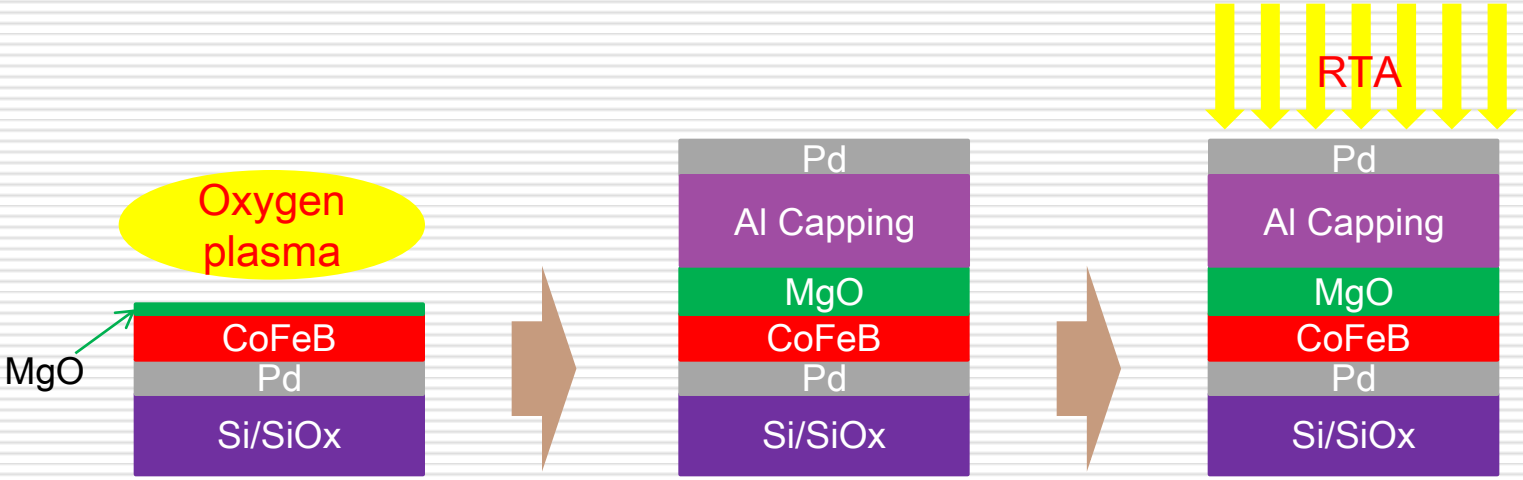

Magnetic properties

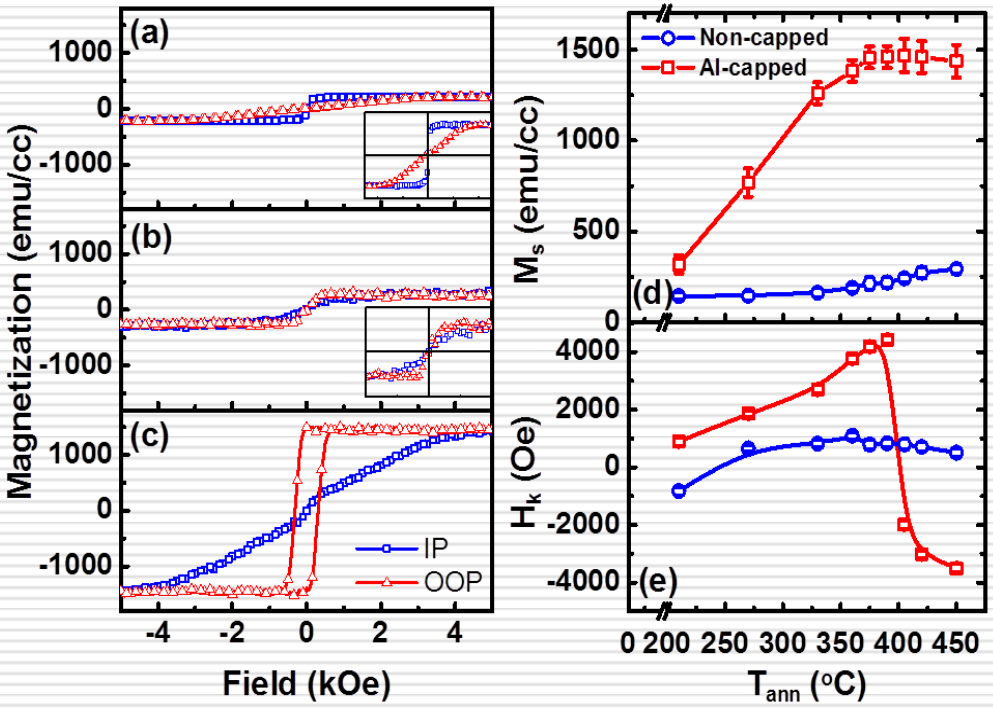

(a) As-deposit

(b) Pd capping, 360°C RTA

(c) 5nm Al capping, 360°C RTA

(d) M_s growth with T

(e) Anisotropy varies with T; changes direction at certain T

Role of Al capping layer

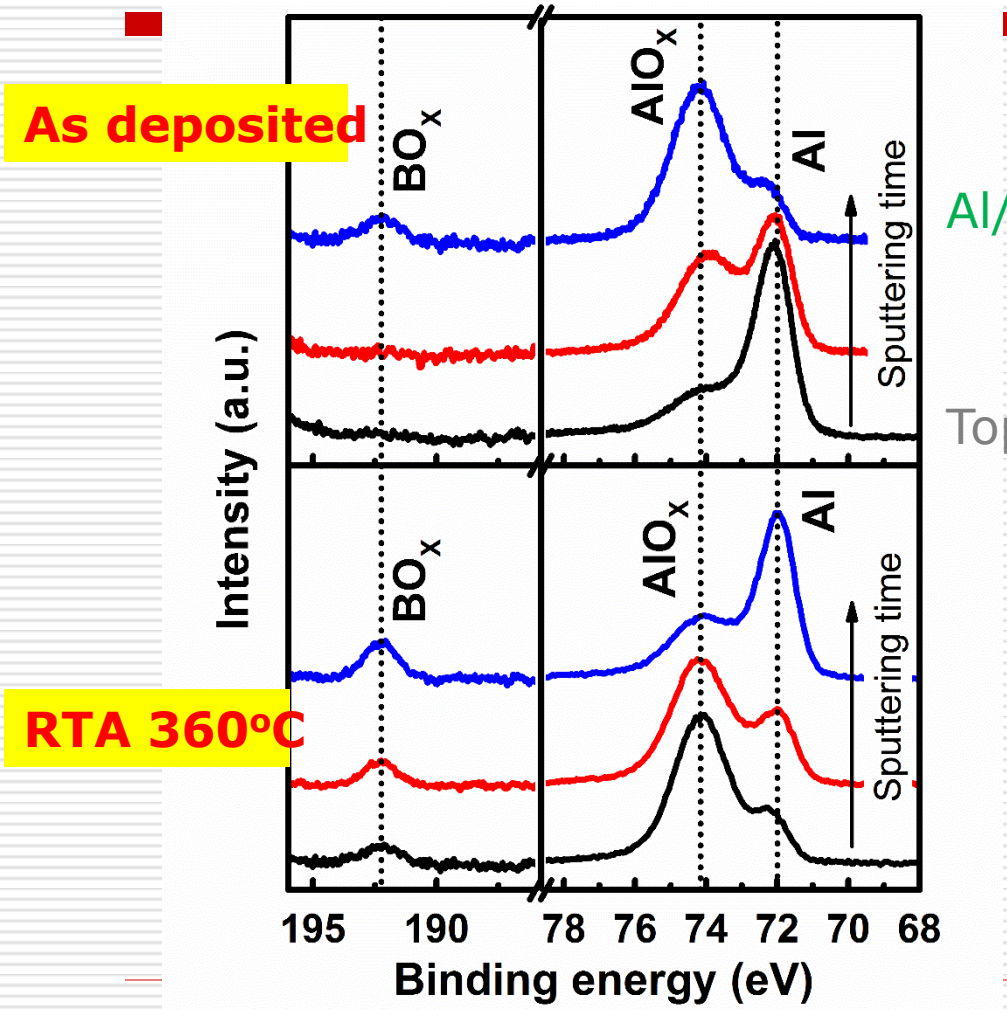

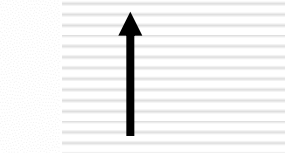

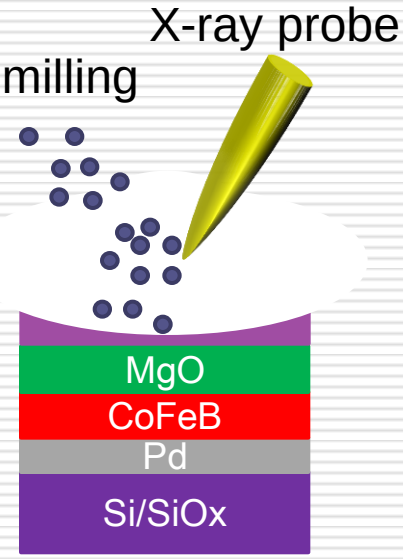

- **O and B were "pumped out" from the bottom**
- **Al capping as O/B absorber during annealing!**

X-ray photoemission spectroscopy @ BL24A, NSRRC, Taiwan

Role of annealing

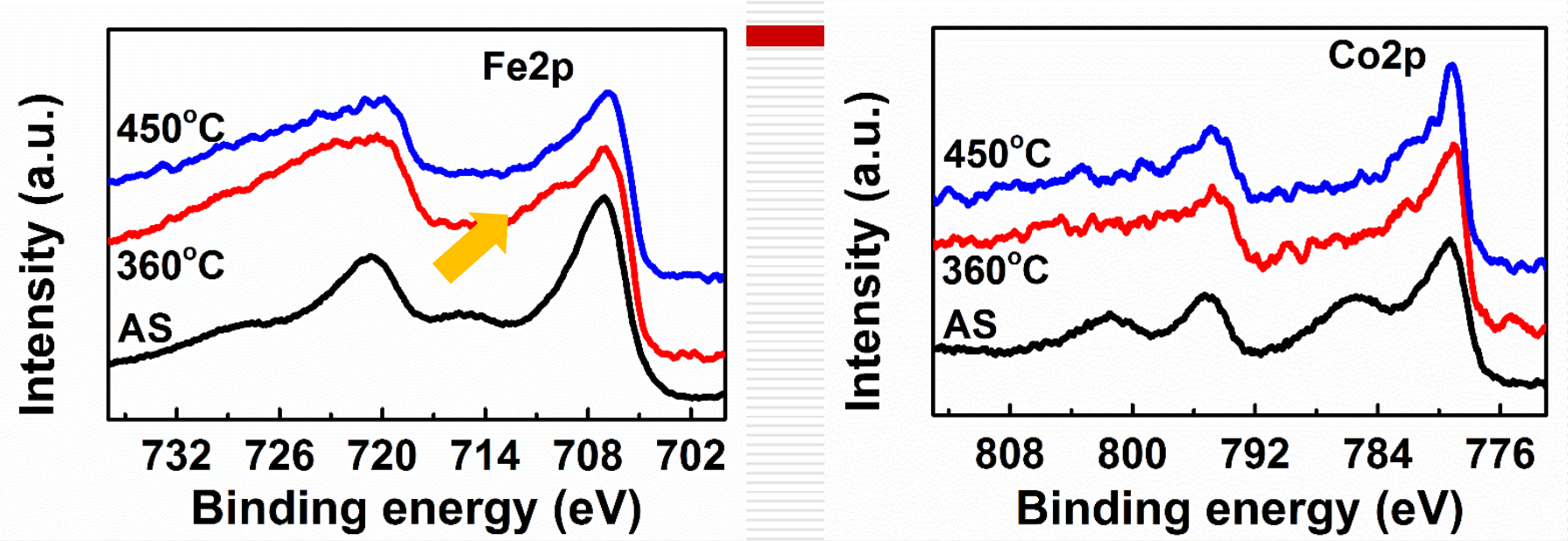

- Reduction of magnetic oxides (FeO_x, CoO_x) → M_s enhancement
- Small amount of FeO_x remain → PMA
- Low α for PMA CoFeB

$$\alpha_{360} = 0.011$$
$$\alpha_{450} = 0.016$$